ADVANCED FUELS CAMPAIGN
2014 ACCOMPLISHMENTS

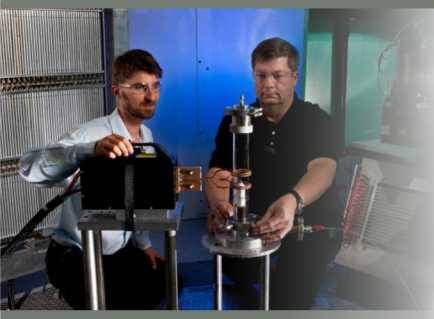

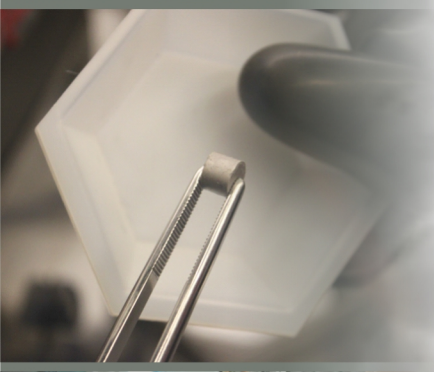

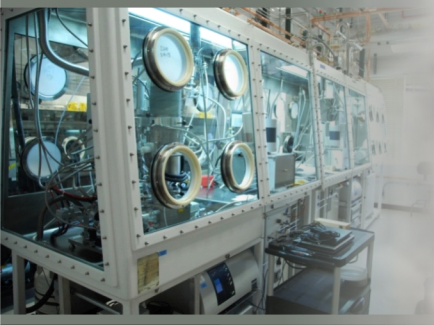

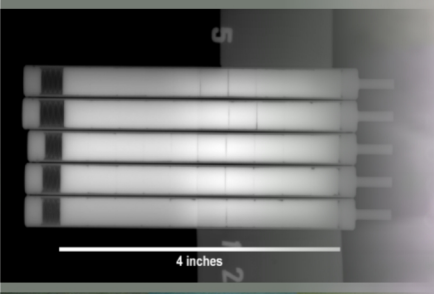

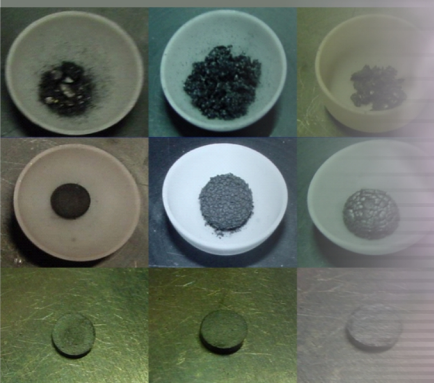

Advanced Fuels Campaign

October 2014

FUEL CYCLE RESEARCH AND DEVELOPMENT

ADVANCED FUELS CAMPAIGN
FY 2014 ACCOMPLISHMENTS REPORT

FCRD-FUEL-2015-000002
INL/EXT-14-33515

October 2014

Compiled and edited by:

Lori Braase (lori.braase@inl.gov)
W. Edgar May (ed.may@inl.gov)
INL Systems Analyses

Approved by:

Jon Carmack
FCRD AFC National Technical Director

October 31, 2014
Date

Prepared for the U.S. Department of Energy
Office of Nuclear Energy
Under DOE Idaho Operaton Office
Contract DE-AC07-05ID14517

This page intentionally left blank.

CONTENTS

FIGURES

TABLES

This page intentionally left blank.

SECTION 1

AFC Integration and Collaborations

1. AFC INTEGRATION AND COLLABORATIONS

1.1 Introduction

The mission of the Advanced Fuels Campaign (AFC) is to perform Research, Development, and Demonstration (RD&D) activities for advanced fuel forms (including cladding) to enhance the performance and safety of the nation's current and future reactors; enhance proliferation resistance of nuclear fuel; effectively utilize nuclear energy resources; and address the longer-term waste management challenges. This includes development of a state-of-the art Research and Development (R&D) infrastructure to support the use of a "goal-oriented science-based approach."

In support of the Fuel Cycle Research and Development (FCRD) program, AFC is responsible for developing advanced fuels technologies to support the various fuel cycle options defined in the *Department of Energy (DOE) Nuclear Energy Research and Development Roadmap, Report to Congress, April 2010*.

AFC uses a "goal-oriented, science-based approach" aimed at a fundamental understanding of fuel and cladding fabrication methods and performance under irradiation, enabling the pursuit of multiple fuel forms for future fuel cycle options. This approach includes fundamental experiments, theory, and advanced modeling and simulation. The modeling and simulation activities for fuel performance are carried out under the Nuclear Energy Advanced Modeling and Simulation (NEAMS) program, which is closely coordinated with AFC. In this report, the word "fuel" is used generically to include fuels, targets, and their associated cladding materials.

The mission of AFC is to perform RD&D activities for advanced fuel forms (including cladding) to enhance the performance and safety of the nation's current and future reactors; enhance proliferation resistance of nuclear fuel; effectively utilize nuclear energy resources; and address the longer-term waste management challenges. This includes development of a state-of-the art R&D infrastructure to support the use of a "goal-oriented science-based approach."

R&D of light water reactor (LWR) fuels with enhanced accident tolerance is also conducted by AFC. These fuel systems are designed to achieve significantly higher fuel and plant performance to allow operation to significantly higher burnup, and to provide enhanced safety during design basis and beyond design basis accident conditions. The overarching goal is to develop advanced nuclear fuels and materials that are robust, have high performance capability, and are more tolerant to accident conditions than traditional fuel systems.

AFC management and integration activities included continued support for international collaborations, primarily with France, Japan, the European Union, Republic of Korea, and China, as well as various working group and expert group activities in the Organization for Economic Cooperation and Development Nuclear Energy Agency (OECD-NEA) and the International Atomic Energy Agency (IAEA). Three industry-led Funding Opportunity Announcements (FOAs) and two university-led Integrated Research Projects (IRPs), funded in 2013, made significant progress in fuels and materials development. All are closely integrated with AFC and Accident Tolerant Fuels (ATF) research.

Accomplishments made during fiscal year (FY) 2014 are highlighted in this report, which focuses on completed work and results. The process details leading up to the results are not included; however, the lead technical contact is provided for each section. The key FY 2014 technical area outcomes are highlighted below.

- ***International Coordination and Collaboration:*** Bilateral agreements are supported with France, Japan, the European Union, the Republic of Korea, and China. The emphases in all collaboration activities are metallic fuel development, irradiation testing and data analyses, and development of

characterization and postirradiation examination (PIE) techniques. New interactions were developed with the Halden Reactor Project (Norway) in advanced LWR fuels, and activities with the Organization for Economic Cooperation and Development /Nuclear Energy Agency (OECD/NEA) were continued in FY 2014. Specific engagement with the Electric Power Research Institute (EPRI) was initiated in FY 2014.

- ***Advanced LWR Fuels with Enhanced Accident Tolerance:*** The primary focus is to continue fundamental RD&D on several promising ATF technologies; establish screening attributes and metrics for ATF concepts; and coordinate research activities between DOE laboratories, Industry FOA teams, University IRP teams and Nuclear Energy University Program (NEUP) investigators. Critical testing capability is required for ATF development. This includes high temperature steam oxidation testing (recently developed specifically for ATF), material property measurement, and irradiation testing.
- ***Transmutation Fuels:*** Primary RD&D areas include casting technology development; fabrication and characterization of minor actinide- and lanthanide-bearing fuel samples; fundamental property measurement and FCCI tests; and irradiation performance testing.
- ***Capability Development:*** Primary RD&D areas include advanced fabrication process development; advanced modeling and simulation (M&S) analysis of fuel systems and fabrication processes; characterization technique development; and unique in-pile and out-of-pile material property measurements.

Accident Tolerant LWR fuel research made significant progress in FY 2014 through completion of Phase 1A activities by the three industry-led FOA awards and initiation of Phase 1B for two additional years of activity. These projects are integrated into the DOE laboratory funded research, development, and infrastructure activities in AFC with the university NEUPs and university-led IRPs. In addition, ATF fabrication support resources were established and demonstrated at Oak Ridge National Laboratory (ORNL), Idaho National Laboratory (INL), and Los Alamos National Laboratory (LANL). Research quantities of ATF compositions were fabricated, demonstrating the capability to support industry FOA fuel fabrication needs as well as the capability to fabricate novel ATF fuel compositions. Design of the initial irradiation of ATF concepts, designated as the ATF-1 test series, was completed. The ATF-1 experiment will be inserted in INL's Advanced Test Reactor (ATR) in FY 2015. The experiment includes fuel concepts from Westinghouse Electric Company (WEC), AREVA, and General Electric (GE); irradiation will continue over the next two years.

The Transmutation Fuels area achieved a major accomplishment in FY 2014 with the successful return of the FUTURIX-FTA experiment from the French CEA Phenix reactor. The FUTURIX-FTA fuel experiment contains four pins of transmutation fuel, two pins of metallic fuel, and two pins of nitride fuel. The results of PIE will allow direct comparison of similar data obtained through fuel testing in the ATR. In addition, revision 6 of the AFCI Materials Handbook was issued.

1.2 Campaign Organization

J. Carmack, Idaho National Laboratory

One of the most challenging aspects of AFC is the management, integration, and coordination of major R&D activities across multiple organizations. AFC interfaces and collaborates with Fuel Cycle Technologies (FCT) campaigns, universities, industry, various DOE programs and laboratories, federal

agencies (e.g., Nuclear Regulatory Commission [NRC]), and international organizations. Key challenges are the development of fuel technologies to enable major increases in fuel performance (safety, reliability, power and burnup) beyond current technologies, and development of characterization methods and predictive fuel performance models to enable more efficient development and licensing of advanced fuels. Challenged with the research and development of fuels for two different reactor technology platforms, AFC targeted transmutation fuel development and focused ceramic fuel development for Advanced LWR Fuels.

Organization

AFC is organized into three technical areas and is integrated with NEAMS for fuels modeling and simulation. The technical areas are 1) Advanced LWR Fuels, 2) Transmutation Fuels, and 3) Capability Development. The technical highlights in this report are organized in the three categories shown in Figure 1.

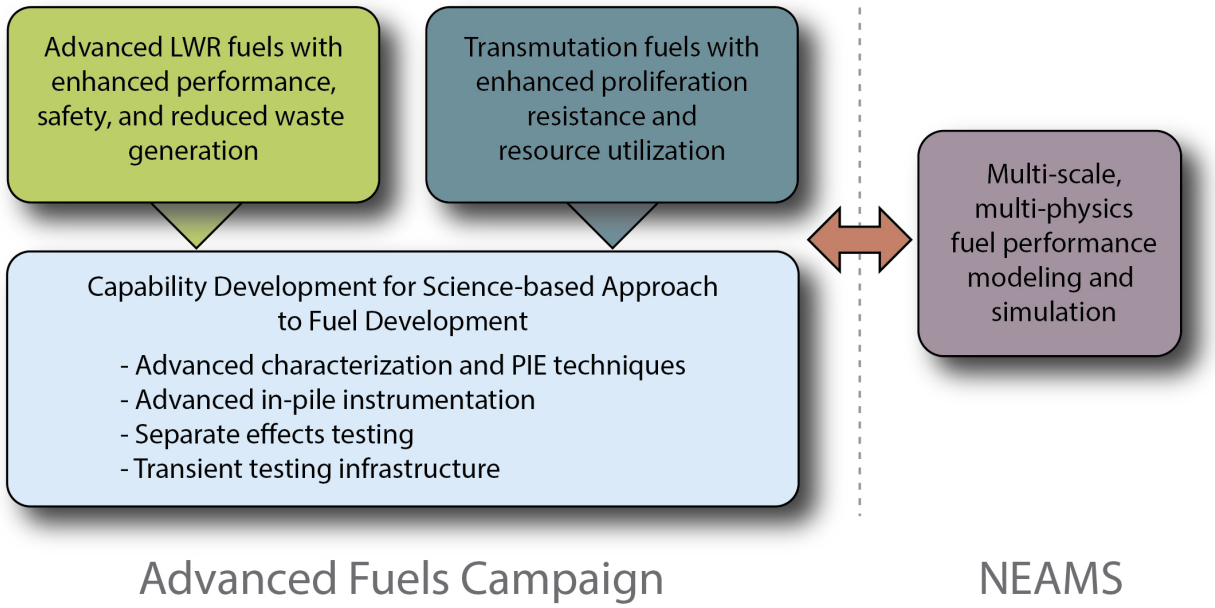

Figure 1. AFC Organization with NEAMS Interface

The AFC leadership team is shown in Figure 2.

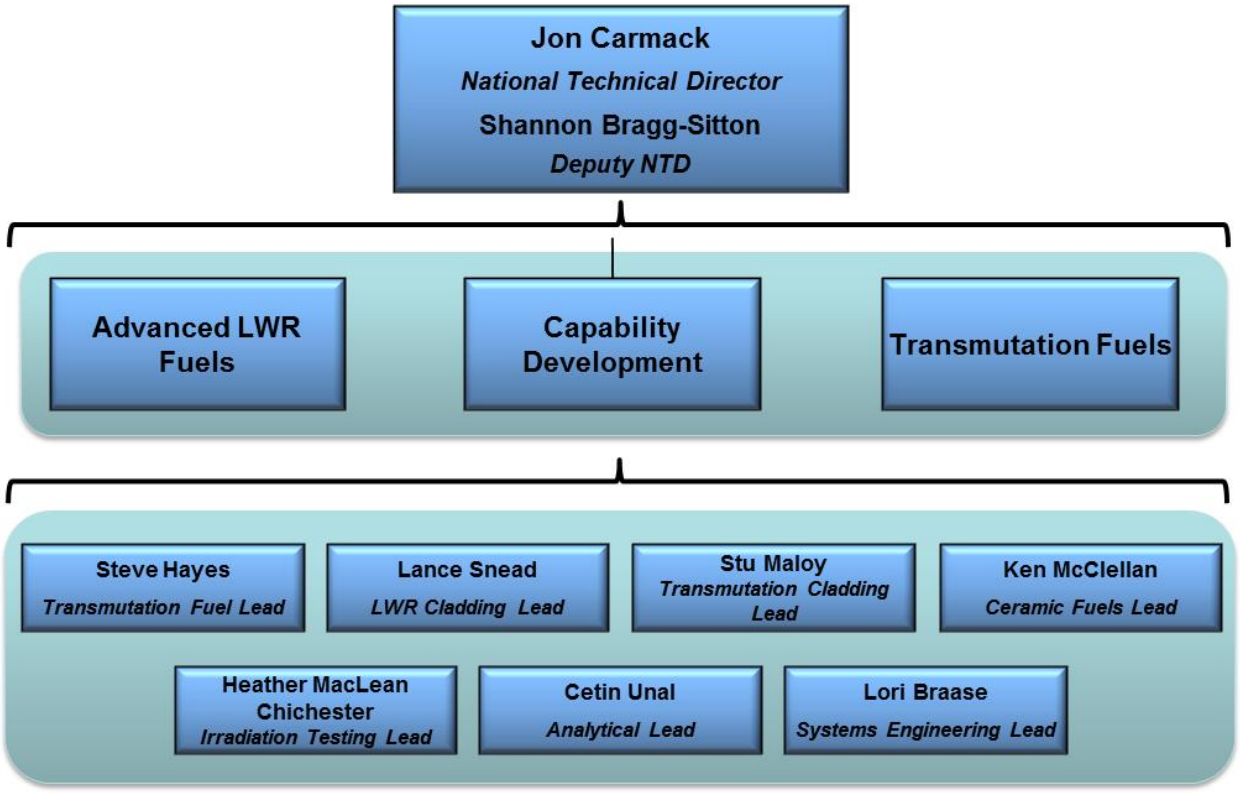

Figure 2. AFC Leadership Team Organization

1.3 Integration and Communication

Two AFC Integration Meetings were conducted during FY 2014. In general, the meetings focused on DOE-NE guidance, industry and university updates, and technical presentations to status R&D efforts. The meeting locations and dates are listed below.

- Oak Ridge National Laboratory, March 12-13, 2014. Highlights include the accomplishment presentations made by the technical principle investigators, a presentation by a new NEUP from the University of California-Berkeley, updates by AFC IRPs (University of Illinois and University of Tennessee), and a technical tour of ORNL's fuels and materials science facilities.
- Idaho National Laboratory, August 26-28, 2014. This was the first AFC integration meeting held at INL, with over eighty people in attendance. A poster session was held on Wednesday evening with 30 presenters from universities, nuclear programs, and student interns. In addition, 30 attendees participated in a tour of the Materials and Fuels Complex.

Workshops

An *Independent Review* of the "failed" AFC-2 A, B, and E ATR irradiation tests, was held January 28-29, 2014. At the request of the program, an independent review committee was convened to review the post-test analyses performed by the fuels development team, to assess the conclusions of the team regarding the cause of the failures, to assess the adequacy and completeness of the analyses, to identify issues that were missed, and to make recommendations for improvements in the design and operation of future tests. The review team included consultants Mike Cappiello (Chair), Richard Hobbins, Leon Walters and Keith Penny (INL). Although there is some difference of opinion, the review committee largely agreed with the

conclusions of the fuel development team regarding the cause of the failures. The review team believed that the most likely cause of failure (fuel melt) in all three tests was a higher than anticipated heat generation rate in the fuel coupled with inadequate heat transfer through the gas gap that exists between a test rod and the safety capsule.

Technology Readiness Levels

The *Technology Readiness Levels for Advanced Nuclear Fuels and Material Development* document was updated from the last issue in 2008. Advanced nuclear fuels research is a critical part of the FCRD program aimed at developing advanced technologies for closing the nuclear fuel cycle. TRLs provide a framework for identification and prioritization of the needed activities associated with nuclear fuels and materials development.

AFC Stakeholder Communications Plan

The *AFC Stakeholder Communications Plan* was completed with an initial focus on ATF. Experts in technical communications at Potomac Communications were consulted to identify the best approaches to communicating with the various stakeholder groups. The purpose of the plan is to foster timely communication with the stakeholders in LWR ATF R&D to ensure a focus on solutions that will garner strong support across those stakeholders and will ultimately be adopted by the commercial nuclear plants.

Stakeholders involved in advanced reactor technology R&D range from non-technical members of the public to the in-depth research community. ATF development is a subset of FCRD AFC, which receives direction through the Fuel Cycle Technology Program in the Department of Energy Office of Nuclear Energy (DOE-NE). Appropriations to DOE-NE are made via the Office of Management and Budget (OMB) with Congressional approval. The ability of AFC to advance ATF concepts is made possible through this hierarchy of entities. Communication with and engagement of these offices is essential to the success of the program.

AFC must periodically interact with external stakeholders and researchers to accomplish the necessary R&D tasks. These external stakeholders (e.g. the Public, Research Community, Industry, Regulators) must be informed of the research goals and objectives of the ATF program and its current status. Feedback from external stakeholders should be considered in the decision making process by AFC leadership.

The communication plan identifies key stakeholders and potential methods of delivering information to each group. Examples of how the plan is being implemented are described below:

- An ATF overview article was published in the March 2014 edition of Nuclear News (ANS monthly publication). The article was authored by S. Bragg-Sitton and includes contributions from lab development teams (Oak Ridge National Laboratory [ORNL], Los Alamos National Laboratory [LANL], INL, Pacific Northwest National Laboratory [PNNL]), FOA teams (WEC, AREVA, GE, and university teams (University of Tennessee [UT], University of Illinois [UI], GeorgiaTech).
- **[INL]** Three information sheets on ATF development were completed and approved. They are intended to provide quick overview information on key areas of ATF R&D. Additional sheets are currently in preparation

for ATF-related topics (e.g. overview of ATF modeling efforts and summary sheets on key facilities supporting ATF fabrication or testing) and will later include transmutation fuel research. These information sheets will be made available to stakeholders via the external website and distributed at industry meetings and other relevant events. Additional sheets will be prepared on topics within AFC. The titles of the documents are

- Enhanced Accident Tolerant Fuels for Light Water Reactors
- Enhanced Accident Tolerant Fuels for LWRs: Industry Teams
- Irradiation Testing of Candidate Accident Tolerant Fuels for LWRs.

- An overview article of the Accident Tolerant Fuel Development Program, authored by Jon Carmack and Shannon Bragg-Sitton was published in the Jan-Feb 2014 *Nuclear Plant Journal*, p. 46-47.

1.4 International Collaborations

AFC researchers are very active in international collaborations with Korea, France, Japan, China, Russia, and the European Atomic Energy Community [EURATOM]. These interactions and collaborations are managed through a combination of participation in Generation IV Global International Forum projects, International Nuclear Energy Research Initiative (INERI) projects, and participation in bilateral and trilateral government-to-government agreements.

The Global Actinide Cycle International Demonstration (GACID) project seeks to demonstrate the irradiation and performance of minor actinide-bearing mixed oxide (MOX) fuel in the Monju reactor in Japan. The Gen-IV Sodium Fast Reactor (SFR) project provides the means for collaboration on the development of advanced fuels including metallic, ceramic, nitride, carbide, and advanced cladding systems. France's Atomic Energy Commission (CEA) and DOE have a joint bilateral to pursue the assessment of the UO2-Am system as a transmutation system for americium. Significant progress was made this year in the U.S. on this subject in the design of an Americium Bearing Blanket (AmBB) irradiation experiment to be conducted in the INL Advanced Test Reactor. CEA efforts have demonstrated the capability to fabricate high concentration Americium bearing ceramic fuel pellets for this irradiation. OECD-NEA supports several collaborations with the US, including organizing international workshops on Accident Tolerant Fuels. EURATOM-DOE collaborative fuel R&D focused on specific technical staff exchanges on fabrication and characterization methods with the Joint Research Center-Institute of Transuranium Elements. AFC engaged with the Halden Reactor Project. ATF material samples were provided to Halden for testing. Discussions were initiated with potential future collaborations including irradiation of accident tolerant fuel and PIE of experiments. Highlights from AFC International Collaborations are included below:

NEA (Multi-National Collaboration / Cooperation)

S. Bragg-Sitton, Idaho National Laboratory

OECD-NEA Nuclear Science Committee approved the formation of an Expert Group on ATF for LWRs (EGATFL). Chaired by Kemal Pasamehmetoglu, INL Associate Laboratory Director for Nuclear Science and Technology, this group will conduct work under three task forces: (1) Systems Assessment, (2) Cladding and Core Materials, and (3) Fuel Concepts. Scope for the Systems Assessment task force includes definition of evaluation metrics for ATF, technology readiness level definition, definition of illustrative scenarios for ATF evaluation, parametric studies, and selection of system codes. The Cladding and Core Materials and Fuel Concepts task forces will identify gaps and needs for modeling and experimental demonstration; define key properties of interest; identify the data necessary to perform concept evaluation under normal conditions and illustrative scenarios; identify available infrastructure (internationally) to support experimental needs; and make recommendations on priorities. Where possible, considering proprietary and other export restrictions (e.g., International Traffic in Arms Regulations), the Expert Group will facilitate the sharing of data and lessons learned across the international group membership. The Systems Assessment Task Force will be chaired by Shannon Bragg-Sitton (INL), while the Cladding Task Force will be chaired by a representative from France (Marie Moatti, CEA) and the Fuels Task Force will be chaired by a representative from Japan (Masaki Kurata, Japan Atomic Energy Agency [JAEA]).

GenIV-Sodium Fast Reactor Arrangement on Advanced Fuels

K. McClellan, Los Alamos National Laboratory

The Sodium Fast Reactor Advanced Fuel (SFR-AF) arrangement started in 2007 with a targeted duration of 10 years within the frame of the Generation IV Sodium Fast Reactor program. The primary objective is to investigate high burn-up Minor Actinide bearing fuels, cladding, and wrapper materials capable of withstanding high neutron doses and temperatures. The project has been structured in 3 steps: evaluation of advanced fuels and materials options, Minor Actinide-bearing fuels evaluation, and assessment of high burn-up capability of advanced fuel(s) and materials. Until this point, participants in the arrangement have been the DOE, CEA, JAEA, Korean Atomic Energy Research Institute [KAERI], and EURATOM. China and Russia have petitioned to join the arrangement with contributions from China Institute of Atomic Energy (CIAE) and ROSATOM (Russian Federation national nuclear corporation), respectively. In 2014, the U.S. served as co-chair for the SFR-AF program management board and hosted the spring meeting in Knoxville, TN. The proposed contributions of China and Russia were discussed with the relevant negotiators, preparation was subsequently approved by the board and the SFR-AF arrangement was modified to incorporate those contributions. The modified arrangement was subsequently approved by the SFR-System Steering Committee and has been transmitted to the signatories of the participating countries for final approval.

US/Japan CNWG Collaboration on Advanced Fuels

K. McClellan, Los Alamos National Laboratory

Cooperative research under the Advanced Fuels area of the Fuel Cycle R&D and Waste Management Sub-Working Group is performed under the general areas of properties, performance and analysis. The goal of this effort is to perform collaborative R&D for evaluation of basic properties and irradiation behavior of advanced fuels. The objectives of the collaboration are to expand the basic properties and performance data and to improve understanding of advanced fuels with an emphasis on employment of advanced experimental techniques. Through incorporation of new minor actinide mixed oxide (MA-MOX) irradiation data the effort will also enable development and application of advanced modeling and simulation tools for design and performance analysis of oxide fuels. In FY 2014, several technical expert meetings were held in Japan and in the US at LANL and INL to advance specific tasks on basic properties of fuels, development of PIE data, and modeling and simulation of irradiated transmutation MOX fuel. Several joint publications from the fuel properties activities were made during the period and initial planning started for future power-to-melt and steady states tests of MA-MOX in the Japanese Joyo reactor.

Halden ATF Candidate Irradiation

K. Terrani, Oak Ridge National Laboratory

AFC representatives actively participated in Halden Program Group (HPG) meetings in FY 2014 and coordinated various synergies between AFC's goals and activities and the Halden joint program. Of particular note was approval of a dedicated test rig for ATF cladding materials in the upcoming 3-year program (2015-2017). The AFC representatives distributed a white paper outlining irradiation testing of a FeCrAl clad UO_2 rodlet (50 cm active fuel length) with various in-pile instrumentation options. In-pile creep testing of FeCrAl and SiC specimens is planned, commencing in January 2015. The specimens, provided by ORNL, are at Halden and are currently being incorporated into their dedicated test rigs.

Finally, AFC is also taking advantage of an upcoming test at Halden (IFA-744: in-pile UO_2 thermal conductivity measurement), originally initiated and designed by EPRI and ORNL, to demonstrate capabilities of the BISON code for detailed 3D analysis of this test rig.

US/EURATOM I-NERI Project on Novel Technology for Synthesis of Nuclear Fuels

K.J. McClellan, LANL

This three-year project was initiated in FY 2014 to investigate advanced net shaping technology for nuclear fuel/target applications. The U.S. contribution to this collaborative research effort is performed under AFC while the EURATOM contribution is performed under the EURATOM FP7 and HORIZON 2020 programs on Safety of Nuclear Fuel. The co-principle investigator (PI) for the U.Ss is Dr. Ken McClellan (LANL) and the co-PI for EURATOM is Dr. Joe Somers, Joint Research Centre Institute for Transuranium Elements (ITU).

The objective is to advance the field of novel compaction technology for advanced fuel systems where conventional routes are not viable. Advanced fuels being studied for enhanced accident tolerance and for actinide transmutation often have unique characteristics which make conventional sintering routes undesirable for or incapable of yielding the required fuel pellet characteristics. This project explores processing routes to enable more efficient fuel synthesis. In order to assess multiple routes for multiple systems, this project integrates the various embryonic advanced processing activities ongoing at each participating institution which will in turn allow this effort to encompass several field-assisted sintering techniques that can be employed for fabrication of a range of ceramic systems. Participating institutions include LANL, INL, ORNL, University of Florida, and ITU.

The first technical meeting was held at ITU in FY 2014. The U.S. accomplishments included thermodynamic screening at ORNL of candidate composite ATF systems consisting of UN-USi_x and UO_2-UB_x. Thermodynamically viable composites were identified for both systems. Initial experimental screening was performed at LANL on these systems. This screening demonstrated that the nitride-silicide systems require processing at higher currents than for UO_2-based composites; however, in both cases higher currents were relative to the single phase UO_2 reference case. ITU has successfully installed a spark plasma sintering (SPS) system within a glovebox to enable exploration of SPS processing of minor actinide-bearing fuels.

US/EURATOM and OECD Projects on Thermodynamics of Nuclear Fuels

T. M. Besmann, S. L. Voit, Oak Ridge National Laboratory; P. E. A. Turchi, Lawrence Livermore National Laboratory; J. R. Kennedy, Idaho National Laboratory; R. J. M. Konings, Centre Institute for Transuranium Elements

Under the OECD-NEA Thermodynamics of Advanced Fuels-International Database (TAF-ID) project, FY14 tasks were grouped into the two areas below. The current version of TAF-ID database contains the description of 178 binary and 47 ternary systems.

- Introduction of existing models from different countries involved in the TAF-ID project. In some cases, several descriptions already exist for some of the chemical systems. For example, metallic fuels models were developed in Japan (Central Research Institute of Electric Power Industry [CRIEPI]), U.S. (Lawrence Livermore National Laboratory [LLNL]) and France (CEA). In such a case, a choice had to be made as to which single description to use in the TAF-ID.

- Full assessment of chemical systems. Where there is no available model in the literature or from the countries involved in the project, a model had to be developed on the basis of available experimental data.

For the US/EURATOM International Nuclear Energy Research Initiative (I-NERI) on Phase Equilibria and Thermochemistry of Fission Products in Urania Fuel, a representation for the thermodynamic properties and the phase equilibria of the U-Y-O system was created using the CALPHAD (CALculation of PHAse Diagrams) approach. To represent YO_2 in the compound energy formalism for U1-yYyO2±X, the lattice stability was calculated using density functional theory. A partially ionic liquid sublattice model is used for the liquid phase, and a Gibbs function for the stoichiometric rhombohedral phase UY_6O_{12} is proposed. All available, self-consistent data was used for the optimization, resulting in coherent models for the U-Y-O system that are consistent across all databases used in the fuels program. An example of the results can be seen in the computed phase diagram shown in Figure 3.

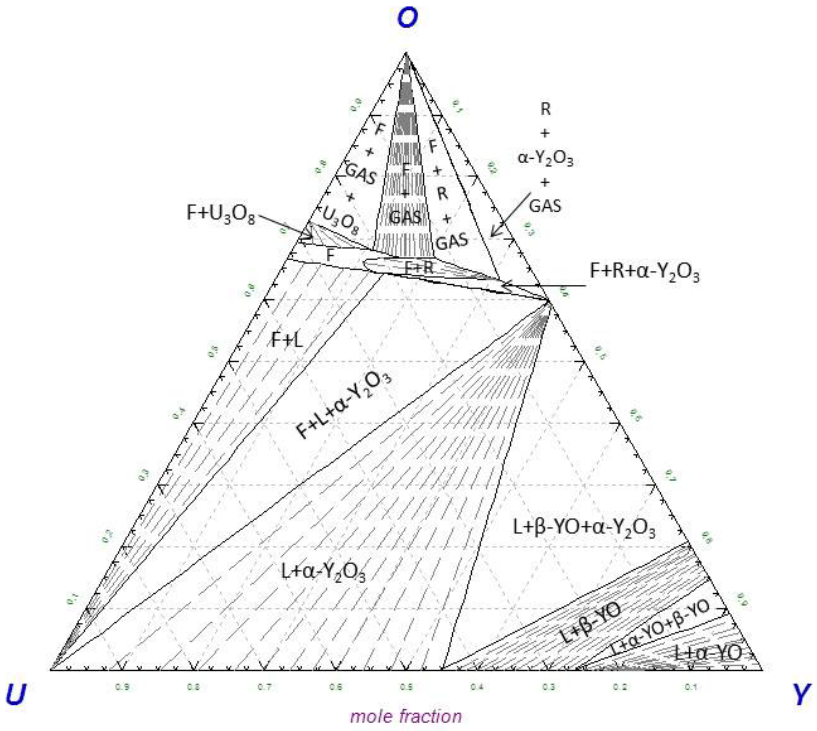

Figure 3. Computed U-Y-O phase diagram at 1500K.

This page intentionally left blank.

Advanced Light Water Reactor Fuels

SECTION 2

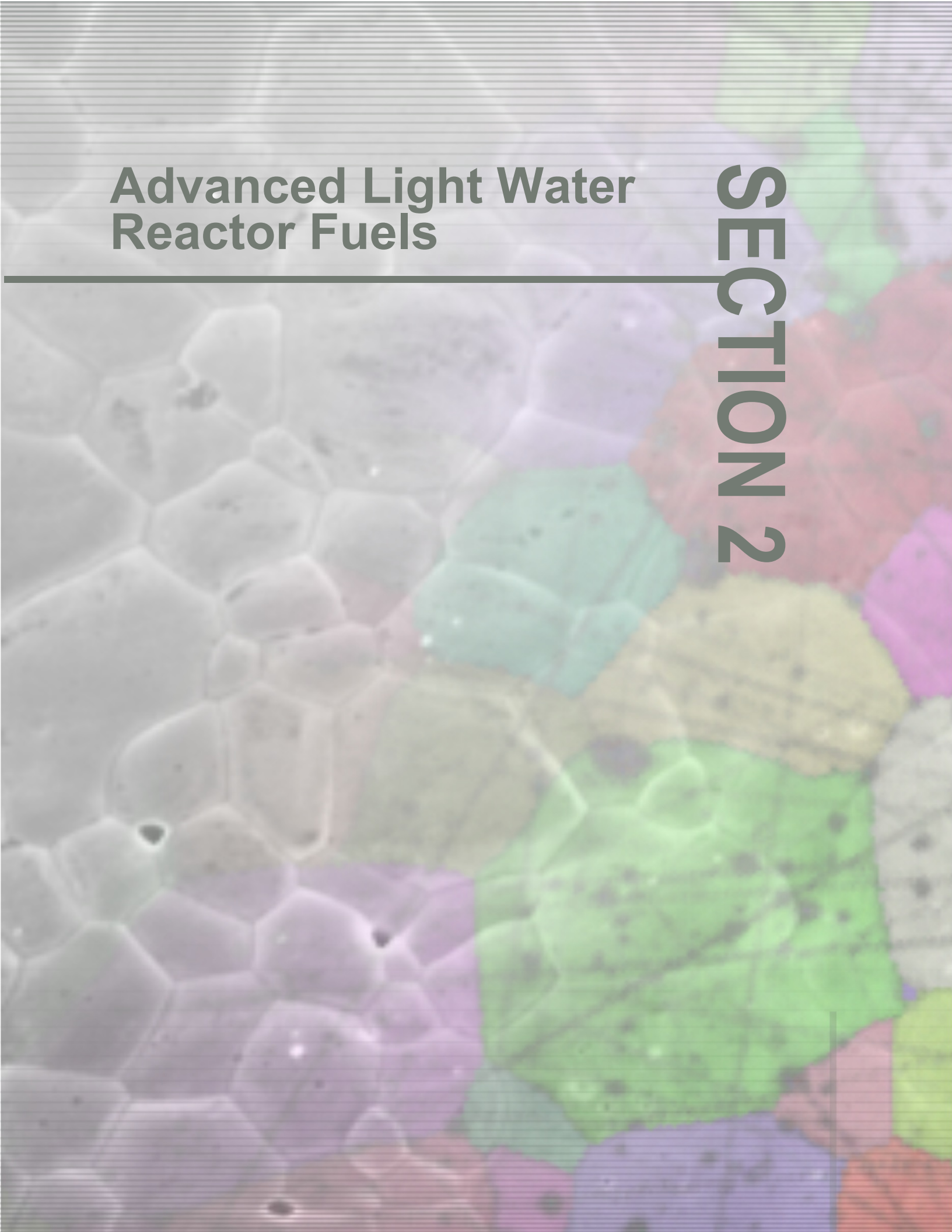

2. ADVANCED LWR FUEL SYSTEMS DEVELOPMENT

Researchers across AFC have been investigating a number of potential fuels and cladding technologies to improve fuel system performance in both normal and accident conditions. Significant progress has been made on establishing oxidation, corrosion, and materials property characterization capabilities and techniques that can be used to assess the performance of potential advanced LWR fuel technologies. In addition, AFC has been preparing for the first irradiation of ATF technologies in ATR in FY 2015.

2.1 Analysis

2.1.1 Accident Tolerant Fuels Metrics

S. Bragg-Sitton, Idaho National Laboratory

The overall goal of ATF development is to identify alternative fuel system technologies to further enhance the safety, competitiveness, and economics of commercial nuclear power. The complex multiphysics behavior of LWR nuclear fuel in the integrated reactor system makes defining specific material or design improvements difficult; as such, establishing desirable performance attributes is critical in guiding the design and development of fuels and cladding with enhanced accident tolerance.

Beginning with the collected guidance on qualitative ATF metrics, a proposed technical evaluation approach has been compiled. The proposed technical evaluation methodology will aid in the optimization and down-selection / prioritization of candidate ATF designs. Detailed evaluation of each concept will gauge its ability to meet performance and safety goals relative to the current UO_2 – zirconium alloy system and relative to one another. This ranked evaluation will enable the continued development of the most promising ATF design options given budget and time constraints, with a goal of inserting one (or possibly two) concepts as an lead fuel rod or assembly in a commercial LWR by 2022.

The proposed methodology was officially released March 19, 2014 (FCRD-FUEL-2013-000264; INL/EXT-13-29957). This report has been distributed to DOE-HQ, AFC technical leads, the AFC Industry Advisory Committee, ATF project leads, and to international contacts in France, Japan, Russia and China under the existing bilateral agreements with these countries. Comments on the proposed evaluation approach are encouraged and will be incorporated into a revised document at a later date.

A summary paper on ATF metrics was presented at the 2014 Water Reactor Fuel Performance Meeting / Top Fuel 2014 in Sendai, Japan. Recognizing that significant changes to the nuclear industry in one country will impact the nuclear plants around the world, presentation of the methodology in an international venue will aid in collecting feedback from the international community with a goal of reaching consensus on the evaluation of enhanced performance fuels worthy of the moniker “accident tolerant.” Preliminary discussions among members of the OECD/NEA Expert Group on ATF Systems Assessment task force suggest that the U.S.-developed metrics document will be used as a starting point for a similar international document.

2.1.2 Industry Advisory Committee

S. Bragg-Sitton, Idaho National Laboratory

The Advanced Light Water Reactor Fuel Industry Advisory Committee (IAC) was established in 2012 to advise AFC's National Technical Director (NTD) on the development and execution of a program focused on advanced fuels for light water reactors. The IAC is comprised of leaders from the commercial light water reactor industry. They represent the major suppliers of nuclear steam supply systems, owners / operators of U.S. nuclear power plants, fuel vendors, and the Electric Power Research Institute. Members are selected on the basis of their technical knowledge of nuclear plant and fuel performance issues as well as their decision-making positions in their respective companies.

The IAC meets monthly via teleconference and in a face-to-face meeting once a year. The IAC met at the Westinghouse Cranberry facility in August 2014. Each IAC member presented ATF development status, potential issues, and the anticipated process that will lead to insertion of a lead fuel rod or assembly in a commercial reactor. The IAC was also asked to provide suggestions for independent experts that could be a part of the planned ATF review committee that will be tasked with prioritizing the various ATF concepts according to the defined metrics. A charter of this committee will be written in FY 2015 to guide the selection of committee members.

2.1.3 Funding Opportunity Announcements

S. Bragg-Sitton, Idaho National Laboratory

Industry-led R&D activities are supported by awards made in 2012 under a DOE Funding Opportunity Announcement. The scope and status of each industry team is provided below. In FY 2014, each research team provided either fuel or cladding samples for irradiation in INL's ATR, completing the FOA Phase 1A scope. Rodlets and capsules were completed and assembled in late summer 2014 for irradiation in 2015. This irradiation test series is referred to as "ATF-1." In September 2014 all three FOA's were selected to continue development of their concepts in Phase 1B, allowing for additional development and testing prior to the planned down-selection / prioritization of ATF concepts in late 2016.

AREVA

The AREVA R&D team is designing both fuel and cladding concepts for enhanced performance and accident tolerance. AREVA provides team leadership and technical guidance related to fuel manufacture and fuel requirements. Additional team members include the University of Florida, developing fuel pellets; the University of Wisconsin and Savannah River National Laboratory, providing cladding coatings; and Duke Energy and the Tennessee Valley Authority, providing utility consultation. Concepts being considered by the AREVA team include:

Modified UO_2 Fuel:

- Chromia doping to reduce fission gas generation, improve load-following characteristics, increase uranium density, improve wash-out characteristics in rod failure, and lock-up cesium in the fuel matrix.
- Embedded SiC fibers to improve thermal heat transfer under normal conditions; this will increase fuel efficiency, improve margin in an accident condition, and lock-up iodine in the fuel matrix.

Modified Zr-alloy Cladding:

- Coatings on existing Zr-alloy cladding to reduce hydrogen pickup, mitigate hydride reorientation in the cladding, and increase coping time during accident conditions.

AREVA ATF-1 rodlets include modified UO_2 fuel fabricated at the University of Florida via Spark Plasma Sintering (SPS) techniques. Fuel is encased standard Zr-alloy cladding for the initial ATR drop-in test.

General Electric Global Research

The GE Global Research and Global Nuclear Fuels team includes the University of Michigan and LANL. The GE team is investigating the replacement of Zr-alloy cladding with advanced steels, such as FeCrAl alloys (APMT), which offer a number of benefits in beyond design-basis accident conditions. Improved properties under normal conditions may provide sufficient benefit to mitigate the increased neutron absorption characteristics of these materials.

Samples of commercial and experimental alloys have been successfully tested for up to 48 h in 100% superheated steam from 600°C to 1475°C. Results to date indicate that the best candidate new alloys, including APMT and Alloy 33, have several orders of magnitude improvement over the current Zr-based alloys in reaction kinetics with steam (Figure 4). These advanced steels have also been tested to demonstrate superior mechanical properties under both normal operating conditions and accident conditions. Ferritic alloys are highly resistant to irradiation damage and to environmentally assisted cracking under normal operating conditions. These materials have been machined into thin walled tubes and end caps have been sealed using orbital weld techniques. Both APMT and Alloy 33 rodlets have been fabricated and assembled.

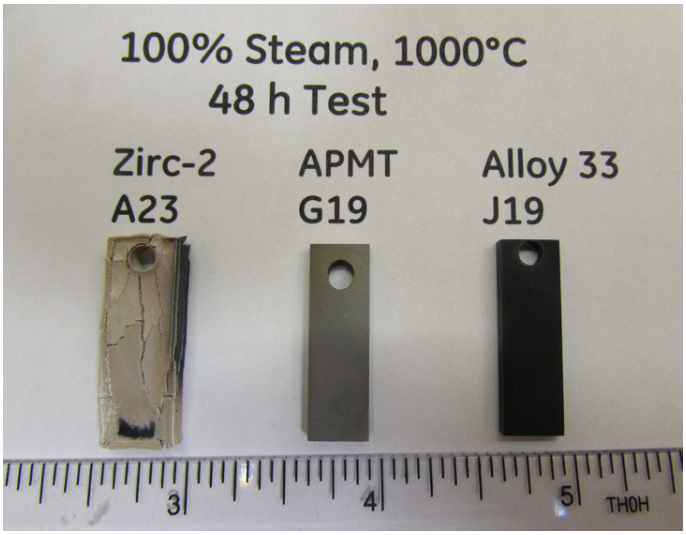

Figure 4. GE Sample alloys following 48 h exposure to 100% steam at 1000°C.

Westinghouse

The Westinghouse Electric Company LLC consortium includes General Atomics (GA), Edison Welding Institute (EWI), the University of Wisconsin (UW), LANL, INL, Texas A&M University (TAMU), the Massachusetts Institute of Technology (MIT) and Southern Nuclear Operating Company (SNOC). Westinghouse has laid out a full development and testing program, and the expected economics of the various options has been determined.

Westinghouse provides team leadership and fuel concept development. Cladding development is provided by GA for SiC-based concepts, while EWI is developing hot-spray coatings for Zr-alloy cladding and UW is developing cold-spray coatings for Zr-alloy cladding (Ti_2AlC and NanoSteel®). Fuel development is conducted by INL for U_3Si_2, LANL for UN, and TAMU for waterproofed UN (using U_3Si_2 additives).

MIT provides steam oxidation, quench and preliminary irradiation testing of cladding candidates. A customer perspective on ATF licensing and economics is provided by the utility partner SNOC.

Fuel development results for both U_3Si_2 and waterproofed UN using U_3Si_2 indicate the feasibility of manufacture of both fuel types. U_3Si_2 has been successfully manufactured into pellets at 97.8% theoretical density (see Figure 5). This fuel offers a 17% increase in ^{235}U loading (at equivalent enrichment) and a five-fold increase in thermal conductivity relative to standard UO_2 fuel. Waterproofed UN would offer up to 35% increase in ^{235}U loading and 10 times the thermal conductivity of UO_2.

Westinghouse cladding development for coated Zr-based alloys has not produced a significant increase in accident tolerance relative to standard cladding to date. These trials provide input to potential coating improvements and will guide future research. Samples of SiC-based cladding have been successfully manufactured and tested in an autoclave at accelerated conditions (425°C). High-temperature (greater than 1200°C) steam tests and irradiation in the INL ATR will follow for preferred cladding concepts. Westinghouse rodlets prepared for ATF-1 include U_3Si_2 fuel in standard UO_2 cladding.

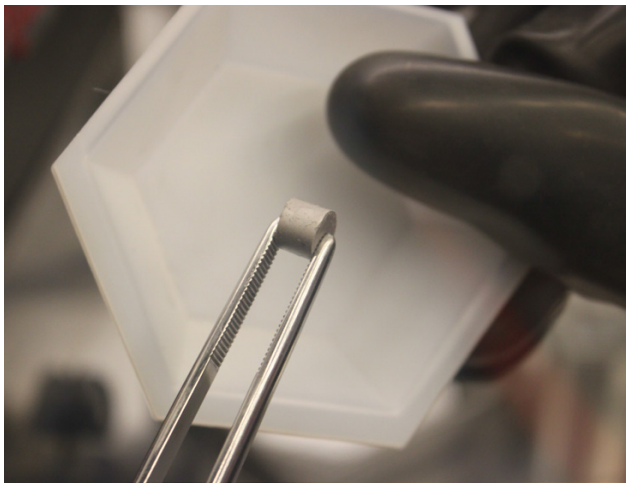

Figure 5. Westinghouse U3Si2 pellet sintered at INL using finely ground powder.

2.1.4 Integrated Research Projects

S. Bragg-Sitton, Idaho National Laboratory

AFC supports two NEUP IRPs for development of accident tolerant cladding. Although these concepts are not yet ready for irradiation testing in ATR, they are undergoing significant out-of-pile testing and testing via ion irradiation. A third related IRP team is developing an Accident Tolerant Reactor design, which would likely utilize ATF. This project is supported under the DOE-NE Nuclear Reactor Technologies office (NE-7) and is led by the Georgia Institute of Technology.

University of Illinois

The University of Illinois IRP team, which includes partners at the University of Michigan, the University of Florida, INL, and ATI Wah Chang, is investigating two solution pathways toward improved ATF cladding. An additional partner, the University of Manchester, is funded by the Research Councils U.K. Energy Program. Both pathways are based on the modification of monolithic Zircaloy cladding to inhibit the rapid oxidation that occurs during elevated-temperature steam exposure and involve either a coating or a low-concentration bulk additive.

A combination of experimental and computation protocols are being employed to design and test modified Zircaloy cladding with respect to corrosion and accelerated oxide growth. Cladding performance evaluation are incorporated into a reactor system modeling effort of fuel performance, neutronics, and thermal hydraulics, thereby providing a holistic approach to accident tolerant nuclear fuel.

Two significant achievements to date are the irradiation of a set of coated samples by high-energy protons to mimic fast neutron damage and the demonstration of delayed oxidation induced by a coating during 700°C steam exposure. Figure 6 shows the coated samples mounted prior to proton irradiation. The proton irradiation was performed at the University of Michigan to 2.3 displacements per atom (dpa). The samples were Zircaloy-2 with FeCrAl coatings of varying composition, ranging from 4000 to 7000 Å thick. These samples will be used in four-point bending tests, high-temperature steam exposure, and autoclave testing. Similar films are planned for irradiation in INL's ATR to similar dpa values; a comparison of proton and neutron irradiation will be useful.

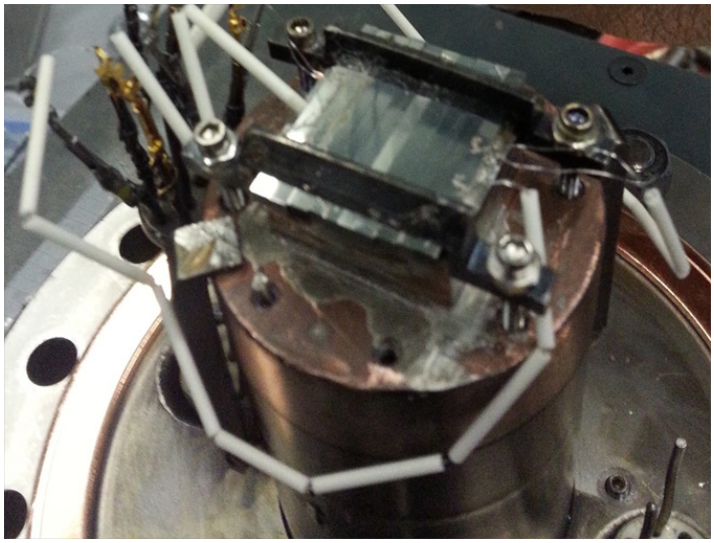

Figure 6. At the University of Michigan, Zircaloy-2 samples with FeCrAl coatings of varying composition prior to 1-MeV proton irradiation. Samples were irradiated to 2.3 dpa at 360 °C.

Oxidation mass gain versus time for uncoated polished Zircaloy-2, for Zircaloy-2–4 (FeCrAl:54/28/18), and for Zircaloy-2–7 (FeCrAl:61/5/34) specimens during 700 °C steam exposure are shown in Figure 7. The delayed onset of oxidation in the Al-rich specimen (Zircaloy-2–7) is clear from the mass gain measured as a function of time, which shows an oxidation delay of approximately 180 minutes.

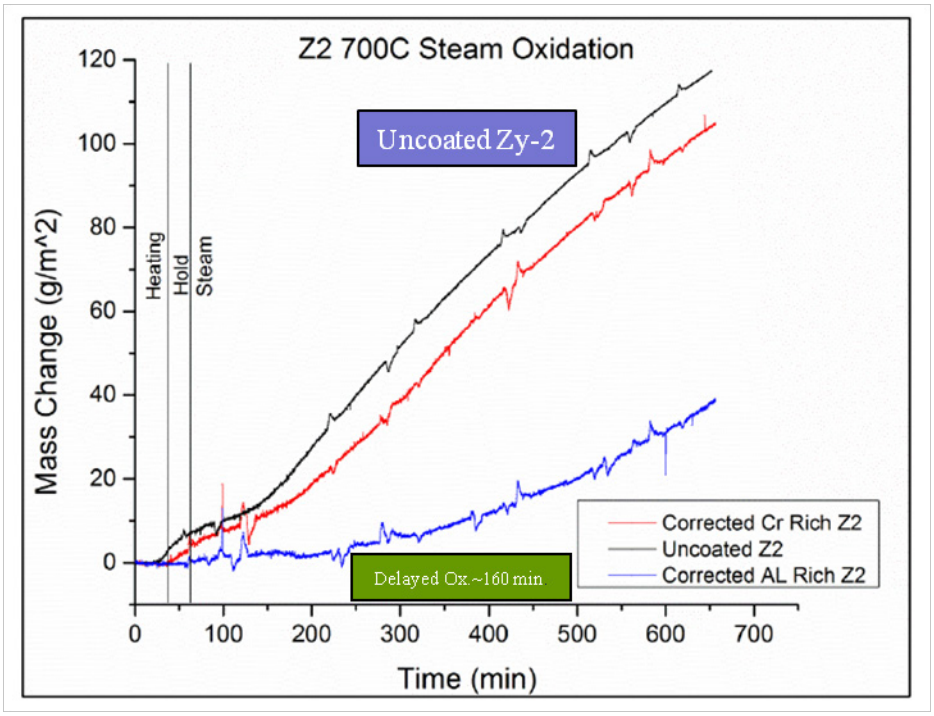

Figure 7. Weight gain measurements in 700 °C steam for two approximately 4000-Å-thick FeCrAl coatings (red and blue lines) and uncoated Zircaloy-2 (black line); one FeCrAl coating delayed oxidation in steam by about 180 minutes.

University of Tennessee

The University of Tennessee, along with Pennsylvania State University, the University of Colorado, the University of Michigan, LANL, Westinghouse Electric Company, Oxford University, the University of Manchester, the University of Sheffield, the University of Huddersfield, and the Australian Nuclear Science and Technology Organization, is working to develop surface modifications of Zr-alloy cladding by applying ceramic coatings. Ceramic Coatings for Clad (The C3 Project) involves coating zirconium alloys with various architectures of ceramic coatings, including nitrides, oxides, and carbides, using various coating techniques such as cathodic arc vapor deposition, magnetron sputtering, thermal spray, pulsed liquid injection, and ion beam–assisted vapor deposition.

Ceramic-coated cladding is expected to improve performance as compared to conventional Zr-alloy cladding in the following respects:

- During normal service, the ceramic coating should decrease cladding oxidation and hydrogen pickup (the latter leads to hydriding and embrittlement).
- During a reactor transient, such as a loss of coolant accident (LOCA), the ceramic coating should significantly delay oxidation of the Zr-alloy cladding, thus reducing the amount of hydrogen generated and the oxygen ingress into the cladding.

Several generations of ceramic-coated Zr-alloy samples have been fabricated. Many of these samples have been corrosion tested in a water-filled autoclave at 360°C for 3 to 14 days, with some samples corrosion tested at higher temperatures (> 700°C). Thus far, the TiAlN coatings have shown the smallest weight gains, suggesting they are the least susceptible to water-based corrosion. Experiments focusing on better ceramic/metal interface adhesion have also been performed. These experiments have focused on how best to prepare the Zr-alloy surfaces for coating deposition. Numerous processing variables were also varied to study the leaching of Al out of the TiAlN samples during corrosion testing. In recent sample

iterations, multilayer coatings that effectively stopped the Al leaching problem were produced. Computational modeling studies of ceramic coated fuel performance under normal and off-normal operating conditions have also been conducted.

Work is under way to develop a better understanding of this improved corrosion behavior for ceramic-coated cladding, and higher-temperature corrosion experiments, which better simulate accident conditions, are currently in progress. Samples are tested at 300-360ₒC at saturation pressure in an autoclave and are tested in 1500 psi steam at 400, 415, 427 and 500ₒC. Figure 8 shows photographs of coated Zirlo cladding material after 14-day autoclave exposure to a 360°C (680°F) aqueous environment. Details of each coating are provided in Table 1.

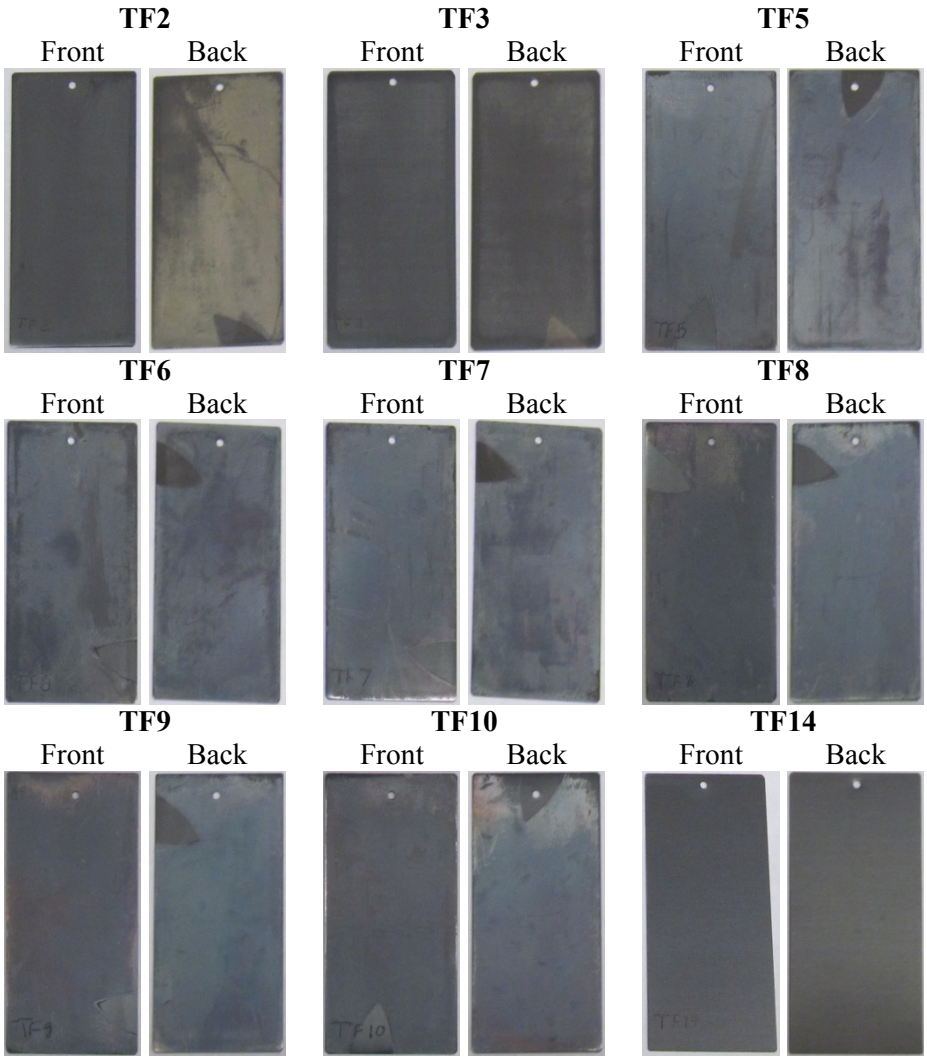

Figure 8. Photographs of Zirlo after 14-day autoclave in 680°F aqueous environment.

Table 1. Sample weight gains after 14-day autoclave in 680°F aqueous environment.

Sample ID	Description	Weight Gain After 3 days [g/dm^2]	Weight Gain After 14 days [g/dm^2]
TF2	Ti_2AlC / TiC /Zirlo	13.50	19.95
TF3	Ti_2AlC / Ti_2C /Zirlo	6.27	12.61
TF5	Ti_2AlC / Ti /Zirlo	22.94	29.85
TF6	Ti_2AlC / Ti /Zirlo	20.74	27.42
TF7	Ti_2AlC / Ti /Zirlo	22.53	29.48
TF8	Ti_2AlC / Zirlo	20.43	27.35
TF9	Ti_2AlC / Zirlo	18.16	25.73
TF10	Ti_2AlC / Zirlo	19.94	26.62
TF14	Zirlo (control)	10.46	17.26

2.1.5 Screening of Accident Tolerant Fuel Candidate Systems: Reactor Performance and Safety Analyses

N. R. Brown, L. Cheng, A. Cuadra, M. Todosow, Brookhaven National Laboratory

An assessment of the viability and potential attractiveness of advanced nuclear fuels must include consideration of how proposed concepts will impact the nominal reactor performance and safety characteristics of current commercial LWRs versus the reference UO_2-Zr system. In FY 2014 Brookhaven National Laboratory (BNL) conducted screening of several uranium nitride composite fuel concepts proposed by LANL, Westinghouse, and others, where the uranium nitride is "shielded" from water by one or more secondary phases. The BNL assessments were performed in support of the ATF Performance Metrics, namely: "*the assessment must address how implementation of the concept will affect reactor performance and safety characteristics.*" This highlight presents assembly-level screening calculations for UN-U_3Si_5 fuel concepts paired with several potential advanced cladding options. In addition, selected equilibrium core analysis results with thermal feedback are compared for UO_2 and UN-U_3Si_2-UB_4 fuels. In this case, the UB_4 content as a tertiary phase has been optimized to match the performance of an Integral Fuel Burnable Absorber (IFBA). We also present results from a transient analysis of a large break Loss-of-Coolant Accident (LB-LOCA) for UO_2 and UN-U_3Si_2-UB_4.

Analysis of "Drop-In" Fuel for UN/U_3Si_5 with Fe-Based Cladding

Several advanced iron-based claddings are under consideration due to increased oxidation resistance versus zirconium-based cladding. We performed assembly-level neutronic analysis for a 17 x 17 PWR assembly with 4.9% enriched ^{235}U to assess the impact of these advanced fuel and cladding materials on reactivity, safety coefficients, and cycle length/burn-up. The focus of this highlight is two commercial alloys: Kanthal AF and Kanthal APMT. The cladding thickness for the predominantly iron-based cladding materials was assumed to be 0.0419 cm versus 0.0572 cm for zirconium-based cladding. The fuel pellet radius was increased and the fuel-clad gap thickness was maintained versus zirconium cladding. Analyses showed a reactivity penalty due to the proposed advanced claddings. In terms of cycle length, the reactivity penalty was compensated via the higher heavy metal loading and increased fuel pellet thickness of the UN-U_3Si_5 fuels, as shown in Table 2. Relative neutron absorption rates in various existing or proposed cladding constituent elements are shown in Figure 9. The element with the highest cumulative absorption rate is Mo, followed by Ni, Cr, Fe, Zr, and Al. The important take-away message

of this study is that, if the fuels are feasible from the perspective of fabricability and performance, high density UN-U_3Si_5 fuels can overcome the reactivity penalty of several proposed cladding materials and are able to closely match UO_2-Zr cycle lengths.

Table 2. Three-batch cycle length and discharge burn-up for various advanced fuel/cladding options at 4.9%-enriched ^{235}U.

Fuel/Clad	Primary phase content	Secondary phase content	Tertiary phase content	Cycle length (EFPD)	Discharge burn-up (GWd/t)
UO_2 – Zr	95.00%	0.00%	0%	532.9	61.6
UN - U_3Si_5 - Zr	50.00%	40.00%	0%	566.5	61.6
UN - U_3Si_5 - UB_2 - Zr	55.00%	34.50%	0.50%	524.4	55.2
UN - U_3Si_5 - AF	55.00%	35.00%	0%	533.1	52.2
UN - U_3Si_5 - APMT	55.00%	35.00%	0%	526.0	51.5
UN - U_3Si_5 - UB_2 - APMT	75.00%	14.50%	0.50%	510.5	44.5

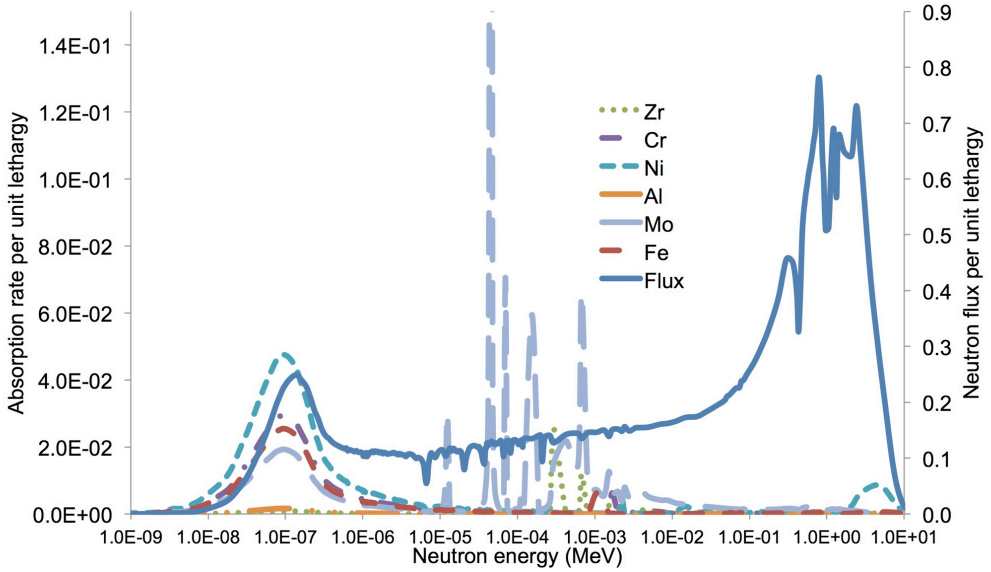

Figure 9. Relative neutron absorption rates in proposed cladding constituent elements.

Equilibrium Core Analysis for UN-U_3Si_2-UB_4

This example shows one role of core analysis with thermal feedback in the analysis of proposed candidate fuel/cladding combinations. This highlight explores a new proposed composite (UN-U_3Si_2-UB_4) with a tertiary component (UB_4) that has been tuned to match the performance of an assembly with 112 IFBA coated fuel rods. This type of configuration is relevant to a recent Westinghouse patent (7,139,360 B2). Several cases were compared for a 17 x 17 assembly and an AP1000-like core: a nominal UO_2-Zr case with 112 IFBA coated rods, a UN/U_3Si_2-Zr case with 112 IFBA coated rods, a UN/U_3Si_2/UB_4-Zr case with 5 concentric depletion zones ("rings") per fuel pin. In the UN-U_3Si_2-UB_4 case the same mass of natural boron from the 112 IFBA coatings is conserved, but is dispersed throughout all 264 of the fuel pins in the assembly as UB_4. The PARCS regulatory-grade core simulator was utilized in a full three-dimensional model of the reactor core including thermal-hydraulic/temperature reactivity feedback. Equilibrium cycle fuel shuffling was performed with the fresh assemblies located near the periphery of the core and the once- and twice-burned assemblies located throughout the central core region. Radial power peaking in the core at end of equilibrium Cycle (EOC) is shown in Figure 10 for UO_2-Zr and

$UN/U_3Si_2/UB_4$. Assembly-average fuel temperatures are shown in Figure 11. This analysis shows that this advanced composite fuel, even with burnable absorber integrated into the pin as a tertiary phase, can closely match the core performance of a nominal UO_2-Zr fuel. In addition, the fuel temperatures will be much lower due to the enhanced thermal properties of the fuel. These results demonstrate how analyses such as these can provide information on the potential for changes to margins for a given candidate fuel system.

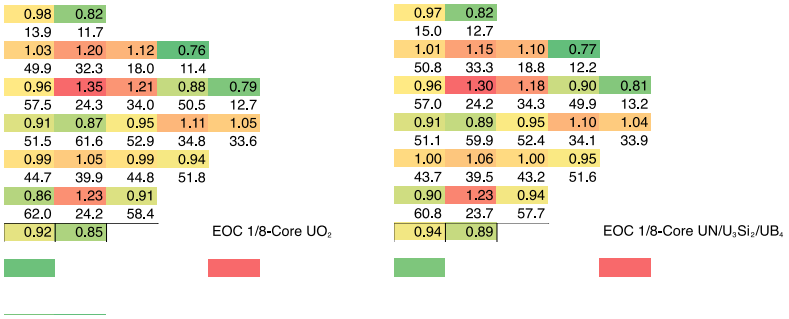

Figure 10. Radial assembly power peaking at EOC for an AP1000-like reactor core.

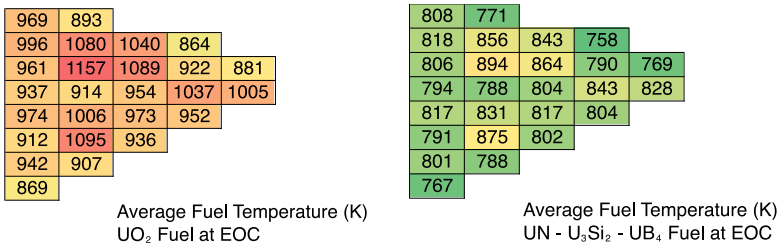

Figure 11. Assembly average fuel temperatures for an AP1000-like equilibrium reactor core at EOC.

Transient Analysis of a Large Break LOCA Event

This section demonstrates how transient safety analyses can provide information on margins and estimated time to a safety limit. The focus of this example is a prediction of how $UN/U_3Si_2/UB_4$ composite fuel will perform in a Large Break (LB)-LOCA event coincident with loss-of-offsite power. This primarily thermal hydraulic transient is evaluated using a detailed TRACE plant model based on a Westinghouse PWR with point-kinetics utilized for the reactor neutronics. The fuel response in the event depends on the thermophysical properties of the fuel, the fuel/clad/gap geometry and gap conductance, the system thermal hydraulics, and the neutronic feedback. The LB-LOCA is primarily a thermal hydraulic transient, and the initiating break and subsequent Emergency Core Cooling System (ECCS) flow dictate the peak clad temperature (PCT) in the event. A large break in the cold leg of primary loop 1 was simulated with a loss of off-site power coincident with the reactor trip. For this fast transient the thermal-hydraulics and fuel thermal properties dictate the overall response more so than the reactivity feedback. Figure 12 shows the PCT and fuel centerline temperature for the two fuel types. The PCT for the nitride fuel is ~30 K lower than the oxide fuel. Initially the nitride is much cooler than the UO_2-Zr fuel, but the temperature difference decreases during the accident event cascade. Although the heat transfer properties of the $UN\text{-}U_3Si_2$ fuel are improved, the decay heat of the reactor and the heat removal capability of the ECCS are key boundary conditions for the transient fuel temperature response.

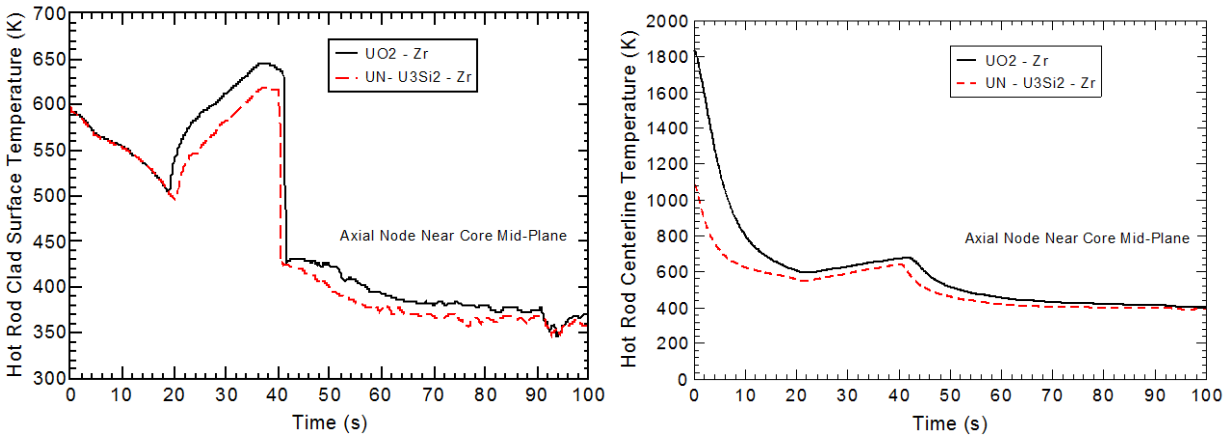

Figure 12. Hot rod clad surface temperature (left) and hot rod centerline temperature for LB-LOCA event in UO_2 and UN-U_3Si_2 fuelled PWRs.

Publications

1. N. R. Brown, A. Aronson, M. Todosow, R. Brito, K. McClellan, "Neutronic performance of uranium nitride composite fuels in a PWR," *Nuclear Engineering and Design,* 275, 2014, 393-407.
2. N. R. Brown, M. Todosow, K. J. McClellan, "Uranium nitride composite fuels in a pressurized water reactor: exploration of multi-batch cycle length and UB4 admixture for reactivity control," *Proceedings of PHYSOR 2014 – The Role of Reactor Physics Toward a Sustainable Future*, Kyoto, Japan September 28 – October 3, 2014.

2.1.6 Thermodynamic Assessment of Accident Tolerant Composite Fuel Candidate Systems

T. Besmann and S. Voit, Oak Ridge National Laboratory

Uranium-based advanced ceramic composite fuel systems are proposed that will improve the normal and off-normal performance while delivering acceptable neutronic characteristics and maintaining economic competitiveness relative to the commercial UO_2. Candidate ceramic composite fuel compositions may be UO_2 with a second phase addition or a non-oxide ceramic composite. In FY 2014, an initial thermodynamic assessment was performed on proposed ceramic composite fuel compositions to determine phase compatibility. Candidate binary fuel systems were chosen and compounds within the candidate systems were identified. Selected binary compounds were paired together and a thermodynamic assessment was performed to determine the stability of the phase assemblages. The following temperature-dependent phase stabilities were computed for proposed two-phase composites, with 10 mol% second phase. Each two-phase composite is labeled with either a "✓" indicating that the combination passed the initial thermodynamic screening or an "✗" if it failed.

- $UN - UB_{4/2}$ ✓
- $UN - U_3Si_2$ ✓
- $UN - U_3Si_5$ ✓
- $U_3Si_5 - UB_{4/2}$ ✗
- $UO_{2\pm x} - UB_{4/2}$ ✓
- $U_3Si_2 - UB_{4/2}$ ✗
- $UN\text{-}10\%U_3Si_5\text{-}10\%UB_{4/2}$ ✓

Figure 13 shows a computed phase diagram for the UN-U_3Si_2 system up to 2500°C. The phase assemblage for UN-10%U_3Si_2 shows some USi formation between 300°-1575°C, although the amount of USi is several orders of magnitude less than the primary phases and thus can be considered a viable composite fuel option from a thermodynamic standpoint. A preliminary assessment of possible routes to synthesize feedstock materials for the ceramic composite fuels from uranium hexafluoride (UF_6) was also completed. This initial evaluation examines the thermodynamic possibility of combining UF_6 with a reactant to directly form various uranium borides or uranium silicides. The thermodynamic calculations for synthesis reactions over a wide temperature range produced the following results:

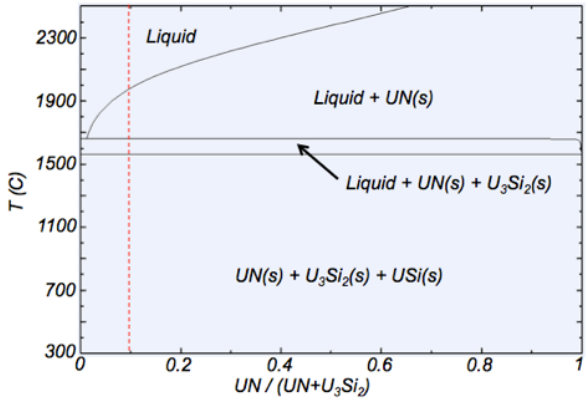

Figure 13. Computed pseudo-binary phase diagram of the UN-U3Si2 system.

- Uranium silicides cannot be prepared from uranium fluorides plus silicon.
- UF_6 or UF_4 will react with boron to form UB_{12}.
- UF_6 or UF_4 will not form the lower borides UB_2 or UB_4.
- BF_3 will not react with UF_6 or UF_4,; thus, borides cannot be formed from BF_3.

2.1.7 Reactor Physics and Severe Accident Analysis of Enhanced Accident Tolerance Fuels in LWRs

J.J. Powers, K.R. Robb, A. Worrall, K.A. Terrani, L.J. Ott, Oak Ridge National Laboratory; N.M. George, G.I. Maldonado, University of Tennessee-Knoxville

An assessment and eventual down-selection/prioritization of candidate enhanced ATF technologies requires definition of metrics to evaluate and compare the candidates as well as analysis of the ATF candidates during normal operations, transients including design basis accidents (DBAs), and severe accident (SA) conditions covering beyond design basis accident (BDBA) scenarios. These analyses include reactor physics, thermal, and systems aspects and approaches.

Several efforts started in FY 2013 continued into FY 2014. These efforts include:

- ORNL provided analysis support to the multi-laboratory effort that culminated in an FY 2014 report defining metrics and an approach that will be used for evaluating ATF concepts, as discussed in section 3.1.1. This evaluation process will include expert solicitation to assess candidate ATF technologies and to establish a prioritization across concepts.
- A preliminary assessment of potential ATF impact on thermal-hydraulic and systems performance during normal operation, DBAs, and BDBAs was performed. This included assessing the impact that changing specific fuel properties (e.g., thermal conductivity) might have on plant response and fuel conditions. Severe accident analyses investigating the impact of ATF concepts on boiling water reactor (BWR) severe accident scenarios continue to evolve through a combination of parametric studies and modeling of specific ATF concepts in using MELCOR.
- Some efforts on fully ceramic microencapsulated (FCM) fuel, which employs tri-structural isotropic (TRISO) coated fuel particles in a silicon carbide (SiC) matrix, carried into FY 2014.

Work on ATF cladding at ORNL focused on an assessment of reactor physics impacts of candidate iron-based and SiC-based cladding materials for pressurized water reactors (PWRs) during FY 2014. Specific options included austenitic stainless steel type 310 (310SS); two ferritic alloys, a generic FeCrAl and an advanced ferritic alloy (APMT™); and a SiC/SiC composite concept. These offer several potential benefits (e.g., reduced oxidation rates) compared with the Zircaloy-4 baseline cladding material but also introduce challenges such as increased neutron absorption in iron-based materials (see Figure 14). Pin-cell depletion calculations were performed and core-level impacts were assessed using batch-weighted power sharing and lifetime-averaged end of cycle reactivity from a reference Westinghouse 17×17 PWR assembly. Analyses also include impacts on neutron spectra, reactivity coefficients, and plutonium breeding. Figure 15 shows several combinations of cladding thickness and fuel enrichment identified that would match the fuel cycle length of the traditional Zircaloy-clad fuel. An economic assessment estimated variations in fuel pellet costs for the cladding material options based on relative UO_2 mass and enrichment in each design. The results indicate FeCrAl and SiC appear feasible as PWR clads from a neutronics perspective.

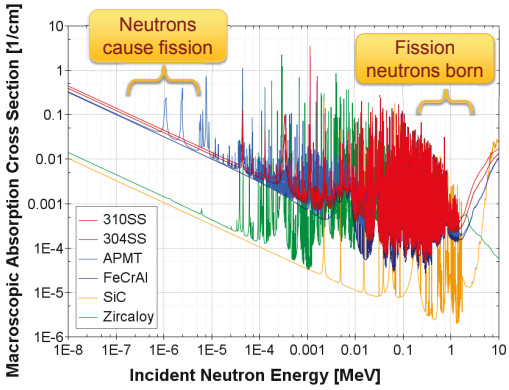

Figure 14. Macroscopic neutron absorption cross sections for cladding materials being investigate. (Note: the APMT composition has since changed)

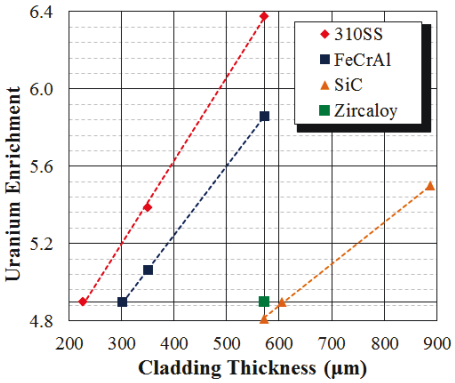

Figure 15. Fuel parameters required to match PWR cycle length of reference Zircaloy case.

Publications

1. S. Bragg-Sitton, B. Merrill, M. Teague, L. Ott, K. Robb, M. Farmer, M. Billone, R. Montgomery, C. Stanek, M. Todosow, and N. Brown, *Advanced Fuels Campaign Light Water Reactor Accident Tolerant Fuel Performance Metrics*, INL/EXT-13-29957 and FCRD-FUEL-2013-000264, Idaho National Laboratory, February 2014.
2. L. J. Ott, K. R. Robb, and D. Wang, "Preliminary assessment of accident-tolerant fuels on LWR performance during normal operation and under DB and BDB accident conditions," *Journal of Nuclear Materials,* 448, 2014, 520–533.
3. M. T. Farmer, L. Leibowitz, K. A. Terrani, and K. R. Robb, "Scoping Assessments of ATF Impact on Late Stage Accident Progression Including Molten Core-Concrete Interaction," *Journal of Nuclear Materials,* 448, 2014, 534–540.
4. J. J. Powers, N. M. George, A. Worrall, and K. A. Terrani, "Reactor Physics Assessment of Alternate Cladding Materials," *Transactions of the 2014 Water Reactor Fuel Performance Meeting / Top Fuel / LWR Fuel Performance Meeting (WRFPM2014/TopFuel 2014),* Sendai, Japan, September 14–17, 2014.

5. N. M. George, I. Maldonado, K. Terrani, A. Godfrey, J. Gehin, and J. Powers, "Neutronics Studies of Uranium-bearing Fully Ceramic Microencapsulated Fuel for Pressurized Water Reactors," *Nuclear Technology*, in press, 2014.
6. N. M. George, K.A. Terrani, J. J. Powers, A. Worrall, and G.I. Maldonado, "Neutronic Analysis of Candidate Accident-Tolerant Cladding Concepts in Pressurized Water Reactors," *Annals of Nuclear Energy*, in press, 2014.

2.1.8 Accident Tolerant and Neutronically Favorable LWR Cladding

J. Galloway and C. Unal, Los Alamos National Laboratory

The viability of stainless steel-based cladding in traditional LWRs was assessed at LANL using various computational tools. Neutronic simulations of APMT cladding and Zircaloy cladding were performed using *Monteburns*, an MCNP-based burnup code. A $1/8^{th}$ symmetric simulation of a 17x17 PWR assembly was employed. Simulating the assembly captures the correct neutron moderation by accounting for the additional water in the guide and instrumentation tubes while also accounting for the correct amount of cladding, with the associated neutronic penalty, in both the fuel rods and guide/instrumentation tubes.

Cladding thickness was varied from the full thickness of standard Zircaloy cladding (0.55-mm) to a fraction of 0.25 of Zircaloy thickness (0.1375-mm). Intermittent thicknesses at fractions of 0.75 (0.4125-mm) and 0.5 (0.275-mm) were also included. The goal of the analysis was to determine the thickness of stainless steel-based cladding necessary to replace Zircaloy without negative reactivity impact. The most robust definition of "no negative reactivity impact" is to match reactivity on a burnup basis. When the clad is thinned, the decreased clad thickness is added to the fuel, increasing the fuel pellet outer diameter, thus increasing the total weight of Uranium in the bundle. To match reactivity on a burnup basis, the cycle length needs to be increased or the power increased; in this study the cycle length was increased to match burnup. Alternatively, effective full power days (EFPD) could be selected as the target for matching reactivity performance. The downside to matching EFPD is that the fuel will have a lower discharge exposure since more fuel is present, which is undesirable with respect to fuel cycle economics.

In this study two interpretations, a three and four batch core, were assumed. The three batch core assumes discharge exposures of 25, 45 and 60 GWd/MTU for fresh, once and twice burned fuels. The four batch core uses the same first three discharge exposures but extends the cycle length with a fourth discharge exposure of 70 GWd/MTU. Weighting factors were then applied to each batch for both of the core configurations. Figure 16 shows the reactivity results for 3%, and 4.95% enrichment, respectively, with each plot containing 1.0, 0.75, 0.5 and 0.25 fractional thickness, with respect to Zircaloy. First, it is clear in the 1.0 plot that the APMT steel has a much higher absorption cross-section than Zircaloy. Additionally, even at 0.25 of Zircaloy thickness APMT still does not achieve early life reactivity equivalent to Zircaloy; however, given enough burnup accumulation, both the 0.25 and 0.5 cases eventually "catch up" to Zircaloy reactivity. Second, it is important to notice the shift with increasing Uranium enrichment. At lower enrichment the flux required to achieve power increases much more than at higher enrichments. This increased flux provides a larger benefit to APMT-based claddings as more ^{238}U is converted into highly reactive Pu isotopes, thus causing a greater reactivity recovery late in life. This trend was observed continually from 3.0% up to 5.5% initial enrichment; the lower the enrichment, the "better" APMT performed relative to Zircaloy.

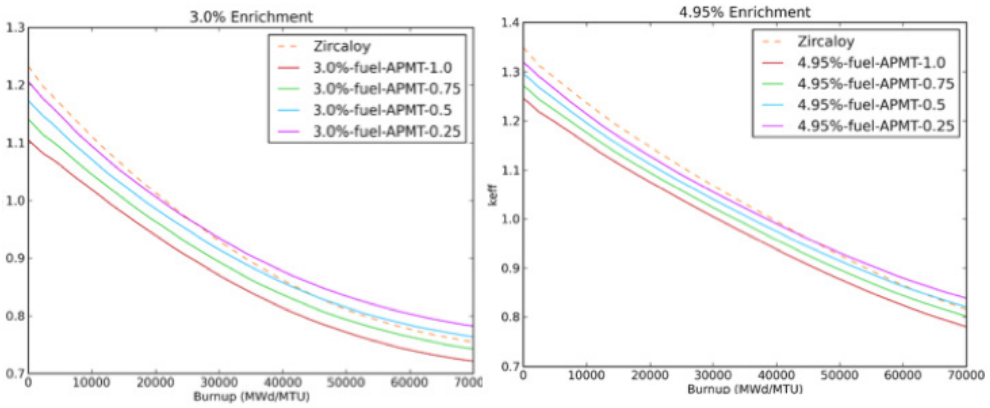

Figure 16. Enrichment Reactivity vs Burnup (MWd/MTU)

With respect to early life reactivity, Zircaloy performs much better than any of the APMT geometries studied. However, a nuclear reactor is fueled with a mix of fresh, once, twice and sometimes thrice burned bundles. Thus, the aforementioned weighting scheme to estimate reactivity for the three and four batch cores was performed.

Fuel performance simulations were performed for both the baseline Zircaloy simulations at full clad width and the subsequent 0.75, 0.5 and 0.25 fractions. BISON, a fuel performance code developed at INL, was used for the fuel performance calculations. Full-length simulations covering the full 12 feet of active fuel height, including a fission gas plenum above active fuel and modeled as 308 fuel pellets, were performed in 2D-RZ geometry.

Table 3 summarizes the results for a fixed geometry across all initial enrichments. The trend noted in the reactivity plots is clearly observed here. As initial ^{235}U enrichment increases the relative performance of APMT-based fuel decreases, by nearly a factor of three for the 3-batch core from 3.0%-5.5%. Additionally the reactivity gain of adopting a higher discharge burnup, four batch core is observed in the decreased reactivity penalty observed in the four batch core.

A second analysis shown in Table 3 (right side) gives the performance of APMT based fuel compared to Zircaloy for 4.5%, and 4.95% enrichment at all four fractions. The penalty for using an unadjusted Zircaloy thickness is quite significant, 5-6% cycle penalty if there is no thickness reduction. While there is interplay between cladding thickness and initial enrichment in determining the "break even" point where APMT based fuel has equal performance to Zircaloy based fuel, determining the thickness in the ~4.5% enrichment range proves fairly consistent with current fuel loadings. Highlighted in yellow are the two cases that illustrate approximate break-even points. Assuming a 3-batch core, the required thickness reduction is ~0.25 of the baseline thickness. Again the adoption of a 4-batch higher burnup core would be of benefit if the performance characteristics of APMT steel clad allow for it.

Table 3. Reactivity Comparison-Burnup Basis

APMT 0.5-Zircaloy

^{235}U-Fraction	3-Batch	4-Batch
3.0%-0.5	-0.750%	-0.322%
4.0%-0.5	-1.419%	-0.875%
4.5%-0.5	-1.696%	-1.160%
4.95%-0.5	-1.914%	-1.393%
5.25%-0.5	-2.004%	-1.520%
5.5%-0.5	-2.112%	-1.651%

APMT-Zircaloy

^{235}U-Fraction	3-Batch	4-Batch
4.5%-1.0	-5.708%	-5.417%
4.5%-0.75	-3.617%	-3.197%
4.5%-0.5	-1.696%	-1.160%
4.5%-0.25	***0.049%***	***0.713%***
4.95%-1.0	-5.626%	-5.363%
4.95%-0.75	-3.683%	-3.282%
4.95%-0.5	-1.914%	-1.393%
4.95%-0.25	***-0.308%***	***0.334%***

When simulating APMT, unirradiated properties are known; however, irradiation properties are not yet characterized. The known properties of APMT were added to BISON for the performance calculations. Regarding irradiation properties, HT9 steel has been used in operating reactors and some irradiation data exists. In the absence of APMT irradiation data, HT9 steel properties were used since both are iron-based stainless steels, although the compositions differ.

Full-length simulations were performed for two cases, the baseline Zircaloy case and a 0.5 fraction APMT case. Both of these simulations were run in 2D-RZ geometry, with symmetry employed about rod centerline. The selected time dependent power profile corresponded with the lower initial power but higher end of life (55% peak) power, which was expected to cause higher stresses at end of life, especially in the APMT fuel. The axial power profile was obtained from the neutronic bundle simulation with allowed neutron leakage at the fuel ends. Power peaking factors of 0.32 in the top and bottom six inches, 0.86 in the next six inches then on the order of 1.0-1.1 for internal nodes were used. In most cases the results are shown in a severely compressed visual, with the z-axis being scaled by 0.005 to fit all the results in one plot. Additional pin level results are also shown for representative fuel pins. Initial fuel pellets are all geometrically identical with chamfer and dishing representative of PWR pellet manufacturing; the fuel pellet geometry is shown in Figure 17 with the true aspect ratio.

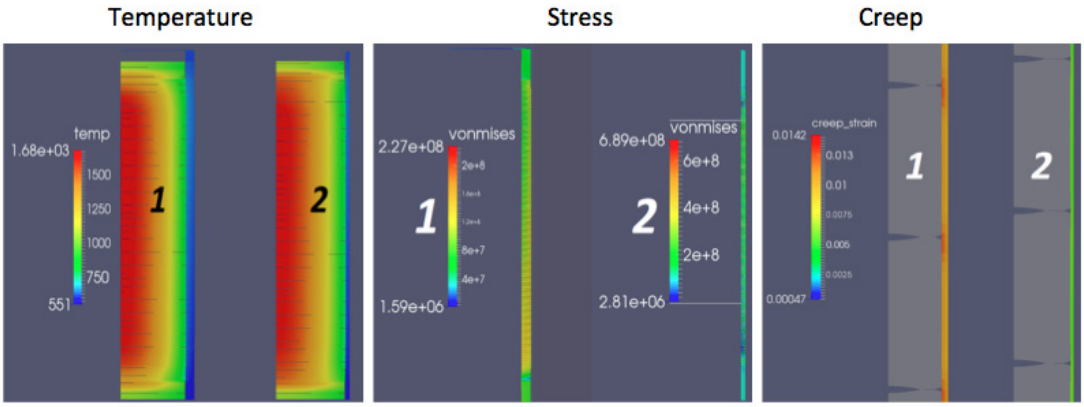

Figure 17. Zircaloy(1) and APMT 0.5(2) Hot Condition Full Rod Temperature, Stress, and Creep Results

Figure 17 shows temperature results at the hottest state point in the middle of the cycle for both the Zircaloy (1) and APMT (2) cases. A curious result occurs with a temperature spike towards both the bottom and top of the fuel rod. Upon close inspection, at these axial locations the fuel is observed to be peeling away from the inner clad surface. Thus, while fuel/clad contact is present along the majority of the axial length there is no contact at these locations, greatly degrading the thermal conductivity.

Results for the Von Mises stresses in the middle of the cycle (the most penalizing for Zircaloy under the given power profile) show drastic differences between the two cladding types for peak stresses. The stresses observed in the APMT cladding are three times higher than those at the same state point for Zircaloy cladding; however, both have nearly the same margin (~200 MPa) from the estimated irradiated yield stresses given above. While not shown here, it was observed that at the end of the cycle the stresses in the Zircaloy cladding had decreased. Conversely, the stresses in APMT cladding had increased to a peak value of 800 MPa for the selected power profile.

The reason Zircaloy maintains comparatively lower stresses despite experiencing very similar power histories is primarily due to its malleability. While being very strong, APMT steel also does not have as much malleability as Zircaloy. The right-hand image in Figure 17 shows the difference in creep strain for Zircaloy (1) and APMT (2). When zoomed in at the fuel pellet level, it is observed that the greatest forces are applied at the chamfered edges of the fuel pellets. Zircaloy has the ability of Zircaloy to deform around these edges, but the rigidity of the APMT steel causes it to be much less prone to deform. The difference in the rigidity properties for each cladding material is the primary reason for the drastically different stresses encountered in each cladding type.

Conclusions

The reactivity penalty inherent in moving away from Zircaloy cladding to APMT steel cladding can be mitigated through a combination of geometry and isotopic changes. In assessing the reactivity penalty it is important to first define what basis is used to evaluate the fuel performance. If matching reactivity on a burnup basis is desired, either very thin clad (0.13-mm) (0.25 fraction of Zircaloy) is required. This thickness is beyond current manufacturing abilities. A 0.26-mm clad (0.5 fraction) is required if combined with enriching the clad constituents. Although burnup is matched in both of these cases, either the cycle can be run longer, or the power increased, to match burnup. Alternatively, if EFPD is chosen as the target for matching reactivity a thickness of 0.26-mm (0.5 fraction) can be used to match cycle length. This, however, results in a 13% loss in discharge burnup, a less efficient usage of fuel.

The 0.5 fraction thickness is nearing the limit of manufacturing tolerances. If this thickness is selected and the cladding is not enriched, an initial ^{235}U enrichment increase of ~0.35% is required to match full thickness Zircaloy behavior. If the accident tolerant characteristics of advanced cladding allows for higher discharge burnups, the reactivity comparisons look more favorable for APMT steel claddings. This conclusion is evidenced by the 4-batch results due to the increased Pu production induced by the presence of the more parasitic APMT steel.

Cladding mechanical performance comparisons of Zircaloy and APMT steel showed very interesting results. The malleability of Zircaloy, and the propensity to creep, results in lower peak stresses relative to APMT simulations. It should again be stressed that each cladding type experienced the same burnup, but the APMT steel simulations required more time “in core” to achieve equivalent burnup. Additionally decreasing the gap-to-fuel ratio will tend toward increased stresses since there is more material to swell thermally, and due to fission product accumulation. However, the simulations clearly indicate higher stresses at the chamfered edges in APMT steel cladding due to the rigidity of APMT.

2.2 Fuel Properties

2.2.1 Severe Accident Test Facility

L.L. Snead, B.A. Pint, K.A. Terrani, Oak Ridge National Laboratory

The LOCA test module for the in-cell Severe Accident Test Station was completed (Figure 18). Rod alignment, hardware and software calibrations were completed. A standard operating guideline was developed with extensive consideration for safety, quality and operational needs to ensure safe operation in hot cell. A 3-D Computer Aided Design (CAD) model was prepared to assist with the installation into the hot cells and any repairs that might be required later (Figure 19).

Multiple participants from across AFC utilized the Severe Accident Test Station (SATS) at ORNL to examine candidate ATF cladding materials. A wide range of Fe-based, Mo-based, and SiC-based materials as well as MAX phase ceramics were exposed to steam environments over a wide range of temperatures up to 1700°C. FOA participants, namely General Electric, Westinghouse, and EPRI (under AREVA collaboration) had the opportunity to test their samples at SATS. These results are critical for informed development of these advanced concepts with the aim of enhancing safety margins in light water reactors under severe accidents.

Figure 18. Severe Accident Test Station at ORNL 3525 hot cells

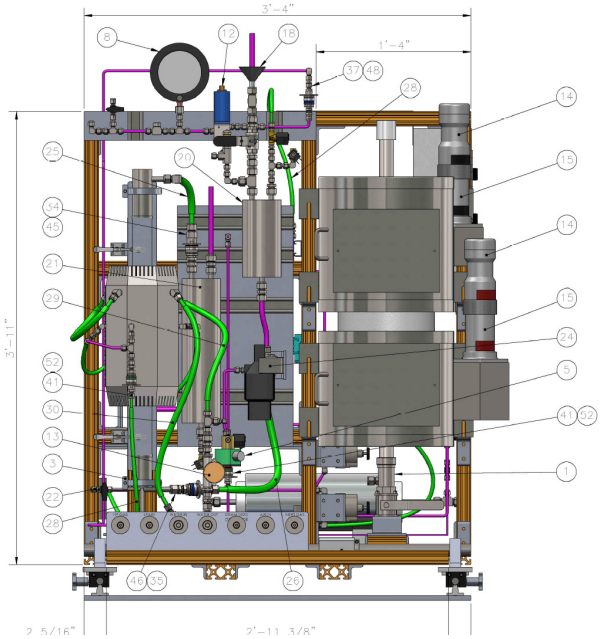

Figure 19. Severe Accident Test Station – front view of 3D Model

Measurements

Of particular note was the extensive testing on high-purity SiC-based materials (monolithic and composite) that are being actively pursued as ATF candidate materials. This work takes advantage of a range of facilities and capabilities at ORNL along with SATS. The results were reported as a Feature Article in the *Journal of American Ceramic Society* where the journal cover was also dedicated to a figure from this study (Figure 20). (K. A. Terrani, B. A. Pint, C. M. Parish, C. M. Silva, L. L. Snead, and Y. Katoh, "Silicon Carbide Oxidation in Steam up to 2 MPa," *Journal of the American Ceramic Society*, vol. 97, 2014, 2331–2352.)

Figure 20. Cover of the August 2014 issue of the Journal of the American Ceramic Society showing a steam-oxidized micro-crack present in a SiC/SiC composite prior to oxidation at 1500°C at ORNL's Severe Accident Test Station.

2.2.2 Uranium silicide fuel phases: Assessment of thermophysical properties, oxidation behavior and cladding compatibility

J.T. White, E.S. Sooby, A.T. Nelson, D.D. Byler, J.T. Dunwoody, D.J. Safarik, and K.J. McClellan, Los Alamos National Laboratory

The uranium-silicon binary system possesses a range of compounds that have been historically investigated and utilized to a limited extent as nuclear reactor fuels. Of the multiple compounds, U_3Si and U_3Si_2 are most familiar; their high uranium densities have made them an intriguing choice for incorporation into composite plate fuels in research reactors and other low power core redesigns where retained neutronic performance was desired at lower enrichments. This increased uranium density compared with uranium dioxide (UO_2) has made these composites attractive to a new generation of nuclear fuels research driven by the renewed push for accident tolerant fuels for use in existing and Gen III+ LWRs. An increased uranium density may facilitate incorporation of cladding variants that incur a neutronic penalty compared to the zirconium cladding alloys used currently. Performance gains may also be realized through advancement of composite fuel designs that aim to incorporate oxidation resistant phases into the fuel/cladding system in order to increase coping time during a LOCA, *e.g.* see the BNL highlight on screening of ATF systems via reactor performance and safety analyses.

The importance of temperature in governing many aspects of reactor performance demands knowledge of thermophysical properties from room temperature to anticipated operating conditions and through temperatures brought about by potential transients. Even the more familiar U-Si compounds U_3Si and U_3Si_2 have received minimal attention with respect to their thermophysical properties at elevated temperatures. An experimental campaign was undertaken in FY 2014 to provide thermophysical and oxidation data and facilitate the evaluation of potential of U-Si compounds for LWR applications. Monolithic specimens for thermal conductivity and oxidation testing were prepared by arc melting high purity feedstocks of depleted U and Si. Resulting buttons were comminuted, pressed and sintered to desired geometries using standard powder metallurgical routes in a W-metal furnace. X-ray diffraction (XRD), scanning electron microscopy (SEM), and chemical analyses were conducted to verify the composition of U-Si specimens to be phase pure within acceptable limits.

The results of thermal conductivity measurements performed from room temperature to the melt points of the four U-Si binary compounds investigated are shown in Figure 21. Reference data for UO_2 and UN are included for comparison. The conductivity for each of the U-Si compounds increase with temperature,

and are generally greater in value than UO_2 at LWR operating temperatures. Early reports of a martensitic phase transformation in U_3Si (which were recently discounted in the literature), was confirmed in all of the thermophysical measurements. Characterization of the high temperature δ′-U_3Si thermophysical properties was also determined for the first time and published in the *Journal of Nuclear Materials*. Results for U_3Si_5 exhibit a low temperature reaction that has not been measured previously in the literature. Properties for U_3Si_5 have been accepted for publication in the *Journal of Nuclear Materials*. These data have been transmitted to collaborators at INL, BNL, and WEC to facilitate design of ATF-1 irradiation experiments to be performed at ATR in the coming year.

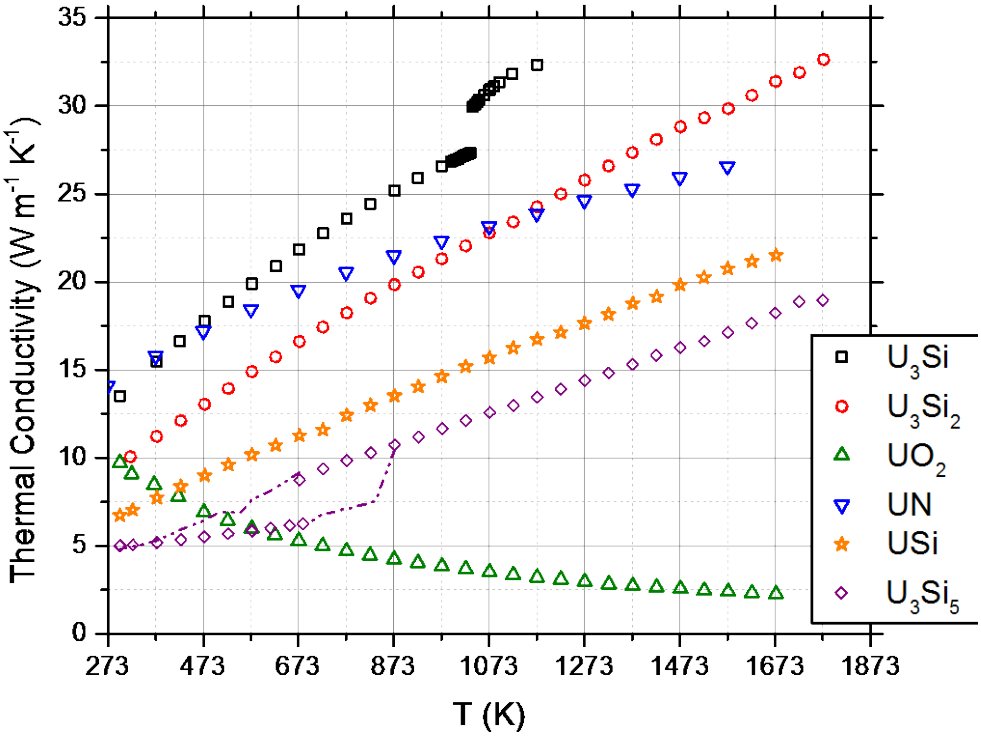

Figure 21. Thermal conductivity of U-Si binary compounds as a function of temperature to the melt points of the various compounds. Values are compared to reference data for UO_2 and UN.

Oxidation testing was conducted on U-Si compounds in air and steam environments to simulate performance under ambient storage and LOCA conditions, respectively. U-Si compounds, UO_2, and UN that are exposed to air at elevated temperature degrade to a black powder. This effect is not observed until above 250ºC, which is above the temperature where UN degrades. Macroscopic photographs of U_3Si_2 and U_3Si_5 compared to UO_2 after isothermal holds under 75%-H_2O/Ar atmospheres are shown in Figure 22. U_3Si_2 fragmented under all test conditions, while U_3Si_5 exhibited some evidence of mechanical integrity. UO_2 pellets gained mass under the test conditions, but did not degrade after exposure to steam. Further isothermal testing on U_3Si_5 in 75% steam/Ar reveals that U predominately oxidizes in the initial stages followed by retarded oxidation of the Si. This work suggests that minimal improvement in the oxidation performance of LWR fuels would be attainable by inclusion of the two U-Si compounds investigated.

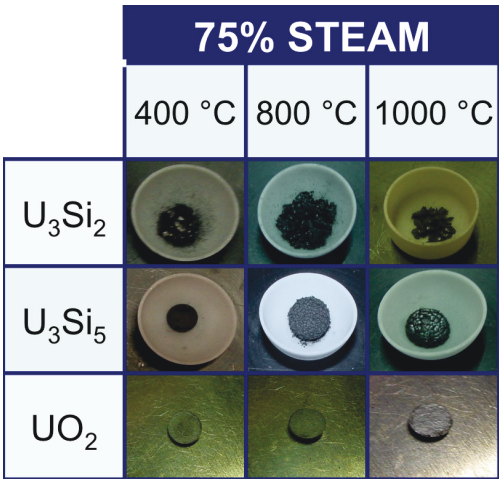

Figure 22. Macroscopic photographs of specimens after exposure to steam at a variety of temperature.

A matrix of candidate accident tolerant fuels and UO_2 paired with candidate cladding materials underwent testing with varied thermal profiles to both screen general fuel/cladding compatibility as well as to investigate the formation of secondary phases that could induce pellet-cladding chemical interactions during reactor service. An assembly was designed to maintain intimate contact between the pellet and the cladding sample at temperatures below 1300°C. The test assembly consists of an outer stainless steel tube fixed with Swagelok fittings on both ends. This complete containment serves to limit the spread of liquid phases that may form as a result of inter-diffusion. A steel spring fixed in length to provide 3 MPa of load upon the assembly closure at room temperature maintained the contact between the fuel pellet and cladding through the experiments.

No significant reactions were observed following exposure for temperatures up to 1000°C and time intervals up to 100 h. Compatibility was generally good for the couples tested. Formation of a U-Al-O phase appears to be a possibility for U_3Si_2 and Fe-Cr-Al alloys. Furthermore, qualitative investigation suggests that U_3Si_2 may getter oxygen more effectively than candidate Fe-Cr-Al materials. This dramatic reversal from the operational experience of UO_2 and a zirconium alloy cladding, in which the cladding oxidizes much more readily than the fuel, is likely to have significant impact on how a reactor fuel responds to either a cladding breach during normal operation or possible transients. Finally, the stability of both uranium silicide and uranium nitride fuels and SiC cladding is in question based upon thermodynamic calculations. Ongoing experimental work will investigate the kinetics of these reactions to evaluate the potential design impact.

Publications

1. J. T. White, A.T. Nelson, D.D. Byler, J.A. Valdez, K.J. McClellan, "Thermophysical properties of U3Si," *Journal of Nuclear Materials*, 452, 2014, 302.
2. J. T. White, A.T. Nelson, J.T. Dunwoody, D.D. Byler, D.J. Safarik, K.J. McClellan, "Thermophysical properties of U3Si5 to 1773 K," accepted in the *Journal of Nuclear Materials,* 2014.

2.2.3 Oxygen Thermochemistry of Urania-Rare Earth System: UO_2-CeO_2

S. Hirooka, T. Murakami, JAEA-Tokai, A.T. Nelson and K.J. McClellan, Los Alamos National Laboratory

Collaboration between the U.S. DOE and Japan on characterization of nuclear materials' properties under the Civil Nuclear Energy Research and Development Working Group (CNWG) remains an area of active

progress. CNWG aims to co-develop nuclear fuel technology by leveraging facilities and resources belonging to both Japan and the US. Although the Japanese Atomic Energy Agency (JAEA) research focuses on $(U,Pu)O_2$ as mixed oxide (MOX) fuel and the DOE program's focus currently is on metallic transmutation fuel, the effects of Ce on the thermochemistry and thermophysical properties of oxide fuel represent a common interest to both programs given the utility of Ce as a surrogate for Pu as well as its importance as a fission product. Many studies have been reported on $(U,Ce)O_2$ as UO_2 with a fission product and a surrogate material of $(U,Pu)O_2$ since Ce is one of most prevalent fission products forming full solid solution over 1000°C. Furthermore, its 3+/4+ valence mirrors that of Pu, making it a suitable thermochemical surrogate.

Thermal conductivity is one of the most critical thermophysical properties for nuclear fuel operation. It is well understood that both cation defects and oxygen defects will significantly affect thermal conductivity. Both are present in MOX fuel, but characterization of their respective roles is challenging given the requirements of Pu operations. Thermal conductivity of $(U,Ce)O_2$ has been systematically studied as a function of Ce content; however, reports on the oxygen non-stoichiometry of $(U,Ce)O_2$ are limited. It is necessary to have a firm understanding of the relationship between oxygen activity and the oxygen-to-metal ratio (O/M) in order to precisely control the latter to facilitate thermophysical property measurement as a function of specific defect structures.

Experimental measurements of the oxygen potential were conducted on 20% and 30% Ce compositions using the gas equilibrium method where oxygen partial pressure in the atmosphere was controlled with mixing dry/wet Ar/H_2 gas. The composition simulates Pu content in advanced MOX fuel in JAEA. More than 100 data points were obtained in the O/M range of 1.945 ~ 2.000 at 1200°C, 1400°C and 1600°C. Ongoing work is focused on executing identical measurements on more dilute Ce contents that better represent levels expected of Ce as a fission product.

The experimental result of $(U_{0.7}Ce_{0.3})O_2$ is shown in Figure 23 together with the calculated result by defect chemistry and $(U_{0.7}Pu_{0.3})O_2$ data. The experimental results are well reproduced by the defect analysis and the error was observed to be 8.7kJ/mol (n=57). From the comparison with that of $(U_{0.7}Pu_{0.3})O_2$, applicability of the same defect chemistry and S-style curve shown in the Fig 1 are common. $(U,Ce)O_2$ requires a higher oxygen potential for an equivalent O/M ratio compared to $(U,Pu)O_2$. This oxygen potential data has enabled ongoing property studies, and is important information in evaluating the analogies as a surrogate of $(U,Pu)O_2$.

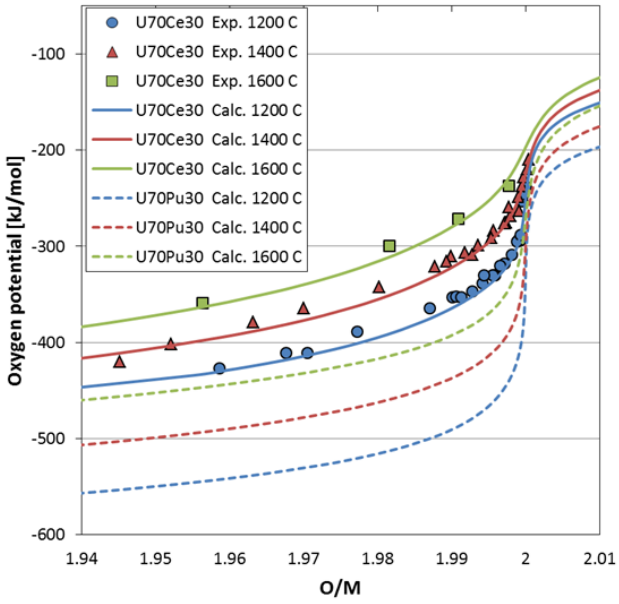

Figure 23. Oxygen potential – O/M ratio developed for U70Ce30 and U70Pu30 analyzed by defect chemistry based on the experimental results by gas equilibrium method.

Publications

1. A.T. Nelson, D.R. Rittman, J.T. White, J.T. Dunwoody, M. Kato and K.J. McClellan, "An evaluation of the thermophysical properties of stoichiometric CeO2 in comparison to UO2 and PuO2," *Journal of the American Ceramic Society*, DOI: 10.1111/jace.13170 (online 7 Aug 2014).
2. M. Kato, T. Murakami, T. Sunaoshi, A. T. Nelson, and K. J. McClellan, "Property measurements of (U0.7Pu0.3)O2-x in Po2-controlled atmosphere," *Proceedings Global 2013*, Salt Lake City, Utah, Sept. 29- Oct. 2, 2013.

2.2.4 Thermo-mechanical Properties of Urania with Additives to Tailor Microstructure and Properties

R. McDonald, H. Lim, P. Peralta, Arizona State University; A. Nelson, E. Luther, R. Leckie, K. McClellan, Los Alamos National Laboratory

In the area of Advanced Accident Tolerant Ceramic Fuel Development, the majority of the FY14 effort at LANL focused on composite fuel seeking transformational R&D, but some effort continued on incrementally advancing fuel technology, e.g. relatively minor modifications to UO_2 to enhance properties that would yield benefit in accident behavior.

Table 4. Grain diameter (with average deviation) of UO2 samples containing oxide additives.

Additive	Avg. Diameter (μm)	Additive	Avg. Diameter (μm)
No Additive	13 ± 1	0.1 wt% Al_2O_3	9.8 ± 0.5
0.1 wt% Cr_2O_3	12 ± 1	0.2 wt% Al_2O_3	9.8 ± 0.7
0.2 wt% Cr_2O_3	15 ± 2	0.1 wt% SiO_2	12 ± 1
0.1 wt% TiO_2	26 ± 1	0.2 wt% SiO_2	11.5 ± 0.7
0.2 wt% TiO_2	28 ± 1	.05 wt% Y_2O_3	12.0 ± 0.3
		0.1 wt% Y_2O_3	12.1 ± 0.6

Small concentrations of oxide additives have been shown to improve the mechanical and physical properties of UO_2 and provide avenues to control its microstructure. Hence, hardness, fracture toughness, and yield strength have been probed in samples containing small concentrations of various oxide additives at temperatures up to 1200°C. Vickers indentation is used as a screening technique to determine which additives may enhance UO_2 for reactor applications. The additives used in this study include: Al_2O_3, Cr_2O_3, SiO_2, TiO_2, and Y_2O_3. Concentrations range between 0.05 and 0.2 wt%, depending on the additive type. The high temperature indentation experiments were performed at Arizona State University (ASU) on an indentation assembly capable of doing 1kgf indents at temperatures up to 1200°C.

Initial work focused on analyzing the microstructure of each sample to characterize the effects of the additives on grain size. The average grain diameter was calculated using Orientation Imaging Microscopy (OIM™) analysis or through the linear-intercept method from SEM pictures. Results are given in Table 4. Adding Al_2O_3 resulted in an average grain diameter 24% smaller than the un-doped sample. Cr_2O_3 additions did not lead to a noticeable change in average grain diameter. A bimodal microstructure occurred in the Cr_2O_3-doped samples, i.e., there was a high number of larger grains surrounded by smaller ones, which differs from the equiaxed grains seen in other samples. This can be seen in Figure 24. SiO_2

and Y_2O_3-doping did not yield any meaningful changes in average grain size. TiO_2-doping led to an average grain diameter more than double what was seen in the un-doped sample.

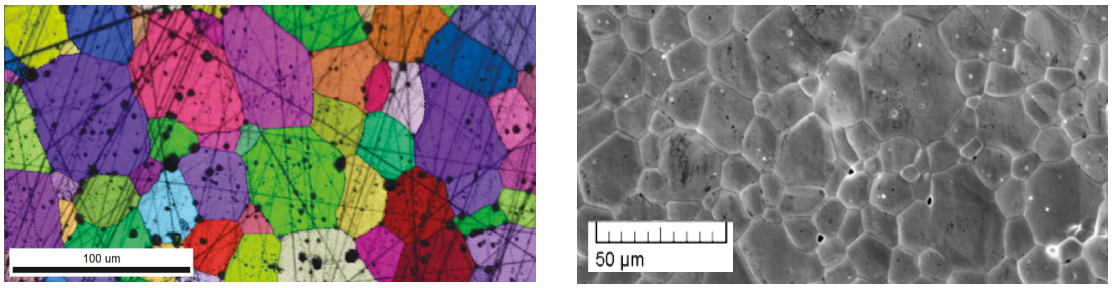

Figure 24. A) OIM map of a 0.2 wt% TiO_2-doped sample. B) Bi-modal microstructure seen in a 0.2 wt% Cr_2O_3-doped sample.

Vickers hardness at each temperature was determined from a direct measurement of the indent size. Across a temperature range of 450-1200°C, the hardness of samples containing Al_2O_3, Y_2O_3 and SiO_2 was not significantly different from the un-doped sample. Cr_2O_3-doping produced samples that were 15 to 20% harder than the un-doped sample at temperatures above 500°C. TiO_2-doping yielded samples that were 17% harder at 500°C, and twice as hard at 1200°C. These results are shown in Figure 25. Experiments are still underway to form a more comprehensive picture of each sample's hardness at 100° C temperature intervals.

Fracture toughness has been calculated only at room-temperature using equations empirically established by Niihara and Morena for brittle cracking due to Vickers indentation [1]. High-resolution imaging and measurement of the cracks is done using SEM. Al_2O_3-doped samples show fracture toughness over 20% higher than the un-doped sample. The sample doped with 0.1 wt% Y_2O_3 showed a 10% increase in fracture toughness. The rest of the dopants led to samples with decreased fracture toughness at room temperature. Determining the fracture toughness at elevated temperatures is currently underway.

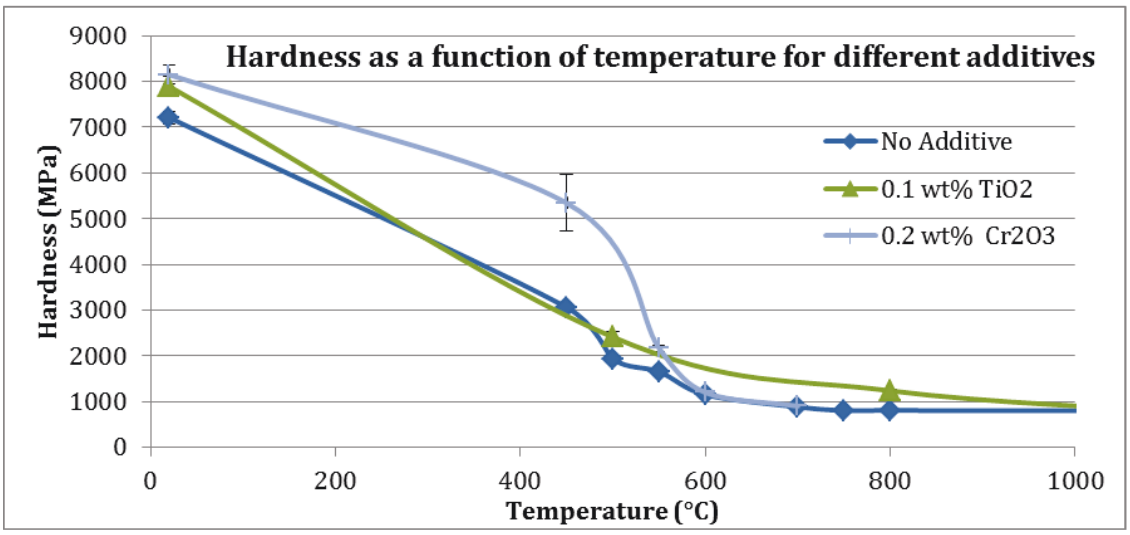

Figure 25. Vickers hardness for the 0.1 wt% TiO_2-doped and 0.2 wt% Cr_2O_3-doped samples. The other additives types did not cause substantial changes in hardness.

Yield strength can be calculated in the high-temperature regime by measuring the extent of material pile-up around each indent. The pile-up area is measured using an optical profilometer, and yield strength is

calculated from equations established by Giannakopolous and Larsson [2]. Experiments are still in progress to determine how each additive alters the yield strength at high temperatures.

References

1. K. Niihara and R. Morena, "Evaluation of K_{IC} of brittle solids by the indentation method with low crack-to-indent ratios," *Journal of Material Science Letters,* 1, 1982, 13-16.
2. A. Giannakopolous and P. Larsson, "Analysis of Vickers indentation," *International Journal of Solids Structures,* 31(19), 1994, 2679-2708.

2.3 Advanced LWR Fuel Development

2.3.1 An Assessment of the Field Assisted Sintering Technique Applied to Ceramic Fuel Constituents

J.A. Valdez, D.D. Byler and K.J. McClellan, LANL

Flash sintering is a fairly new technique in the material processing field in which an electric field (DC or AC) is applied to a ceramic at either the onset of heat-up or at an isothermal temperature that causes ultra-fast sintering at temperatures hundreds of degrees below conventional temperatures. For example in wide band gap insulators such as zirconia, ultra-fast sintering at low temperature has been shown in work by Downs et al. [1] in which they sintered YSZ to high density at 390°C using an applied field of 2250 V/cm. For comparison, typically zirconia is sintered at ~ 1400°C using conventional pressureless sintering. There are many examples of materials such as ionic conductors, electronic conductors, semi-conductors and insulators that have been flash sintered and possible mechanisms responsible for this effect have been proposed.

Typically, a flash sintering apparatus consists of a furnace and power supply with leads in contact with a sample for application of the electrical field. Sample sintering is tracked either by a camera (image analysis is performed to calculate shrinkage) or a linear voltage displacement transducer. The simplicity and low cost, of this technique makes it adaptable to production settings as well as laboratory environments. Flash sintering applied to nuclear fuels may be used either as an initial processing step to increase green pellet strength or as an actual sintering step depending on the requirement. A schematic representation of a typical flash sintering apparatus, with the key components labeled, is shown in Figure 26.

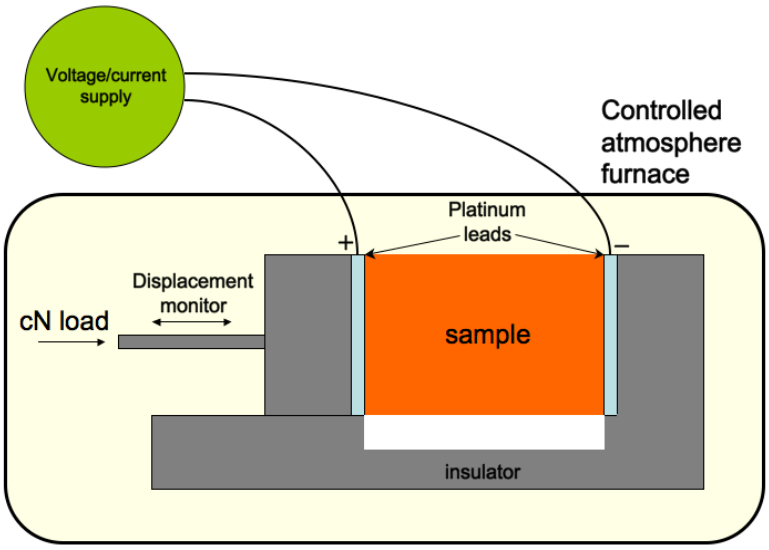

Figure 26. Schematic representation of the LANLs flash sintering apparatus.

This configuration was the basis of the flash sintering setup LANL developed and used to complete an assessment of advance field-assisted sintering techniques for ATF fabrication, which was focused on surveying Urania and ATF composites $UO_{2.00}$-UB_2 and UN-U_3Si_5. The sintering that occurs at lower temperatures when using flash sintering takes place at ultrafast sintering rates (nearly instantaneously) as compared to conventional sintering; sintering occurs in seconds rather than hours. Our studies on $UO_{2.16}$ showed that flash sintering produces comparable densities to those that are achievable using conventional sintering although at lower temperatures and much less time. This observation is shown in Figure 27. Specifically it shows that when using flash sintering the linear shrinkage that results in a final density of ~93% theoretical takes place in *3234% less time* and at a *temperature that is 40% lower* than the temperature required to achieve similar linear shrinkage using conventional sintering.

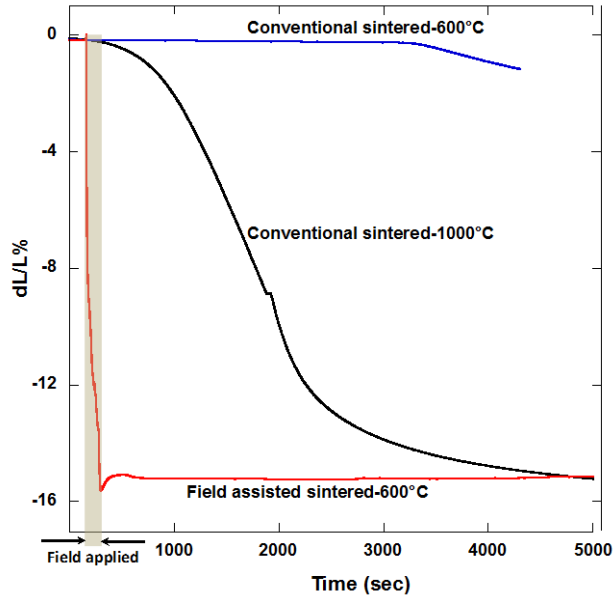

Figure 27. Sintering strain (dL/L_o%) obtained from $UO_{2.16}$ comparing FAS sintering at 600°C conventional sintering at 600°C and 1000°C.

The resulting microstructure of a $UO_{2.16}$ pellet that was sintered using the flash method can be seen in Figure 28. The micrograph shows a density gradient consisting of lower density regions on the pellets ends and a high-density region in the middle of the pellet. Experiments using longer hold times have been shown to produce increased pellet geometric uniformity; therefore, it should be possible to produce a uniform microstructure throughout the pellet with optimization of the processing parameters, mainly temperature, power-density and hold time. Experiments were also performed on $UO_{2.00}$. The results from these experiments showed that $UO_{2.00}$ also densifies at higher rates and lower temperatures compared to conventional sintering, although the final density was lower in $UO_{2.00}$ using identical parameters that produced higher final density in $UO_{2.16}$.

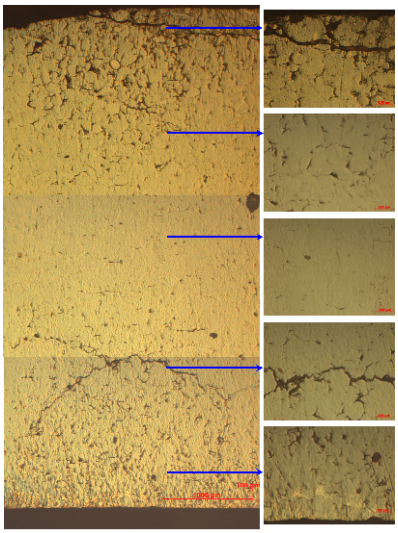

Figure 28. Optical image of a cross-sectioned $UO_{2.16}$ pellet

Several other flash sintering experiments were performed on matrix and constituent phases, both individually and as composites. To assess the flash sintering response of the previously mentioned materials, the selected parameter envelope was developed and optimized to achieve high final densities in $UO_{2.16}$. A summary of the experimental findings is shown in Table 5. The table shows densification using flash sintering was achievable in 8-YSZ (used to compare with literature values), $UO_{2.16}$, $UO_{2.00}$, and $UO_{2.00}$-UB_2 (localized), whereas using the parameters that produce densification in the previously stated materials showed no measurable densification in UB_2, UN, U_3Si_5, or UN-U_3Si_5 composites.

Table 5. Flash sintered materials surveyed

Material system	Flash sintering densification	Comment
8 YSZ (yttria stabilized zirconia)	yes	Densification less than reported in literature, most likely due to geometric effects.
$UO_{2.16}$	yes	Good densification
$UO_{2.00}$	yes	Excellent densification
UB_2	no	Poor densification
UN	no	Poor densification
$UO_{2.00}$-UB_2	yes	Localized densification
UN-U_3Si_5	no	Poor densification

With the lack of densification in the previously stated materials, these material systems might be candidates for experiments using other field assisted sintering (FAS) techniques such as spark plasma sintering (SPS). The concept of investigating other FAS techniques on composite systems surveyed under this work package will be presented to both our jointly funded collaborators at the University of Florida studying SPS (NEUP) and the US/EURATOM (United States/European Atomic Energy Community) I-NERI project (International Nuclear Energy Research Initiative) investigating FAS techniques. Additionally, there also exists the possibility of achieving high densification using flash sintering in the proposed ATF composites and end-member phases by broadening the processing parameter envelope through more detailed studies performed by LANL.

References

1. Downs, V.M. Sglavo, "Electric field assisted sintering of cubic zirconia at 390°C," *Journal of the American Ceramic Society*, 96, 2013, 1342–4.

2.3.2 Microencapsulated Fuels

K.A. Terrani, L.L. Snead, Oak Ridge National Laboratory

Major accomplishments toward production of the LWR-optimized Fully Ceramic Microencapsulated (FCM) fuel form were demonstrated. Of particular note are optimization of TRISO particle overcoating process to control packing fraction and particle-to-particle spacing, incorporation of a thin buffer layer, and production of high-density UN kernels that are essential for LWR application of coated fuel particles. These accomplishments have now paved the way for production of LEU FCM pellets in FY 2015 that will be available for irradiation testing.

2.3.3 U-Mo Advanced LWR Fuel

R. Omberg, C. Lavender and C. Henager, Pacific Northwest National Laboratory

The development and demonstration of extrusion and co-extrusion capability was a focus area for PNNL with considerable progress in FY 2014. Difficult to extrude alloys such as MA-956 were investigated and characterized. Both extrusion and co-extrusion are processes that are important to the Advanced Fuels Campaign. Extrusion is an efficient, high-yield commercial process that is capable of producing lengths of tubular rods at high extrusion rates, with excellent material yields. PNNL achieved three important accomplishments that moved the state-of-the-art forward in these areas.

The first achievement comprised the design and processing of model rodlets, which demonstrated the ability to co-extrude a metal fuel element with an integral cladding layer using a commercially-viable direct extrusion process. The co-extrusion process would provide near net-shape metal fuel elements that can be directly machined for welded end caps, eliminating multiple machining steps and the generation of large amounts of scrap fuel material. The extrusion force required to extrude solid and tubular fuel pins meeting the general dimensional requirements of the ATF-1 capsule-rodlet assembly were determined to be within the capability of commercial extrusion systems. Figure 29 below shows the completed rodlet.

Figure 29. Finished model rodlet with machined viewing windows.

As a second achievement, U-10Mo/Zr was co-extruded successfully as shown in Figure 30. The stresses were at an acceptable level, and the resulting extrusion was sound with no incipient melting.

Figure 30. Successful co-extrusion of U-10Mo/Zr.

Finally, PNNL is also developing a triple layer co-extruding concept to mitigate potential corrosion concerns. Currently, the triple layered extrusion concept under exploration involves U-Mo surrounded by an inner layer and then a cladding layer as shown in Figure 31. The cladding will be a Fe-based alloy for accident tolerant purposes. Investigation to date indicates that MA956, 14YWT and Kanthal APMT are all promising, and that MA956 and Kanthal APMT will likely work. The 14YWT, however, has a hot strength that is higher, which may be a challenge. The inner layer is provided for corrosion resistance and hydrogen gettering for the cladding and inner layer breach. Potential materials for the inner layer could be Zr, Nb or others. The Zr and Nb have the benefits from alloying and compatible processing, and they will be used to examine the eutectics, corrosion resistance and hot strength.

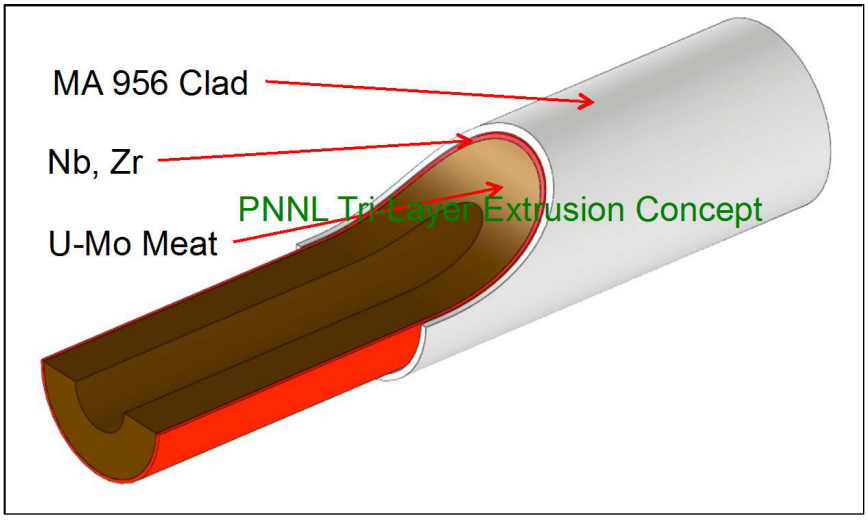

Figure 31. Triple co-extrusion concept under development at PNNL.

2.3.4 Understanding and Improving the Carbothermic Reduction/ Nitridization Route for UN Synthesis

A. J. Parkison, Los Alamos National Laboratory

Uranium mononitride (UN) has been of historical interest as a nuclear fuel due to its high actinide density, high melting point, and high thermal conductivity. Although traditionally considered for fast reactor and

transmutation fuels, its favorable attributes have made it a candidate for a constituent in ceramic composite ATF concepts for LWR service. For example, UN-U_3Si_2 composite fuel is a system being investigated under the Westinghouse-led FOA project. In addition to superior thermophysical properties that will reduce fuel centerline temperatures, thereby minimizing restructuring and fission product transport, its candidacy is driven by its high uranium density (40% greater than uranium dioxide), which could facilitate replacement of zirconium cladding with stainless steel without a large penalty to reactor operation, *e.g.* see the BNL highlight on screening of ATF systems via reactor performance and safety analyses. One of the multiple research pathways necessary to advance UN as an LWR fuel option is an improved understanding of the thermodynamic drivers that will govern the chemistry and structure of UN feedstock. These characteristics dictate the structure-property relationships of dense fuel product and in-pile performance.

The carbothermic reduction/nitridization (CTR-N) route has been extensively utilized to synthesize bulk UN. This process uses uranium dioxide/carbon pressed pellets as the starting material and molecular nitrogen as the nitriding agent. This route was chosen because it is assumed to be the UN fabrication route most amenable to immediate industrial scale processing. Although conventional wisdom suggests that a fuel that incorporates UN will require a MOX-like glovebox line during fabrication, there has been recent evidence that the CTR-N process has the potential to be conducted at existing UO_2 fabrication plants with only minimal changes to standard processing procedures. This process has been employed extensively at LANL for synthesis of UN for multiple programs at kilogram levels. However, the precise time-temperature-atmosphere profiles have underwent minimal optimization over the years. While legacy conditions have been found suitable to yield a product of acceptable impurity levels, the precise rate limiting factors that dictate purity are not well understood. These must be assessed not only to improve both the product and efficiency of laboratory scale synthesis, but also to evaluate future industrial feasibility and costs.

This CTR-N process is currently being studied using ZrO_2 as a surrogate material instead of radioactive UO_2, because this allows greater freedom in material handling during the initial investigations. A full systematic study of the UO_2 CTR-N process will begin near the transition to FY 2015. The current effort focuses largely on the coupling of thermogravimetric analysis (TGA) and quadruple mass spectrometry (QMS). TGA is capable of measuring the mass changes associated with competing mass loss (evolution of carbon monoxide) and mass gain (addition of nitrogen) mechanisms. Synchronized QMS allows one to differentiate between these mass gain and mass loss mechanisms, resulting in kinetics information for these individual reactions. The material is also being analyzed using XRD and SEM. The XRD analysis will give information on the relative phase abundance as the oxide transitions to the carbide, to a mixed carbonitride, and finally to the nitride. The SEM analysis will grant information on the microscopic physical changes as they occur during the CTR-N reaction.

Initial findings using ZrO_2 surrogate material have demonstrated the importance of feedstock morphology on the resulting kinetics of nitride formation. Strong evidence has been found that variables such as starting particle size, particle shape, and milling time play significant roles in the conversion from oxide to nitride. Figure 32 and Figure 33 show the effect that milling time and starting C:O ratio have on the starting morphology of the feedstock. It was found that the reduction portion of the CTR-N reaction has a squared dependence on milling time. This squared dependence is a result of the material being fractured during the milling process, thus increasing the starting contact area between the ZrO_2 and the graphite. However, it remains unclear how this greater starting contact area will affect the availability of nitrogen to the interior bulk material, as the nitrogen requires a pathway to the interior that is diminished as the material is homogenized. The starting C:O ratio was also found to be important in engineering this

reaction. It was found that a C:O ratio of 2.5 provided the most rapid reduction. Again, it remains to be seen how this will affect the conversion to nitride or the ability to produce a high purity material.

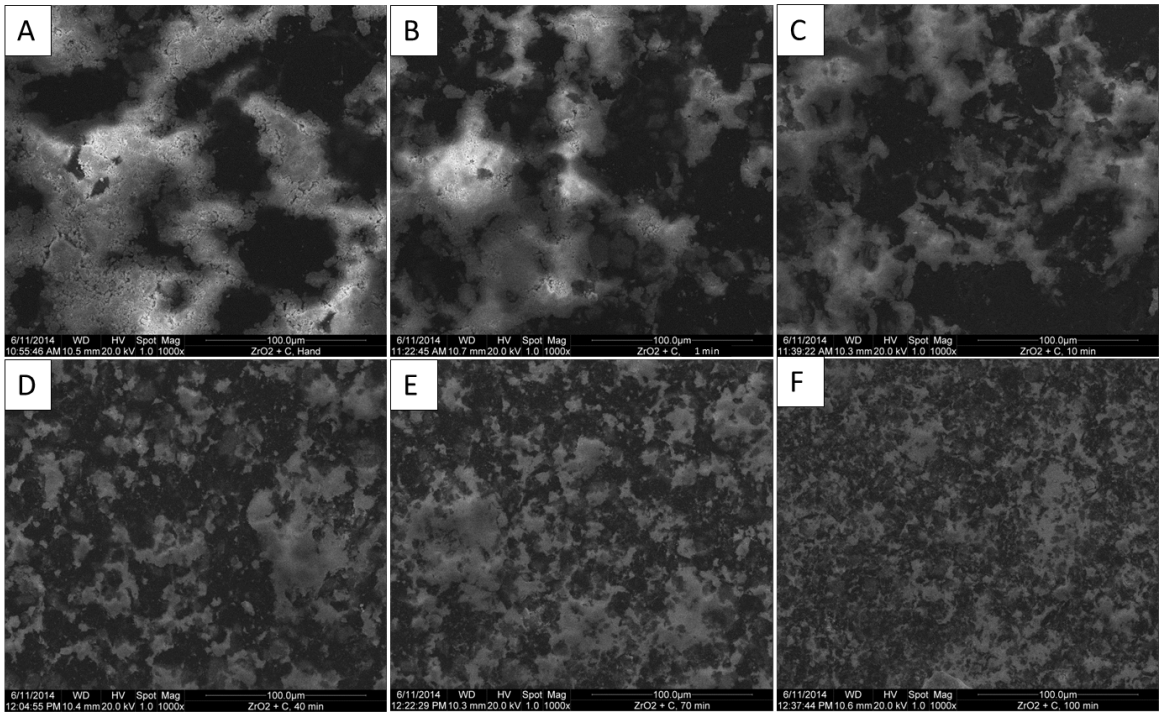

Figure 32. The effect of milling time on starting morphology for ZrO_2-graphite mixtures. Homogenization is seen to occur as milling time increases. The C:O ratio was 1.5. [A) hand milled, B) 1 min Spex mill, C) 10 min Spex mill, D) 40 min Spex mill, E) 70 min Spex mill, F) 100 min Spex mill]

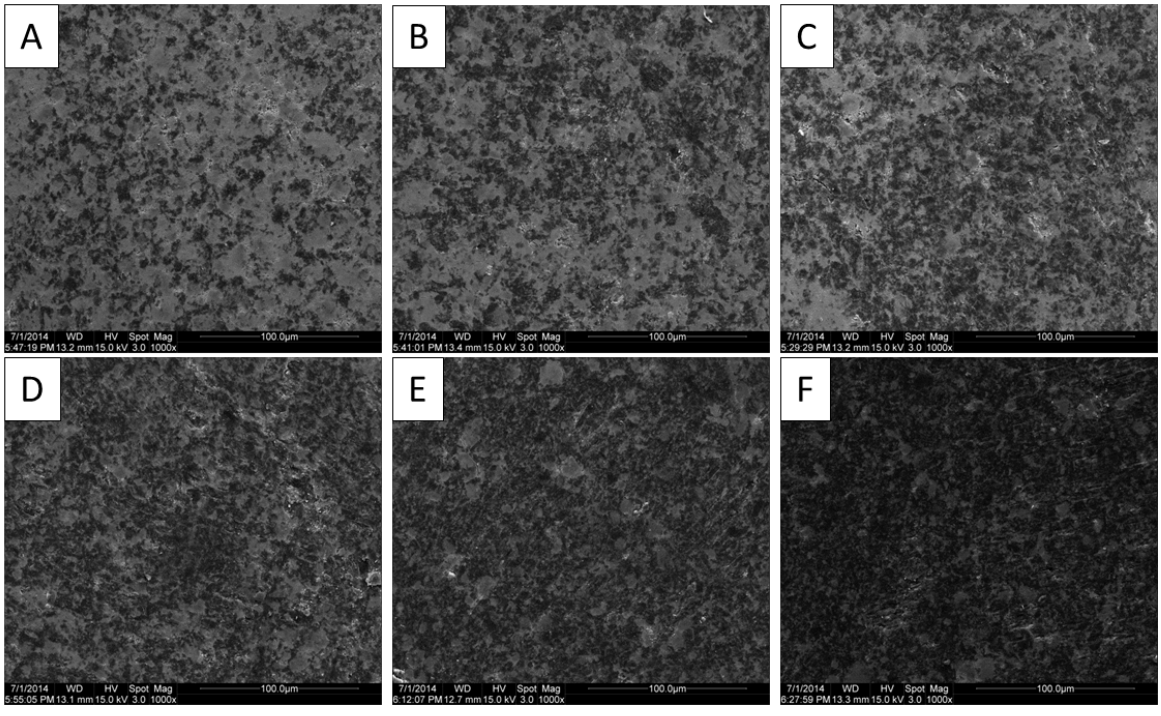

Figure 33. The effect of C:O ratio on starting morphology for ZrO_2-graphite mixtures. The milling time was 100 minutes. [A) C:O of 0.5, B) C:O of 1.0, C) C:O of 1.5, D) C:O of 2.0, E) C:O of 2.5, F) C:O of 3.0]

Effects such as pore formation and sintering are believed to play major roles in not only the conversion rate, but also in the purity of the final material. It therefore becomes critical to understand the effect that the microstructure has as the reaction progresses so that the process may be engineered and optimized for industrial use. Figure 34 shows the changes to the microstructure that take place during the conversion to nitride. It appears that all graphite is essentially transformed into pores/channels which provide the nitrogen access to the bulk material. This stresses the importance of understanding the starting morphology as shown in the two previous figures. The interplay between all of these variables is complex, but it is in the process of being understood.

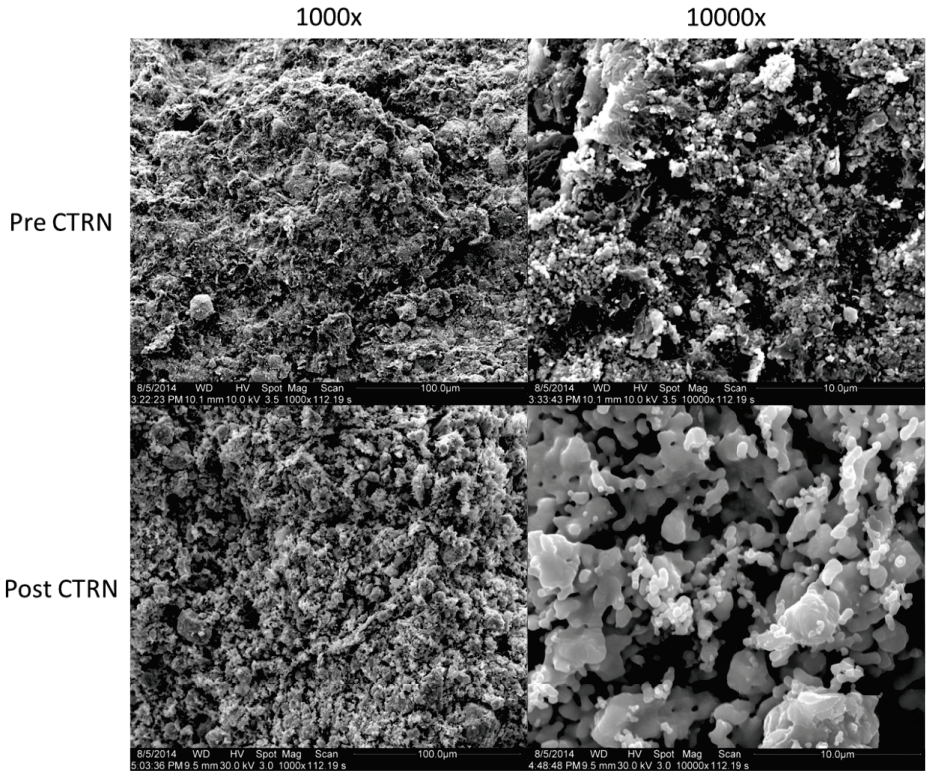

Figure 34. Scanning electron microscope (SEM) image of zirconium oxide mixed with graphite before the CTR-N reaction (top), and the material after the CTR-N reaction (bottom). Notice the pore formation and sintering that took place during the reaction. Reaction temperature was 1425 °C, milling time was 100 minutes, and C:O ratio was 1.5.

The ultimate goal of this project is to determine the order, timing, and kinetics of the transition from oxide to carbide, to carbonitride, and finally to nitride as the CTR-N reaction progresses. This will allow process variables such as temperature and atmosphere to be adjusted at the precise time needed for optimized conversion. Figure 35 plots the reaction rate as a function of reaction progression for several temperatures and atmospheres. The reaction rate and progression are determined by measuring the competing mass changes mentioned above using TGA. This gives information on the rate limiting mechanisms as well as the nature of the progression of these reactions during the CTR-N process. Perhaps most striking is the "hump" seen near the 79% mark, which likely corresponds to the onset and progression of the conversion of carbide or carbonitride to nitride. There also appears to be a change in reaction mechanism near the 98% mark, possibly corresponding to the onset of carbonitride formation. These and similar hypotheses are currently under investigation. The kinetic detail elucidated in these studies provides the tools necessary to understand and optimize the synthesis of high purity UN. This

level of understanding is critical for facility and process design should this process be implemented on an industrial scale.

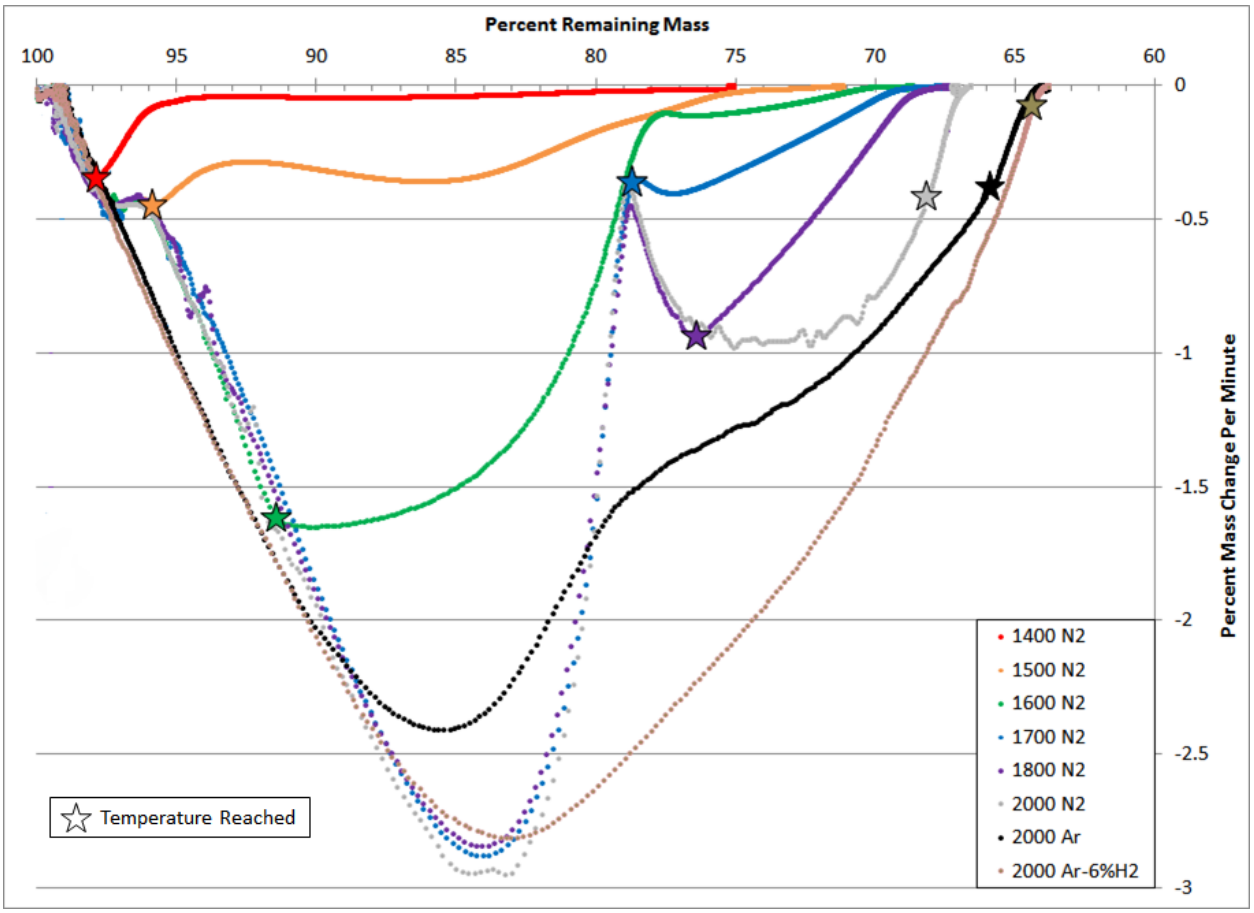

Figure 35. Zirconium oxide was mixed with graphite and allowed to react in a nitrogen atmosphere for temperatures between 1400 and 2000 °C. This material was also reacted in nitrogen, argon, and argon-6% hydrogen at 2000 °C. Ramp rate was 20 °C/min.

2.4 Cladding

2.4.1 Engineering Grade ATF Alloy Development and Properties

Y. Yamamoto, B. Pint, S. N. Dryepondt, Oak Ridge National Laboratory

Based on the systematic studies of model FeCrAl alloys (Phase I) in terms of fabricability, mechanical properties, oxidation resistance, aging effects, and weldability, together with concerns about the potential irradiation resistance [1], Fe-13Cr-5Al-Y (wt%) was down-selected as an initial base alloy composition for the 2nd generation (Phase II) ATF FeCrAl alloy development. The Phase II alloy design focused on strengthening the alloys through minor alloying additions, such as Mo, Si, Nb, and C, to introduce either solution-strengthening and/or precipitate-strengthening, together with minimizing negative impacts on the other properties such as fabricability, oxidation resistance, etc. The alloy compositions were selected with guidance of computational thermodynamics and a design strategy to control stable microstructure in a

wide temperature range from room temperature to elevated temperatures, such that stable properties would be expected not only at the service temperature of ~320°C but also under both design-basis and beyond-design-basis nuclear reactor accident scenarios. Based on mechanical property evaluation as well as oxidation testing, one of the Phase II FeCrAl alloys with the nominal alloy composition of Fe-13Cr-5Al-2Mo-1Nb-0.2Si-0.05Y, wt.% (C35MN) combined with a controlled sub-grain structure (Figure 36) was down-selected for further evaluation. Various property evaluations were initiated including thermal stability, steam oxidation, irradiation exposure, tube burst testing, hydrogen permeation, creep-rupture properties, weldability, and fabricability. It was found that the Nb addition was the key to increaseing the thermal stability of the microstructure by formation of Fe_2(Mo,Nb)-Laves phase precipitates, and the proper thermo-mechanical treatment would allow better fabricability and microstructure control to obtain improved mechanical properties.

Further alloy development to seek the base alloy compositions with improved oxidation resistance was also initiated by using high Al containing model (Phase I) FeCrAl alloys. Acceptable room temperature fabricability was observed up to 7 wt.% Al containing alloys which exceeded the upper limit Al content to avoid unexpected embrittlement reported in the literature [2]. Improved oxidation resistance was observed even with relatively lower Cr content, indicating that the high Al containing alloys would realize less susceptibility of irradiation embrittlement without sacrificing the oxidation resistance. Based on the results, a revised development of Phase II ATF FeCrAl alloys with minor alloying additions (Al, Zr, Y, Mo) were initiated and the optimization of the alloy compositions will continuously be conducted in FY 2015.

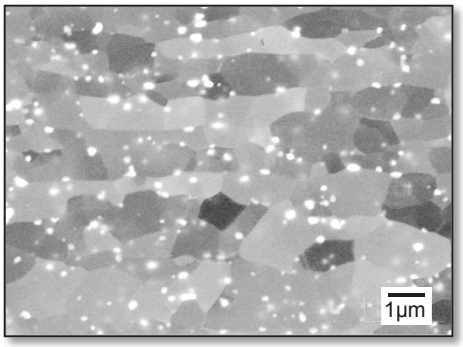

Figure 36. SEM-BSE image of C35MN with controlled sub-grain structure. The bright particles correspond to Fe_2(Mo,Nb) Laves phase precipitates.

Oxide dispersion strengthened (ODS) FeCrAl alloys are being developed with optimum composition and properties for accident tolerant fuel cladding. Two ODS Fe-15Cr-5Al-0.5Ti+Y_2O_3 alloys were fabricated by ball milling and extrusion of gas atomized metallic powder mixed with Y_2O_3 powder. To assess the impact of Mo on the alloy mechanical properties, one alloy contained ~1wt% Mo. As can be seen in Figure 37a, the yield strengths of the 155YT and 155YMT alloys were very similar, and significantly higher than the yield strengths of advanced Zircaloy-4 and wrought FeCrAlY alloys. The alloy yield strengths were also superior to the fine grain ODS PM2000, particularly at temperature > 600ºC. These high tensile properties are likely due to the combination of a very fine grain structure and the presence of nano oxide precipitates. The total plastic deformations at rupture for the 155Y(M)T alloys were, however, lower than the deformations for the Zircaloy-4 and wrought FeCrAlY alloys in the 10 to 20% range at all temperatures (Figure 37b). To estimate the maximum temperature of use for the two alloys in steam, ramp tests at a rate of 5ºC/min were carried out in steam. Like other ODS alloys, the two alloys showed a significant increase of the mass gains at ~ 1380ºC compared with ~1480ºC for wrought alloys of similar composition. The beneficial effect of yttrium for wrought FeCrAl does not seem to be effective for most ODS FeCrAl alloys. An Fe-12Cr-5Al+Y2O3 +ZrO2 ODS alloy fabricated for a different project exhibited similar tensile properties and oxidation resistance as the 155Y(M)T alloys, but better creep properties at 800ºC. A lower Cr, high strength ODS alloy with a higher maximum use temperature should be achievable.

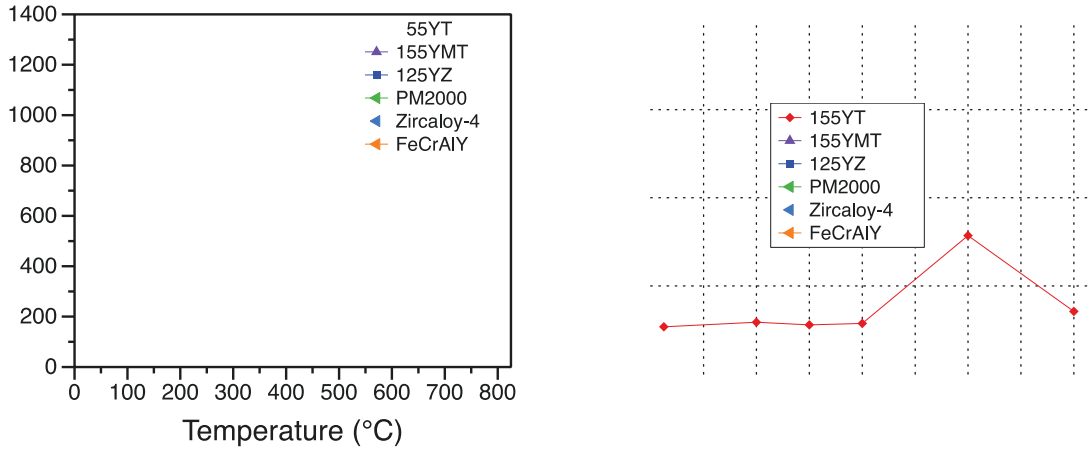

Figure 37. a) Comparison of the tensile properties of the two 155Y(M)T ODS alloys with the tensile properties of Zircaloy-4 alloy [3], an advanced wrought FeCrAlY alloy, ODS fine grain PM2000 [4], and an Fe-12Cr-5Al+Y2O3 +ZrO2 ODS alloy, a) Yield strength and b) Total plastic deformation

Publications

1. B. A. Pint, S. Dryepondt, K. A. Unocic and D. T. Hoelzer, (2014) "Development of ODS FeCrAl for Compatibility in Fusion and Fission Applications," submitted to JOM.
2. K. A. Unocic, D. T. Hoelzer and B. A. Pint, "The Microstructure and Environmental Resistance of Low-Cr ODS FeCrAl," Materials at High Temperature, in press.

References

1. L. L. Snead, Y. Yamamoto, K. A. Terrani, B. A. Pint, "Development of Oxidation Resistant Iron Alloys for LWR Cladding," Proceedings of the LWR Fuel Performance Meeting (TopFuel 2013), Sep. 15-19, 2013, Charlotte, NC.
2. C. S. Wukusick, J. F. Collis, "An Iron-Chromium-Aluminum Alloy containing Yttrium," *Materials Research and Standards*, December 1964, 637-646.
3. S. K. Kim, J. G. Bang, D. H. Kim, I. S. Lim, Y. S. Yang, K. W. Song, D. S. Kim, *Nuclear Engineering and Design,* 239, 2009, 254.
4. P. Schwarzkopf, PM 2000, "Sheet Grain Class 4 ODS Iron Alloy Sheet," Material Property Datasheet, Material No.: 1.4768, Abbreviated DIN name: CrAI 21 6.

2.4.2 Scale-up and Tube Fabrication

L. Snead, Y. Yamamoto, Oak Ridge National Laboratory

Parallel to the property evaluation of the down-selected Phase II alloys (C35MN, Fe-13Cr-5Al-2Mo-1Nb-0.2Si-0.05Y, wt.%), the process development of thin-wall tube fabrication of the FeCrAl alloys was pursued which utilized commercially available processing steps. Potential commercialization processes of tube fabrication include casting, forging/rolling, piercing, extrusion, swaging, drawing, pilgering, and heat treatments. The current work package mainly focuses on coordinating of the thin-wall tube manufacturing by using commercial companies who has capability to provide vacuum induction melting up to 500 lbs., and thin-tube manufacturing via cold or warm drawing process. The vacuum induction melt ingot with 3.4" diameter x 18" length was prepared by Sophisticated Alloys, Inc., Butler, PA. The ingot was homogenized at 1200ºC, and then machined two billets with a hole, and then hot-extruded with a mandrel at 1150ºC to make master tubes with 1.5" outer diameter x 0.3" wall thickness x 38-40" length, processed

at ORNL (as shown in Figure 38). The master tubes were sent to Rhenium Alloys, Inc., North Ridgeville, OH, for surface machining prior to the drawing process, and then they were pre-annealed for solution heat treatment (see Figure 39). The tube drawing is currently in progress at the same manufacturer. The expected delivery date is in October 2014.

Figure 38. Master tube fabrication sequence conducted at ORNL.

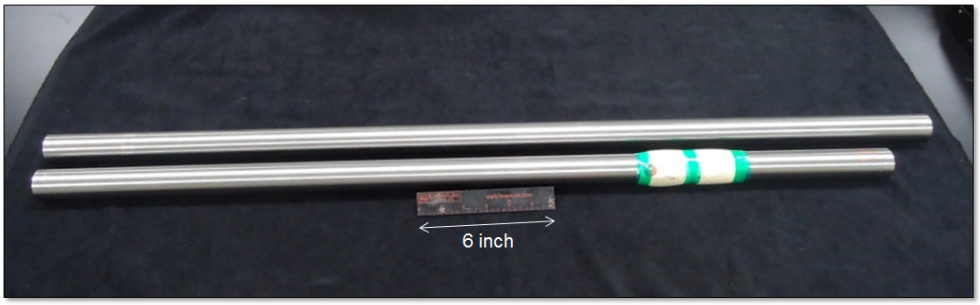

Figure 39. Machined master tubes at Rhenium Alloys, Inc. prior to tube drawing process.

2.4.3 Tube Development

Maloy, Yamamoto, Los Alamos National Laboratory

Initial tube drawing studies were performed on Phase I alloys (T35: Fe-13Cr-4.5Al-0.15Y, T54:Fe-15Cr-4.0Al-0.15Y) through a subcontract with Century Tubing (San Diego, CA). Solid rods originally ~10 in. long and 1 in. in diameter were supplied by ORNL, center drilled and drawn over a mandrel to fabricate thin-walled tubing. Approximately 16 cold reduction passes were performed over a mandrel through a carbide die of 14-24% reduction per pass. Intermediate anneals were performed at 850ºC in hydrogen. Final dimensions obtained were 10 ft long with a 0.374 inch outer diameter and 0.014 inch wall thickness. Figure 40 shows the final tubing produced by Century Tubing.

Figure 40. Photo showing tubing produced from Phase 1 FeCrAl alloys by Century tubing (from left to right, Chris Truong, Vincent Le, Ly Pham, Joe Carr, Dave LaBerge and Dan Tran).

2.4.4 Weld Development for Thin-walled FeCrAl Cladding

J. Gan, Idaho National Laboratory

The weld development of thin-walled FeCrAl alloy cladding is important in support of LWR ATF development. R&D was conducted to join the endplug to thin-walled FeCrAl alloy cladding to result in a configuration consistent with current LWR fuel pins and adequate for fuel pin fabrication. Two level-3 milestone reports were completed in FY 2014. Both laser weld (fusion based) and pressure resistance weld (solid state joining without melting) were under investigation to achieve strong bond strength along both radial and axial dimensions at the weld without significant degradation of the material microstructure in the weld-affected zone. It was found that the optimal weld parameters for laser weld established in FY 2013 work for the cladding of 250 micron wall thickness was not applicable for the thicker cladding (350 micron) in FY 2014 work. An iteration of laser weld studies was performed to identify the optimal parameters with good heat penetration and minimum material loss from ablation.

A cross sectional optical micrograph of a laser welded ORNL Gen-2 FeCrAl thin plate in a butt joint configuration is shown in Figure 41(top). The dark contrast revealing the weld zone confirmed that joining from both sides is achieved with limited material loss from ablation. The laser weld of emulated thin-wall cladding fabricated from ORNL Gen-2 FeCrAl alloy will be performed and tested in the 1st quarter in FY 2015. Preliminary test results for pressure resistance welding (PRW) on a commercial FeCrAl alloy (Kanthal-D) is shown in Figure 41(bottom). A cut-off view from a 3D X-ray CT scan revealed severe deformation of thin-wall cladding at the weld zone as a result of excess applied pressure. It is a significant challenge to identify the optimal parameters for PRW to establish a strong bond without creating undesired deformation in the heat-affected zone.

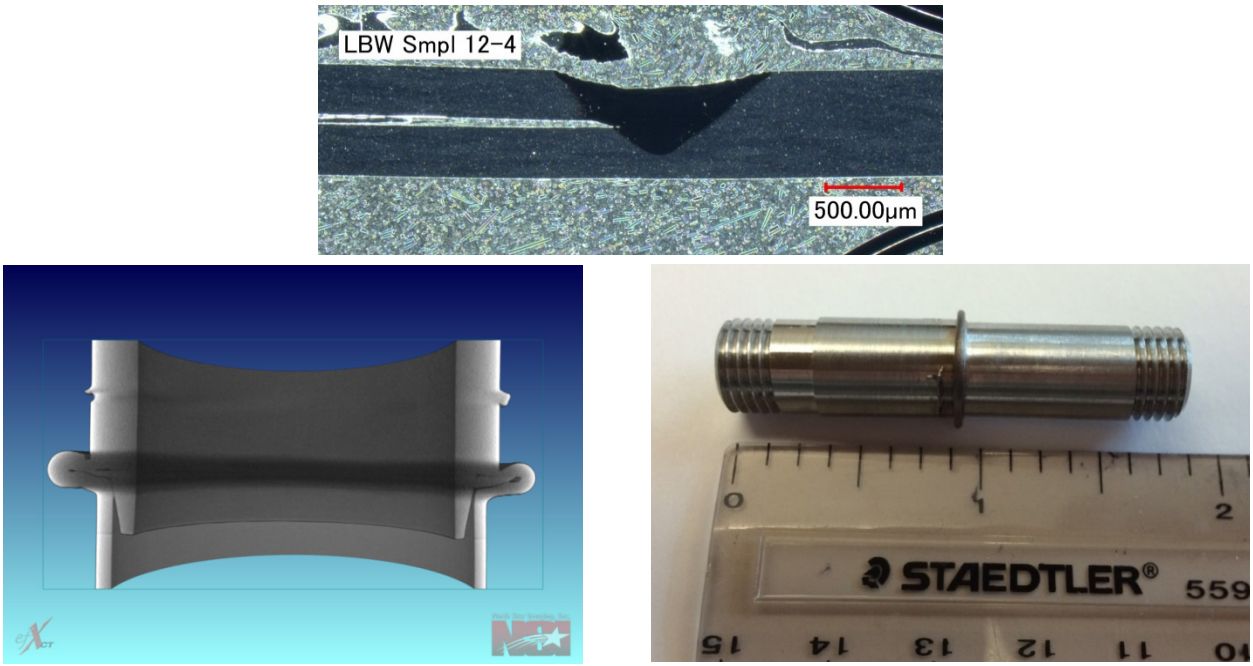

Figure 41. (Top) Optical cross section view of a laser welded set of ORNL Gen-2 FeCrAl thin plates where dark contrast indicates the weld zone. (Bottom left) A cut-off view from 3D X-ray CT scan of a pressure resistance welded commercial FeCrAl (Kanthal-D) emulated thin-wall cladding revealing the deformed region of the cladding at the joining point due to excess applied pressure; (bottom right) a photo of the welded section..

2.4.5 Welding Development of ATF FeCrAl

K. G. Field, Oak Ridge National Laboratory

The development of test rodlets for the ATF-1 irradiation campaign includes developmental welds used to create hermetic seals. Three welds are utilized: two circumferential welds, which metallurgically bond the top and bottom caps to the rodlet tube, and a spot closure weld on the top cap to seal in the He back-fill gas. A down-selected FeCrAl alloy, C35MN5-B, was subjected to welding and destructive testing to evaluate the unirradiated performance of well-controlled welds in an engineering grade FeCrAl alloy. Plate sections of the C35MN5-B alloy were welded in accordance with developed parameters. Four guided bend test specimens and five SS-J3 specimens were fabricated for destructive testing. Welding resulted in a loss of strength and ductility, as reported in Field et al. [1]. Two face and two root bend tests were conducted; these tests showed satisfactory results. Successful completion of the initial destructive testing allowed for completion of final prototype testing before full fabrication of rodlets for the ATF-1 irradiation campaign. Shortened rodlets were welded in correspondence with the fabrication protocols developed for the ATF-1 irradiation; Figure 42 shows an example of the weld prototypes. Prototype parts were He leaked checked with leak rates less than 8.5×10^{-8} std. cc/s. Hydrostatic loading of the parts indicated no failure or deformation at either weld. These results indicate that the C35MN alloy can be successfully welded using the ATF-1 joint geometries.

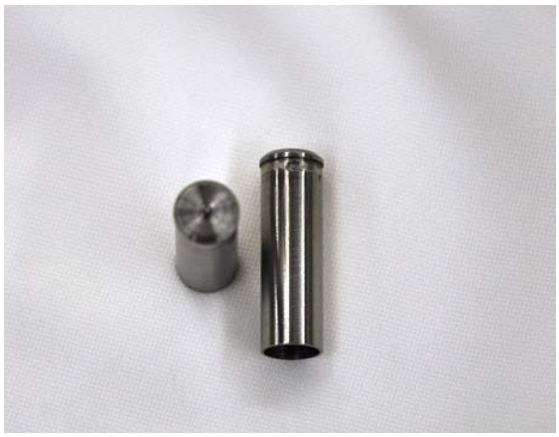

Figure 42. Prototype parts showing closure welds and electron beam circumferential welds.

References

1. K. G. Field, M. N. Gussev, Y. Yamamoto, L. L. Snead, "Deformation Behavior of Laser Welds in High Temperature Oxidation Resistant Fe-Cr-Al Alloys for Fuel Cladding Applications," *Journal of Nuclear Materials*. 454(1-3), November 2014, 352–358, ISSN 0022-3115, http://dx.doi.org/10.1016/j.jnucmat.2014.08.013

2.4.6 Characterization and Properties of LWR ATF cladding

O. Anderoglu, Los Alamos National Laboratory

Ferritic FeCrAl-based alloys are highly resistant to oxidation due to formation of stable oxide scale at elevated temperatures. Therefore, they are considered to be promising candidate materials for accident tolerant cladding. In this project, tensile testing of 1st and 2nd generation nuclear grade ferritic FeCrAl alloys developed at ORNL was completed at room temperature, 300°C, and 600°C. In addition, tensile testing of thin-walled tubes of FeCrAl alloys was also completed at the same temperatures as seen in "a" Figure 43. The alloys show the typical tensile behavior expected from ferritic steels. Uniform elongation is >20% at room temperature and 300°C. The inset in (a) is an SEM image of the fracture surface of the sample tested at room temperature, showing dimples on the surface. EBSD analysis in "b" Figure 43 shows that the tube microstructure contains mostly large grains of 100-150 μm. No significant texture is observed in thin-walled tubes. In summary, the newly developed nuclear grade FeCrAl alloys show good mechanical properties and microstructure for LWR cladding applications.

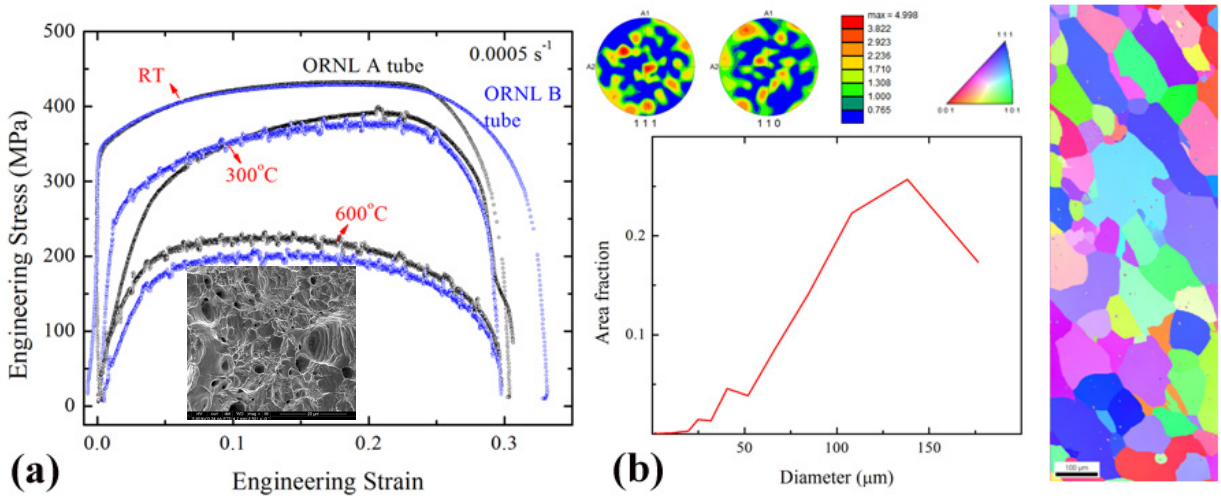

Figure 43. (a) Tension test results on two thin walled tubes of FeCrAl alloys, ORNL A and B show good strength and ductility at elevated temperatures. The SEM image of the fracture surface shows dimples which are characteristics of ductile failure. (b) EBSD results show distribution of grains mostly of 100-150μm. No significant texture is observed in the thin walled tubes.

2.4.7 Molybdenum LWR Clad Development through CVD Processing

S. Maloy, D. Devlin, I. Usov, Los Alamos National Laboratory

Molybdenum (Mo) and its alloys are considered promising candidates for accident tolerant nuclear fuel cladding. The most attractive properties of Mo are its high strength, high creep resistance and moderate stability in water vapor at elevated temperatures. It is believed that mechanical and radiation tolerance properties can be improved even further for high purity and grain refined Mo. Currently, the major hurdle in industrial applications of Mo is a lack of a fabrication method for thin wall (~ 0.25 mm) and fine grain (submicron grain size) tubing. Conventional metallurgical methods failed to produce Mo with appropriate mechanical strength. Mo tubing fabrication using fluidized bed chemical vapor deposition (FBCVD) processing was proposed and is under investigation.

The conditions for FBCVD of Mo using the $MoCl_5$ as a precursor have been explored in FY 2014, including temperature, precursor concentration and fluidizing conditions. We have shown that isotropic material with microstructures identical to those obtained from fluidized bed carbon deposition can be achieved. Figure 44 shows a thick-wall free-standing Mo tube with a dense granular microstructure. Figure 45 shows a Mo deposit under conditions resulting in continuous nucleation and a grain refined isotropic microstructure. Through FY 2014 research a more complete understanding of the tube growth process has been developed, providing indication of possible directions to further evaluate the process:

1. Investigate methods of separating nucleation and growth processes. The simplest approach is to look at the effect of lowering the reaction temperature and increasing the reactant concentration. The point here is to increase the gas phase particle nucleation rate while reducing the surface reaction rate. It is believed that this will lead to a dense smooth microstructure.
2. Investigate substrate surface conditions. It is clear that this process is very sensitive to surface roughness.
3. Borosilicate glass tubing has a smooth surface and a coefficient of thermal expansion (CTE) close to Mo. Glass tubing may make an ideal substrate for deposition and should be further explored.

The combination of these two effects, nucleation vs. growth and surface roughness, may be sufficient to achieve the desired microstructure at a reasonable deposition rate.

Figure 44. A thin walled free-standing Mo tube produced using FBCVD.

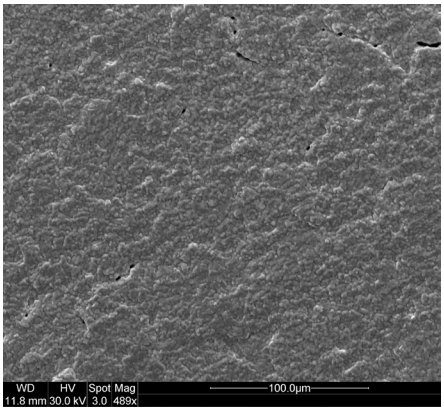

Figure 45. Grain refined isotropic Mo deposited by FBCVD.

Publications

1. Nelson, A.T., E.S. Sooby, Y.J. Kim, B. Cheng, and S.A. Maloy, "High temperature oxidation of molybdenum in water vapor environments," *Journal of Nuclear Materials*, 448(1-3), 2014, 441-447.

2.4.8 SiC Joining and End-Plug Technology Development

L. Snead, Y. Katoh, Oak Ridge National Laboratory

Development of robust SiC joints that retain adequate structural and functional properties in the anticipated service environment is a critical milestone toward establishment of advanced SiC composite technology for the accident tolerant fuels and core structures. During the present reporting period, the following tasks achieved significant progress toward this overarching goal.

1) Joining technology development – fabrication processes for robust joints of SiC ceramics and composites were successfully developed utilizing the transition metal diffusion routes and the pressure-less transient eutectic phase route [1,2]

2) Test technology development – significant progress was made in development of test standards for shear strength of flat ceramic joints in ASTM Committee C28 [3]; moreover, designing and evaluation of new test methods for joints in end plug-relevant configurations were initiated

3) Environmental effects – planning and specimen preparation were completed for testing of candidate joints in the Severe Accident Test Station

4) Irradiation effects – a collection of SiC joint torsional shear specimens were prepared; irradiation vehicles were designed, constructed, and safety approved; neutron irradiation in the High Flux Isotope Reactor was initiated [4]

5) Industrial interactions – coordination, guidance, and assistance were provided to the end plug technology development programs in DOE-funded industries.

Note that the irradiation study task was supported by the Light Water Reactor Sustainability Program during FY 2014. All technical tasks will be continued in FY 2015 under the Advanced Fuels Campaign.

Systematic Technology Evaluation Program for SiC-based LWR Fuel Cladding

The initial technical plan for the "Systematic Technology Evaluation Program for SiC/SiC Composite Accident Tolerant LWR Fuel Cladding and Core Structures" was developed and published[5]. The primary objective of the planning was to develop a blueprint of a technical program that addresses the critical feasibility issues; assesses design and performance issues related with manufacturing, operating, and off-normal events; and advances the technology readiness levels in essential technology elements for SiC/SiC composite-based LWR fuel cladding and core structure concepts. A web-assisted SiC ATF Technology Workshop was organized in February 2014, the outcome of which was incorporated in the program plan.

The planning exercise consists of three main tasks: technology review, critical technology gap analysis, and technical program planning. Various technical gap issues were identified during the technology review process and the analysis revealed that many of them are related to three key feasibility issues for SiC/SiC composite fuel cladding: hydrothermal corrosion, cracking failure, and fuel-clad system compatibility. Additional very important gap issues have also been identified and analyzed. The technical program plan was designed to systematically address these key technology gaps and feasibility issues, and then lay out the tasks in a work breakdown structure (WBS), which consists of three top level categories: Design and Failure, Environmental Effects, and Off-normal Behavior. Simultaneously, the plan attempts to set an early technical program toward advancing the technology readiness levels of essential technologies in these three areas.

References

1. T. Koyanagi, J. Kiggans, C. Shih, and Y. Katoh, "Processing and characterization of diffusion-bonded silicon carbide joints using molybdenum and titanium interlayers," *Ceramic Engineering and Science Proceedings*, (accepted for publication).
2. T. Koyanagi, J. Kiggans, C Shih, Y. Katoh, "Pressureless joining of sic by transient eutectic-phase method," *Transactions of the American Nuclear Society,* 110 (2014).
3. C. Shih, Y. Katoh, J. Kiggans, T. Koyanagi, H.E. Khalifa, C.A. Back, T. Hinoki, M. Ferraris, "Comparison of shear strength of ceramic joints determined by various test methods with small specimens, ceramic engineering and science proceedings," (in press).

4. Y. Katoh, L.L. Snead, T. Cheng, C. Shih, W.D. Lewis, T. Koyanagi, T. Hinoki, C.H. Henagar, M. Ferraris, "Radiation-tolerant joining technologies for silicon carbide ceramics and composites," *Journal of Nuclear Materials*, 448, 2014, 497-511.

5. Y. Katoh, K.A. Terrani, L.L. Snead, ornl/tm-2014/210, Revison 1, "Systematic technology evaluation program for sic/sic composite-based accident-tolerant LWR fuel cladding and core structures," 2014.

2.4.9 MELCOR for Modeling of Advanced Cladding Performance Under Accident Conditions

B. Merrill, S. Bragg-Sitton, P. Humrickhouse, Idaho National Laboratory

Scoping simulations performed using a severe accident code can be applied to investigate the influence of advanced materials on beyond design basis accident progression and to identify any existing code limitations. In FY 2012 an effort was initiated to develop a numerical capability for understanding the potential safety advantages that might be realized during severe accident conditions by replacing Zircaloy components in LWRs with silicon carbide (SiC) components. To this end, a version of the MELCOR code, under development at Sandia National Laboratories in New Mexico (SNL/NM), was modified by replacing Zircaloy for SiC in the MELCOR reactor core oxidation and material properties routines. The modified version of MELCOR was benchmarked against available experimental data to ensure that present SiC oxidation theory in air and steam were correctly implemented in the code. When exposed to a steam environment, SiC exhibits linear volatilization of the SiO_2 that forms on the surface in addition to the parabolic oxidation of the base SiC. Additional modifications have been implemented in the code in FY 2013 and 2014 to improve the specificity in defining components fabricated from non-standard materials. INL has focused on applying this modified MELCOR code to the Three Mile Island Unit 2 (TMI-2) LOCA for SiC-based and FeCrAl-based cladding designs.

Following the initial study that directly substituted CVD SiC for Zircaloy in the PWR simulation, additional work has been completed that allows the user to define both SiC and SiO_2 as unique cladding materials, in addition to Zircaloy, ZrO_2, and Inconel, in both the core physics and materials properties data packages. These modifications also allow the user to apply the properties for CVD SiC and its oxide (silica) or to override these properties with more appropriate values for their application. In this version, the user controls the mass of SiC in the cladding for each core volume. The logic for this modified version of MELCOR assumes SiC to be the outermost material on the cladding surface in that core volume, or the entire cladding composition if no other cladding material is requested by user input. This allows the user to model the SiC as a coating or wrap on the base metallic cladding, or as the cladding material alone, while not affecting the Zircaloy in any other core component or any other core volume of a user's model. When SiC is present as a composite cladding material, the rod failure criterion is changed from that of Zircaloy to the decomposition temperature of SiC. For SiC-coated or wrapped cladding, the code reverts back to Zircaloy oxidation equations and failure and candling criteria if the SiC were to be lost from the surface, for example by oxidation in steam. Upon rod failure, the SiC in that volume enters the debris field in the same volume, where it continues to undergo further oxidation by steam. This modification required considerable changes to MELCOR's material oxidation logic and oxidation routines.

The success of the modifications made for SiC during FY 2013 allowed INL to easily create a second version in FY 2014 for materials that exhibit only parabolic oxidation behavior with both air and steam. This version uses FeCrAl as a new default cladding material option. Like the SiC version, the user can model FeCrAl as a cladding coating, or as the cladding material alone, for any given region of the core

though user input. If the user desires to use a different cladding material option, then the FeCrAl material and oxidation properties can be overridden through user input, as long as the oxidation process for this new material is parabolic.

Work to modify MELCOR has resulted in a numerical capability for understanding some of the potential safety advantages of SiC and FeCrAl over Zircaloy for the cladding of fuel rods during LWR severe accident conditions. The SiC version of MELCOR was successfully benchmarked against experimental data to ensure that present SiC oxidation theory in air and steam were correctly implemented in the code. More recent SiC data is now available, but benchmarking of the modified MELCOR against this experimental data has not been completed. The same is true for the FeCrAl modified version of MELCOR.

2.5 Advanced LWR Fuels Irradiation Testing

2.5.1 Light Water Reactor Accident Tolerant Fuels Irradiation Testing

K. Barrett and H. MacLean Chichester, Idaho National Laboratory

The mission of the ATF-1 experiments is to test novel fuel and cladding concepts designed to replace the current zirconium alloy-uranium dioxide (UO_2) fuel system. The objective of this R&D is to develop novel ATF concepts that will be able to withstand loss of active cooling in the reactor core for a considerably longer time period than the current fuel system while maintaining or improving the fuel performance during normal operations, operational transients, design-basis, and beyond design-basis events [1].

Accomplishments

Irradiation testing in support of ATF-1 included:

1) Purchase and receipt of a GE-100 cask for shipments between the ATR and the Materials and Fuels Complex (MFC)
2) Design, analysis, and fabrication of drop-in capsule ATF-1 series experiments
3) Preparation for irradiation testing of ATF-1 capsules in the ATR
4) Kick-off meeting for design of ATF-2 water loop experiments.

Prior to initiating test specimen design in FY 2014, an ATF Quality Implementation Plan (QIP) was issued to provide guidance to experimenters, engineers, and the fabrication and inspection teams to meet Program expectations.

The ATF-1 drop-in capsule experiments were designed and analyzed in FY 2014 to perform irradiation testing in four ATR small-I positions. These positions were identified to perform irradiation tests under prototypic LWR temperatures and powers.

During the experiment design phase, a sensitivity analysis was performed to identify the most critical parameters for experiment design and risk assessment. Results showed that internal rodlet pressure calculations are most sensitive to fission gas release rate uncertainty while temperature calculations are most sensitive to cladding I.D. and O.D. dimensional uncertainty. The analysis showed that stress calculations are most sensitive to rodlet internal pressure uncertainties; however, the results also indicated

that uncertainties in the inner radius, outer radius, and internal pressure were all magnified as they propagate through the stress equation [2].

Fabrication and inspection of the ATF-1 FOA and ORNL experiments was completed in FY 2014 and five ATF baskets were fabricated and shipped to ATR in preparation for irradiation testing.

As-built projected temperature calculations were performed on the ATF capsules using the BISON fuel performance code. BISON is an application of INL's Multiphysics Object-Oriented Simulation Environment (MOOSE), which is a massively parallel finite element-based framework used to solve systems of fully-coupled nonlinear partial differential equations. Both 2D and 3D models were set up to examine cladding and fuel performance. As-built axial and radial dimensions were measured on each rodlet tube using a Coordinate Measurement Machine (CMM). The CMM data were directly imported into the BISON model and 3D temperature profiles were calculated. Figure 46 and Figure 47 show the preliminary BISON results for one of the ATF-1 concepts. The as-built 3D temperature profiles can then be used to determine if the rodlet clad temperatures (axial and azimuthal) are with the desired test range for the ATF concept design.

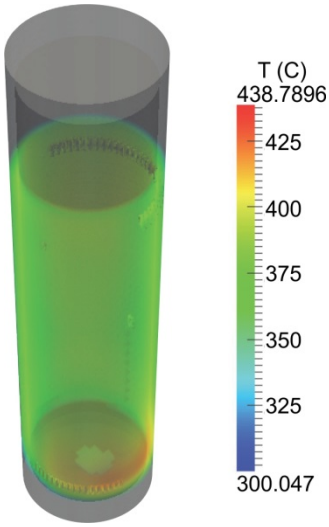

Figure 46. Volumetric view of temperature with a threshold of 300 - 450C.

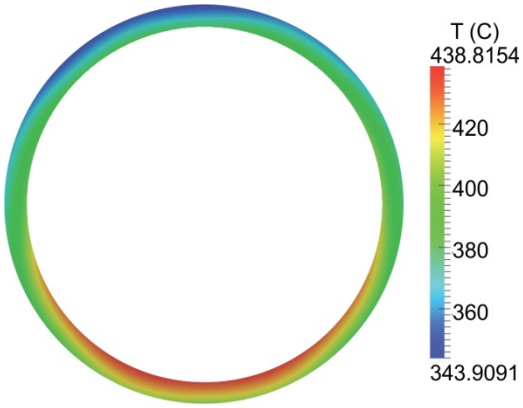

Figure 47. Radial slice of temperature in the cladding at a height of 0.125 inches.

Unfortunately, ATR experienced an operational malfunction in September 2014 leading to an unplanned outage. The malfunction required significant repair/maintenance preventing the ATF-1 capsules from

initial insertion and irradiation testing in FY 2014. However, the capsules are ready for insertion and will begin irradiation testing once ATR is operational.

ATF-2 Loop Experiment

The kick-off meeting for the Accident Tolerant Fuels Loop Design (ATF-2) was held August 25, 2014 at INL. The ATF test plan includes ATR water loop testing starting in FY 2017. In preparation, the test train design will be based, in part, on industry FOA team needs, utility constraints, and ATR Water Loop operational requirements. The purpose of the meeting was to identify loop testing needs from industry partners, constraints from utilities, and operational requirements from ATR.

The three industry teams presented their objectives and testing needs. A draft "testing needs" matrix was developed and will be vetted with the attendees. Some of the overall issues included Nuclear Regulatory Commission (NRC) licensing requirements for a full range of data. The matrix will be used to begin ATF-2 test train conceptual design in FY 2015.

Future Work

ATF-1 experiment capsules will continue irradiation in FY 2015. An existing INL Nuclear Science and Technology database platform is being modified for application to the ATF program. The database will be designed for material and data traceability to each ATF experiment assembly. The database was originally developed at INL for another ATR project; therefore, the scope of work and cost will be significantly reduced compared to development of a new database platform.

New ATF-1 experiment concepts will be designed and analyzed for ATR insertion FY 2015 and FY 2016. The ATF-2 water loop test train will be designed and analyzed in FY 2015. Fabrication will begin in FY 2016 and insertion is planned for early FY 2017.

References

1. *Roadmap: Development of Light Water Reactor Fuels with Enhanced Accident Tolerance*, Idaho National Laboratory Report, INL/EXT-12-25305, September 2012.
2. Barrett, K. E., Ellis, K. D., C. R. Glass, G. A. Roth, and M. P. Teague, "Critical Processes and Parameters in the Development of Accident Tolerant Fuels Drop-In Capsule Irradiation Testing," in review for submission to the *Journal of Nuclear Materials*.

2.5.2 Irradiation Stability of ATF FeCrAl

K. G. Field, Oak Ridge National Laboratory

The iron based FeCrAl alloy system has the potential to form an important class of accident tolerant cladding materials. However, past experience on ferritic Fe-Cr based alloys indicates possible instabilities in the microstructure due to neutron irradiation. Previous research shows an as-irradiated microstructure evolution that includes dislocation loops, void/bubbles, and precipitation of second phases. These defects can significantly alter the mechanical properties at LWR-relevant irradiation conditions. However, the trends associated with the formation of these defects in Fe-Cr-Al alloys have not been fully established. To investigate the irradiation-induced microstructural evolution as a function of alloy composition, 180 tensile specimens of SS-J2 geometry were manufactured and validated for a neutron irradiation campaign. These tensile samples consisted of a series of four model and two commercial Fe-Cr-Al alloys with 10-22 wt.% Cr and 2.9-4.9 wt.% Al. The samples were irradiated in the High Flux Isotope Reactor (HFIR) at temperatures between 340°C and 387°C at doses between 0.3 and 16 dpa. At this time, 108 samples have completed their irradiation cycle with the maximum dose of 1.6 dpa. Mechanical testing of 36 sub-size

non-irradiated and irradiated tensile specimens at room temperature indicates radiation-induced hardening is apparent in all alloys including the model and commercial alloys such a Kanthal K720. Radiation-induced hardening typically corresponded to a marked decrease in the ductility parameters of the alloys.

A subset of specimens including all the model alloys irradiated at 387 °C to 1.6 dpa were selected for extensive post-irradiation examination using advanced characterization techniques. Small angle neutron scattering and atom probe tomography was used to quantify the formation of Cr-rich α' precipitates, while scanning transmission electron microscopy was used to quantify the dislocation loop density and size. Results indicate precipitation of Cr-rich α' is dependent on the bulk Cr composition with the number density being most sensitive to Cr composition. Dislocation loops with Burgers vector of $a/2\langle 111\rangle$ and $a\langle 100\rangle$ were detected and quantified. A radiation induced hardening model was developed based on the dispersed barrier hardening model. This model indicated that the change in yield strength, after irradiation is dominated by the large number density of Cr-rich α' precipitates. Based on these results it is concluded that the stability of Fe-Cr-Al alloys in the presence of neutron irradiation is dependent on the Cr composition, with reductions in Cr content significantly improving the performance of the alloys after irradiation.

ORNL ATF-1 Rodlet Manufacturing, FeCrAl Cladding

The primary objective of the ATF-1 irradiation campaign is to determine the behavior of select ATF systems under prototypical neutron irradiation environments. The irradiation campaign seeks to determine the compatibility between the fuel and the proposed metallic claddings or coatings as a function of neutron irradiation. A second objective is to determine the mechanical and physical behavior of the metallic cladding after irradiation, including the rodlet endcap weld performance and durability and pellet/clad mechanical interaction.

To meet these objects, three miniaturized rodlets (with near 17x17 PWR radial geometries) were developed, fabricated, and delivered for the ATF-1 irradiation. These rodlets utilized a Fe-Cr-Al alloy clad material with the nominal composition of Fe-13Cr-5.2Al-2Mo-0.2Si-1Nb-0.15Y, also known as ORNL heat C35MN. This exploratory alloy is a fine-grained, Fe-Cr-Al alloy that has displayed excellent mechanical properties and high temperature stability. It is anticipated, based on fundamental research executed on Fe-Cr-Al alloys through the ATF program [1], that this particular alloy will have acceptable radiation tolerance due to the reduced Cr content while still having acceptable oxidation resistance due to the increased Al content. Through the fabrication process of the rodlets, the weldability of this alloy heat was successfully demonstrated for the weld geometries investigated. The rodlets were fueled with commercial UO_2 to provide a fuel-clad system closely representative of the envisioned ORNL ATF concept. A radiograph of the assembled rodlets is provided in Figure 48. These rodlets were delivered to INL in September 2014 for insertion into the ATR. Future post-irradiation examination plans, currently in-development between ORNL and INL, will investigate radiation tolerance of the cladding material, fuel-cladding chemical interactions, and performance of the developmental welds. As such, the development and irradiation of these rodlets will facilitate future research into the applicability of engineering grade Fe-Cr-Al alloys for accident tolerant applications.

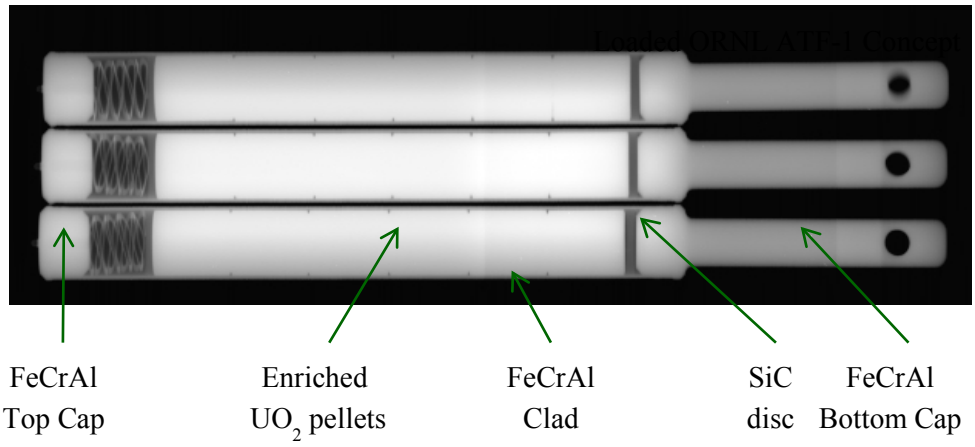

Figure 48. Radiograph of ORNL ATF-1 rodlets after completion of fabrication prior to delivery. Length of rodlet in image is 4.5 inches, nominal.

References

1. K.G. Field, X. Hu, K. Littrell, Y. Yamamoto, R.H. Howard, L.L. Snead, *Stability of model Fe-Cr-Al alloys under the presence of neutron radiation*, FY-14 FCRD Milestone Report: ORNL/LTR-2014/451, September 2014, http://www.osti.gov/scitech/biblio/1157142.

2.5.3 Irradiation Performance of Microencapsulated Fuels

L.L. Snead, Oak Ridge National Laboratory

PIE of a High-Flux Isotope Reactor (HFIR) irradiated sample of microencapsulated fuel that was neutron irradiated to ~7.5E25 n/m^2 (E>0.1 MeV) was completed. Data was generated on dimensional change, thermal conductivity, and irradiation-induced microstructural changes. A summary of results has been published [1]. Additionally, the negligible reaction of matrix SiC with Zircaloy was studied as part of this work. Figure 49 shows a micro-tomography image of the highest-dose irradiated sample of this series indicating a complete lack of decohesion of the TRISO layers due to the irradiation and the stability of the SiC-based matrix, both of which were concerns motivating the study.

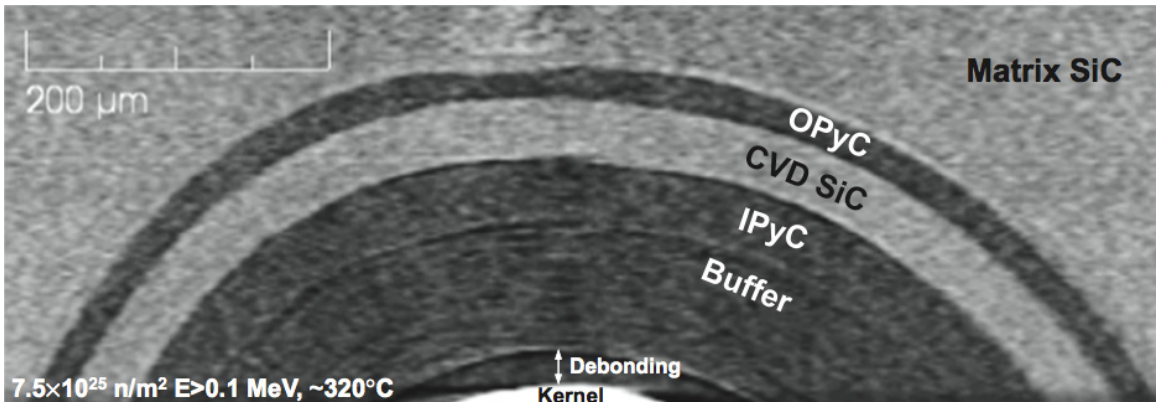

Figure 49. Post irradiation examination of HFIR irradiated sample

References

1. L. L. Snead, K. A. Terrani, Y. Katoh, C. Silva, K. J. Leonard, and A. G. Perez-Berbquist, "Stability of SiC-matrix microencapsulated fuel constituents at relevant LWR conditions," *Journal of Nuclear Materials,* 448, 2014, 389-398.

2.5.4 Fabrication and Assembly of ATF-1

G. Moore, C. Woolum, Idaho National Laboratory

Fabrication of ATF test capsules was performed at INL using fuel pellets provided by AREVA, GE, and Westinghouse. Pellet preparation procedure included ultrasonic cleaning followed by vacuum degassing. Rodlets were either provided by vendors or fabricated on-site at INL; rodlet composition varied by capsule and is listed in Table 6. The rodlets were loaded with fuel pellets, and endcaps were welded onto the rodlets. Rodlets were encapsulated in a SS316L capsule and endcaps welded into place. Welding of both the rodlets and capsules was performed using an Arc Machines Inc. (AMI) orbital welder in a helium environment (Figure 50a).

The certification process includes dimensional analysis, a helium leak check, leak penetration testing, visual inspections, and radiography. Both the rodlet and capsule components undergo dimensional inspection using a Brown and Sharp Coordinate-Measuring Machine (CMM) (Figure 50b). A helium leak check is performed on the rodlet once it has been welded. Liquid penetrant testing is performed on the welded capsule assemblies. Visual inspections and digital radiography are performed after welding on both rodlets and capsule assemblies (Figure 50c).

Seven capsules were certified for insertion into ATR in accordance with the ATF-1 milestone. The capsules qualified for insertion are identified in Table 6. These capsules include 3 capsules of AREVA pellets, 1 capsule of GE pellets, and 3 capsules of Westinghouse pellets. This serves as the initial irradiation experiment of capsule assemblies for advanced fuel and cladding concepts, the first of many such experiments planned with industry, national laboratory, and university partners. Successful completion of these experiments allows for a unique opportunity to grow partnerships with industry. These ATF experiments will provide the qualification data necessary to prepare for commercial irradiation of a lead fuel rod/assembly in 2022.

Table 6. ATF-1 capsule assemblies qualified for insertion into ATR.

Capsule ID	Rodlet ID	Fuel Material	Rodlet Material
ATF-01	A02	AREVA UO_2	Zircaloy-4
ATF-04	A05	AREVA UO_2-Diamond Particles	Zircaloy-4
ATF-05	A06	AREVA UO_2-Diamond Particles	Zircaloy-4
ATF-06	G01	GE UO_2	Alloy 33
ATF-10	W01	Westinghouse U_3Si_2	Zirlo (Zircaloy-4 caps)
ATF-12	W03	Westinghouse U_3Si_2	Zirlo (Zircaloy-4 caps)
ATF-14	W05	Westinghouse U_3Si_2	Zirlo (Zircaloy-4 caps)

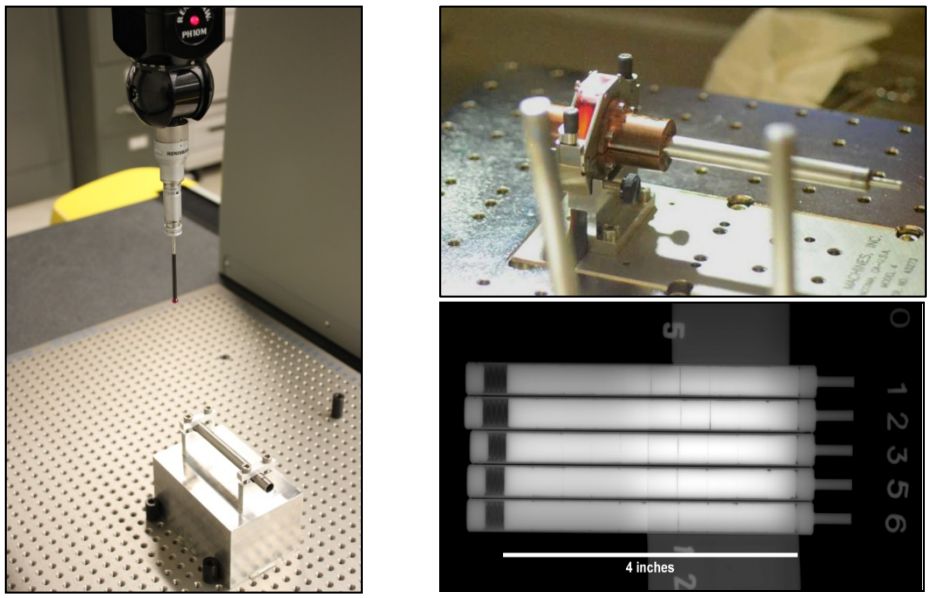

Figure 50. Preparation of ATF-1 capsules (a) AMI orbital welder; (b) Coordinate-Measuring Machine (top); and (c) digital radiography of welded capsule assemblies (bottom).

2.5.5 ATF-1 UN-U_3Si_5 Composite Fuel Development and Irradiation Test Design

K.J. McClellan, D.D. Byler, E.P. Luther, J.T. White, LANL; P. Medvedev, INL

One approach to development of fuels with enhanced accident tolerance is exploration of advanced composite systems (revolutionary path) with the potential to improve the accident performance of LWR fuels and to offer benefits during normal operation. Composite fuels have been of interest for many decades, as a wide range of both ceramic and metallic alloys can be envisioned that would surpass the performance of traditional LWR oxide ceramic fuels. However, when systems are explored within the constraint of use in existing commercial LWRs and fabricated in existing fuel fabrication facilities with minimal modification, the practical limit on uranium-235 enrichment creates significant challenges in the introduction of non-fissile second phases. Any inert second phase incorporated in a proposed fuel must be limited to extremely low volume fractions if reactor performance is not sacrificed and enrichment remains fixed. It is difficult for such concepts to achieve improvement in any of the critical metrics (e.g. thermal conductivity, mechanical properties, or thermochemical stability) when limited in such a way.

An option to overcome this constraint is the use of uranium bearing second phases. Although they may not contain the uranium density of uranium dioxide or uranium nitride, a phase containing even half the uranium density of these reference ceramics may provide sufficient margin to retain reactor operation within a fixed enrichment. A wide range of uranium compounds have been investigated historically, many of which could be envisioned to offer intriguing benefits to accident performance as well as the overall fuel attributes. Certain combinations of these phases have the potential to yield the benefits of composite fuels, such as improved thermal conductivity and increased pellet integrity while maintaining the current commercial fuel enrichment limit (Table 7). Just as importantly as improvements in accident and normal operation from the fuel pellet itself, fuels with uranium densities higher than UO_2 can help enable changes to ATF cladding by offsetting the neutronic penalty of candidate systems such as Fe-based cladding, e.g., FeCrAl alloys.

Initial screening of composite fuel concepts has been performed by coordination of themodynamic, neutronic and assembly level analysis coupled with experimental studies of the fresh fuel properties and

characteristics. Based on the screening results to date, the uranium nitride-uranium silicide composite systems seem attractive and warrant further examination in terms of fresh fuel properties and more detailed reactor performance analysis (see, for example, the highlights on property studies on uranium silicide phases by J.T. White and composite fuel reactor performance and safety analysis by N. Brown). Limited data currently exists for fresh fuel properties of a number of the constituent phases of the candidate composite systems and the composites themselves, but there is even less data in terms of irradiation behavior. Therefore, an initial irradiation test has been planned under the ATF-1 irradiation test series for the UN-U_3Si_5 composite fuel system. As can be seen from Table 7 of the nitride-silicide systems that have been considered, UN-U_3Si_2 is being explored under the Westinghouse FOA. The UN-U_3Si_5 is also a promising system based on early assessment, as the U_3Si_5 phase has a fairly high thermal conductivity and relative to U_3Si_2, has better oxidation behavior in steam and a higher melting point. However, the irradiation stability of the UN-U_3Si_5 composite and of the U_3Si_5 phase is unknown and must be assessed to further evaluate the viability of this system.

Therefore, preliminary design in fuel fabrication process development for an initial drop-in type irradiation test has been in undertaken in FY 2014. The test will be performed in the INL ATR as part of the ATF-1 test series with the designation of "LANL-1" and will consist of two rodlets of UN-U_3Si_5 composite fuel and two rodlets of U_3Si_5 monolithic fuel. The nominal test parameters are shown in Table 7, where highest priority was placed on linear heat generation rate (LHGR) and then on peak internal cladding temperature (PICT). While monolithic U_3Si_5 is not being advocated as a stand-alone fuel concept – due to the relatively low uranium density of 7.5 g/cm^3 a U_3Si_5 fuel would require enrichment great than 5% ^{235}U – the silicide-only rodlets are being irradiated as an efficient way to collect irradiation behavior data for this composite constituent phase.

Table 7. ATF-1/LANL-1 nominal test design parameters.

Fuel	PICT Target/Max (°C)	LHGR (W/cm)	Centerline Temp (°C)	Cladding Material	Target Burnup (GWd/MTU)
UN/15vol%U_3Si_5	350/400	240	<1650	Kanthal AF	10
UN/15vol%U_3Si_5	350/400	240	<1650	Kanthal AF	20
UN/15vol%U_3Si_5	350/400	240	<1650	Kanthal AF	50
U_3Si_5	350/400	240	<1650	Kanthal AF	10
U_3Si_5	350/400	240	<1650	Kanthal AF	20

The preliminary design of the test required material properties that are not available from literature, so processes were developed to fabricate material property samples with densities of greater than 90% theoretical density (typically >95%) for the UN and U_3Si_5 constituent phases as well as the UN-U_3Si_5 composite . Representative microstructures of the composite samples (Figure 51) show that the silicide phase does not coat the UN grain boundaries and is a discontinuous phase. Key properties, such as thermal conductivity (Figure 52), were measured and subsequently used for preliminary design of the LANL-1 test using the BISON fuel performance code.

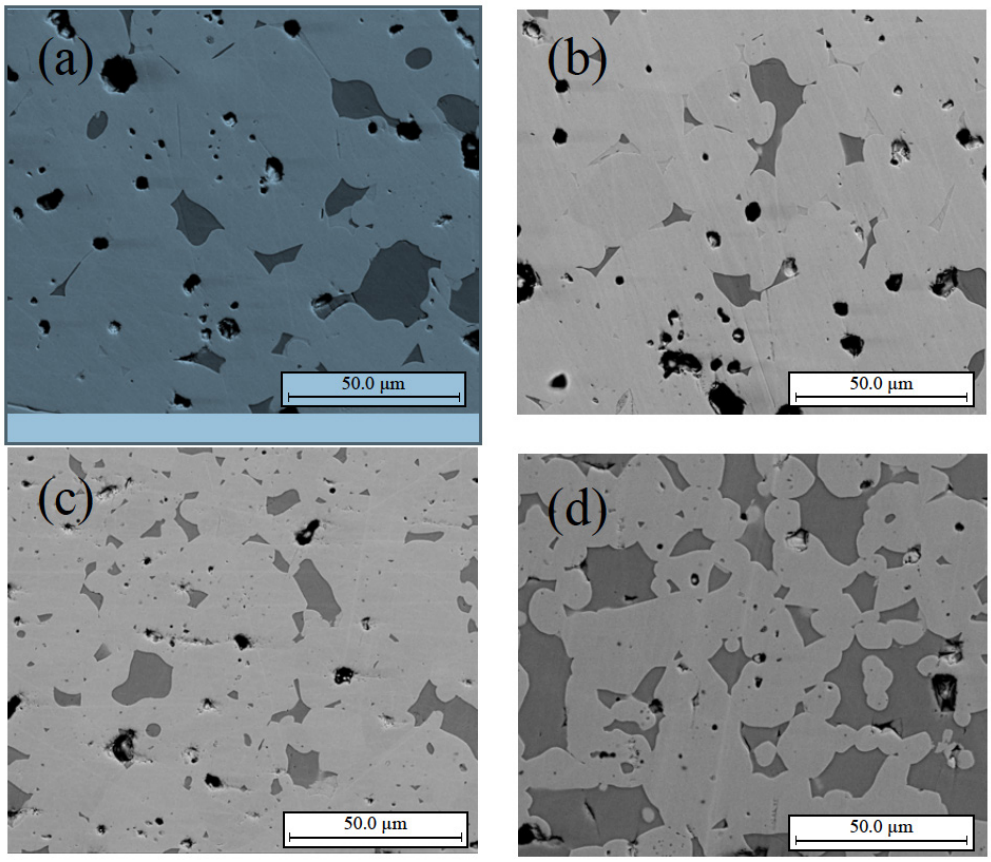

Figure 51. Microstructures of U3Si5-UN collected using a backscatter detector for (a) 5v%, (b) 10v%, (c) 15v%, and (d) 30 v% specimens.

The preliminary LANL-1 fuel and rodlet design was developed using the BISON code, modified to initially utilize composite fuel properties based on a rule-of-mixtures approximation from the measured constituent properties. Subsequently, the analysis was performed using the properties measured on the actual UN-15vol% U_3Si_5 composite samples matching the target fuel density of 95% theoretical density (Figure 52). The composite data was in fairly good agreement with the rule-of-mixtures initial approximation. The preliminary composite test geometry from the BISON analysis is shown in Figure 52. Key test temperatures are shown in Figure 53. The LANL-1 test is designed with a rather large rodlet/capsule gap of ~70µm to facilitate neutron tomography to image the gap before and after irradiation (detector pixel pitch of 55µm). As there is no swelling data for the U_3Si_5 or for the composite at this time (collection of this data is one of the primary objectives of the LANL-1 test), swelling was estimated using a model for UN from fast reactor testing. Using this approximation, the pellet/capsule gap was set at 25 µm, where closure is not predicted until ~35 GWd/t burnup (Figure 54).

The preliminary design developed using BISON has enabled early development of the fuel fabrication process. Final design approval using the ATR-approved tools is anticipated in early FY15. At that point, final refinement of the fabrication process will be completed and fuel pellets will be fabricated and shipped to INL for fabrication of the test rodlets and encapsulation. Insertion of the ATF-1 LANL-1 test is planned for the ATR 158A run cycle.

Rodlet

Design Parameter	Nominal Value
Cladding Material	Kanthal AF (FeCrAl alloy)
Cladding O.D.	0.3708 in (9.4194 mm)
Cladding I.D.	0.3306 in (8.3984 mm)
Bond Material	He

Fuel

Design Parameter	Nominal Value
Fuel Type	UN-15v%U_3Si_5 U_3Si_5
Enrichment	<4.95
Pellet O.D.	0.3287 in (8.3484 mm)
Pellet Length	≥0.362 in (9.18 mm)
Stack Length	3.20 in (45 mm)

Capsule

Design Parameter	Nominal Value
Capsule Material	316L SS
Capsule O.D.	0.4320 in (10.9728 mm)
Capsule I.D.	0.3760 in (9.5504 mm)
Capsule Length	6.16 in (156.46 mm)
Capsule/Rodlet Gap	~0.0028 in (0.071 mm)

Figure 52. Preliminary composite test geometry from the BISON analysis to target a 240W/cm LHGR while maintaining a ≤350°C PICT.

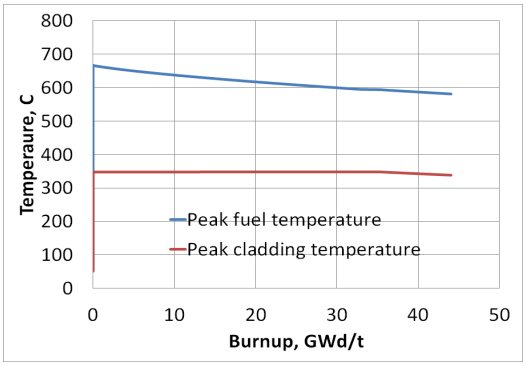

Figure 53. Peak fuel and cladding temperatures as a function of burnup for UN-15vol%U_3Si_5 composite fuel in Kanthal AF cladding from the preliminary BISON analysis.

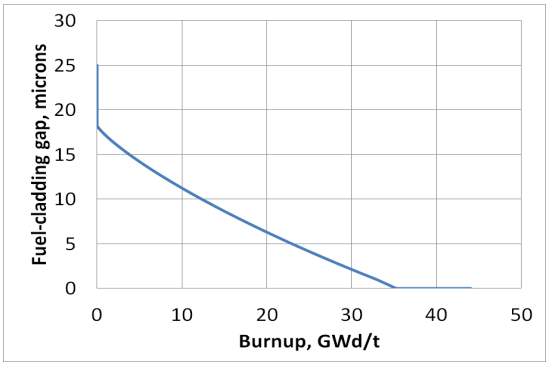

Figure 54. Pell/cladding gap as a function of burnup for UN-15vol%U_3Si_5 composite fuel in Kanthal AF cladding from the preliminary BISON analysis.

Transmutation Fuels Technologies

SECTION 3

3. TRANSMUTATION FUELS TECHNOLOGIES

Metallic-based Fuels Technologies focused on research and development to gain a fundamental understanding of metallic fuels. Priority was on low-loss fabrication methods and capability and on developing a fundamental understanding of the phase, microstructure, and chemical migration behavior of metallic fuel constituents. The desired outcome is to develop an understanding of the key phenomena affecting metallic fuel performance and behavior under irradiation.

3.1 Analysis

3.1.1 Comparison of BISON Calculations with PIE Results for AFC-3A-R4 Annular Metallic Fuel

P. Medvedev, Idaho National Laboratory

In FY 2014, BISON fuel performance modeling results were compared with newly obtained results of the post-irradiation examination of the AFC-3A-R4 annular metallic fuel. The key technical issues were whether the annular fuel would swell inward and fill the annulus, or swell outward, resulting in an undesirable cladding deformation. Prior to completion of the post-irradiation examination it was predicted that the annular fuel will swell inward and partially fill the annulus (INL/EXT-12-27183). Postirradiation examination results were in agreement with the modeling results showing very small diametral strain and axial elongation of the fuel. Comparison of calculated and measured axial fuel elongation is shown in Figure 55. The calculated end-of-life fuel axial elongation is 0.049%, and measured fuel axial elongation is 0.56%. The calculated trend shows initial elongation of the fuel due to the thermal expansion, and later contraction of the fuel due to cooling after the reactor shutdown. Comparison of calculated and measured axial fuel elongation is shown in Figure 56. The calculated end-of-life diametral fuel strain is 0.03%, and measured diametral fuel strain is 1.3%. The calculated trend shows initial increase of the fuel diameter due to thermal expansion, and contraction of the fuel due to cooling after the reactor shutdown.

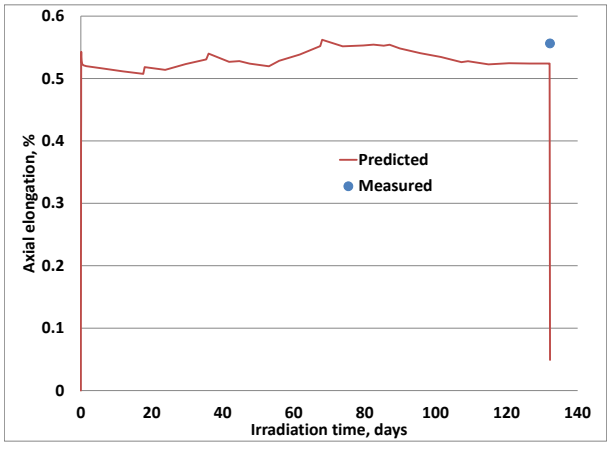

Figure 55. Comparison of calculated and measured fuel axial elongation.

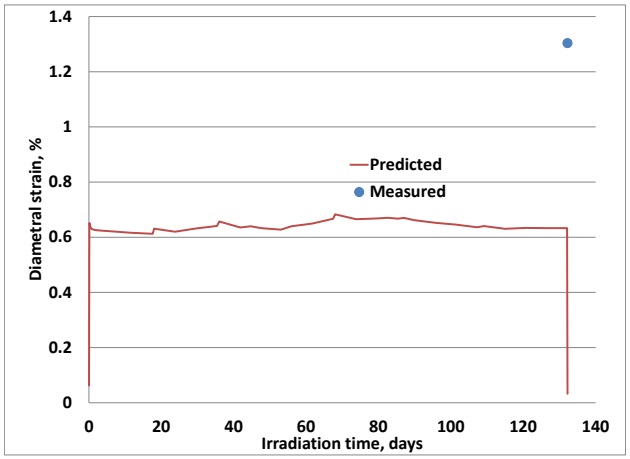

Figure 56. Comparison of calculated and measured diametral fuel strain.

3.1.2 Modeling of Compressible Gas Bubbles in Truchas

J. Bakosi, Los Alamos National Laboratory

A new flow physics option, the adiabatic bubble model, has been implemented in Truchas. This is similar to the "homogeneous bubble model" option available in Flow3D. The rationale behind such a bubble model is two-fold: (1) to speed up large multi-phase-flow calculations with many gas bubbles where the flow field inside the bubbles is of no interest, and (2) to potentially more accurately approximate the underlying physics, as the gas density in such calculations may be orders of magnitude smaller than the liquid density and is compressible, compared to the existing flow algorithm which treats materials as incompressible. Based on designating a material as void, by assigning zero density, bubbles are identified and tracked throughout the evolution of the flow field in space and time. Instead of integrating the flow equations inside bubbles, their pressures are governed by an ideal gas law. Each bubble material is assigned its initial pressure specified by the user via the input deck. The initial bubble volumes are computed based on the geometrical layout of the void materials (designated as bubbles by assigning zero density) in the input deck. The bubble volumes and pressures evolve in time due to forces by the surrounding liquid (or gas) flow computed by the existing fluid flow algorithm in Truchas. The bubble model neglects heat transfer inside bubbles, but assumes that the bubbles are compressible. The computed bubble pressure affects the surrounding fluid via enforcing the bubble pressure on the surface between the bubble and the fluid.

A relatively complex test case is a single light bubble in a heavy surrounding fluid, as depicted in Figure 57. The setup also includes a second bubble at the top, modeling a free atmosphere. The density ratio between the bubbles and the fluid is 1/100. The case was run with and without the bubble model. The initial bubble pressure is assigned to be equal to the hydrostatic pressure at the center of the bubble. Figure 57 depicts the initial condition, and the bubble volume fraction without and with the bubble model.

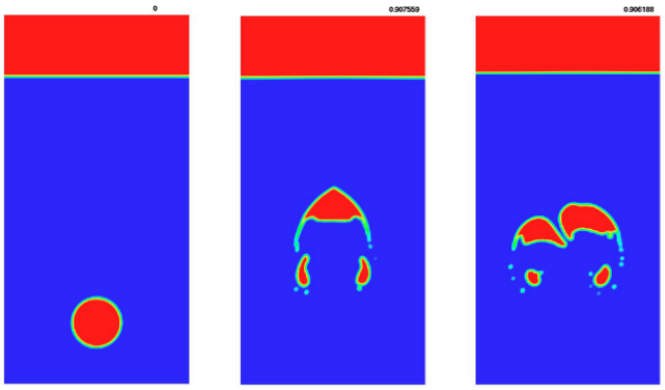

Figure 57. Light bubble rising and splitting with and without the bubble model – void volume fraction. Left -- initial condition; middle -- t=0.9, no bubble model; right -- t=0.9, bubble model.

As expected the two models behave qualitatively similar, i.e., the bubble rises due to its lower density than its surroundings, but the two models compute different solutions for the bubble topology and its rising speed.

3.1.3 Implementation of a Surface Tension Algorithm into Truchas

R. Ranjan, Los Alamos National Laboratory

Surface tension effects occur at an interface of two fluids when modeling multiphase flow. Truchas has surface tension models, which utilize convolution based models that are prohibitively expensive in parallel and engender load-balancing issues where one processor is computing the convolution integral and others await the results from such evaluations. This problem arises due to poor scalability of the convolution algorithm used currently. Applicability of the convolution algorithms on unstructured meshes has been limited because of the lack of appropriate interpretations of the radius of curvature required in the convolution process.

We incorporate a new procedure namely L2 projection and L2 smoothing of the volume of fluid color function to effect smearing. This procedure has been mentioned in literature to provide smearing of the interface by virtue of the existence of the diffusion term that serves to broaden the discontinuous interface. The smoothing operation or this smearing process is incorporated by adjusting the parameter epsilon in the equation below. An example is provided in Figure 58 in which smearing has been achieved effectively for input of a diagonally oriented Volume of Fluid (VOF) field on an unstructured mesh. Both of the opposite diagonals were checked for smearing for verification purposes. However, results are presented only for the top left diagonal.

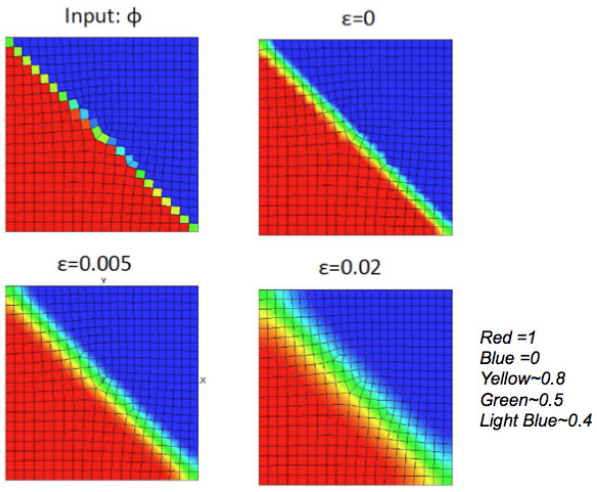

Figure 58. Input VOF field and output for different epsilon values

Further tests were done on this new algorithm for different test problems. The verification problems included the static bubble, advection of a bubble in a channel, and a deforming bubble at different Bond numbers.

Figure 59 shows the unstructured computational domain for the static bubble problem. The simulation was performed with an end time of 0.5 and time step size of $1e^{-04}$. The smoothing constant was taken as 0.005 for the simulation. As can be seen from the figures, the problem when solved on an unstructured mesh creates spurious currents but they remain bounded because there is no excessive motion or deformation of the bubble shapes over time.

Next, the rise of an air bubble in water by buoyancy forces was considered (see Figure 60). The characteristic non-dimensional number for this situation is the Bond number, or the ratio of the gravitational forces to surface tension forces. For this case, the observable difference in the bubble shapes is not evident between the convolution-based and projected algorithms for solving this problem. This is because in this case the surface tension force is not dominant, i.e. the flow is primarily driven by buoyancy forces.

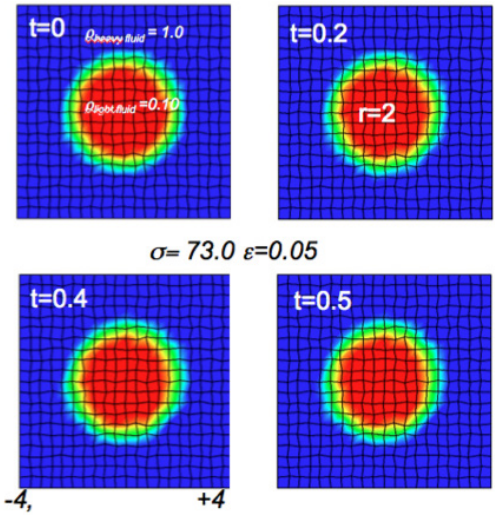

Figure 59. Static bubble solved on an unstructured mesh

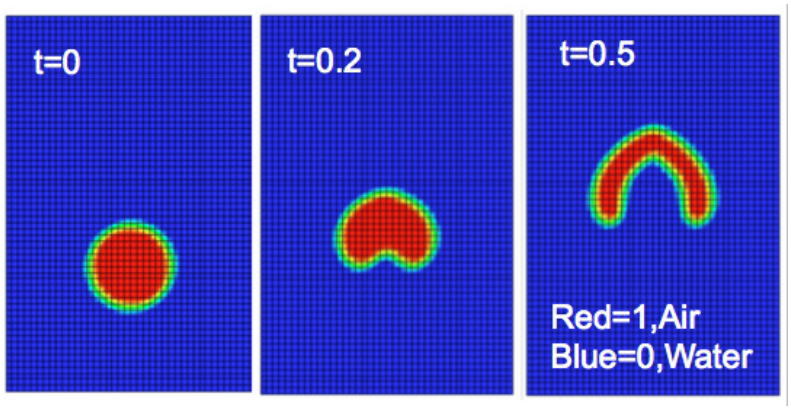

Figure 60. Computed shapes at times t=0, 0.20 and 0.50 with Bond numbers Bo_1=73.4 and Bo_2=59.83x10^3

3.1.4 Flow3D Simulations of U-Zr Casting Experiments

R. Ranjan, Los Alamos National Laboratory

Computational simulations of gravity casting for metallic U-Zr fuel rods were performed with Flow3d. First, experimental test data obtained from INL was used to validate the numerical simulation. The validated model is applied to the second fuel-rod casting experiment. The volume of the rods cast, length of the rods, and temperature profiles were predicted through the transient casting process and were found to match closely with experimental data. A sensitivity analysis was explored with vent locations, pressure, mesh refinement and effects of the surface tension at the interface.

In Figure 61, the transients are shown as the melt flows down the casting apparatus at time 0.18 s and 1.8 seconds for the 200 gm simulation. After 1.8 s of simulation time no appreciable changes were observed in settling of the melt and it could be assumed that the casting part of the problem had reached steady state. Much of the flow and settling down of the melt occurs before three seconds of simulation time. Simulated lengths and volumes of three rods were in good agreement with the measured data. Swirling flow at the entrance of rods is confirmed. Casting design is modified to include groves at the entrance of rods to guide the flow. Simulation of this modification is in progress.

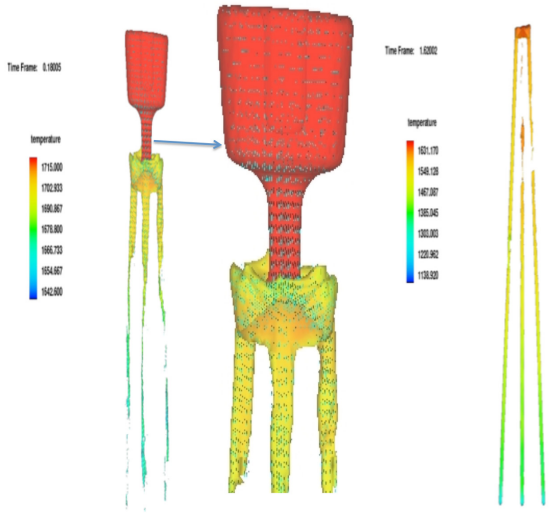

Figure 61. Transient casting simulation for 200 gm charge

During the casting experiments temperature measurements were made at two separate locations along the length of the inner mold. Agreement between the experimental results and predicted simulation results from Flow3d are provided in Figure 62. The maximum deviation between the predictions was found to be within 2.6°C for the bottom temperature predictions and 5.1°C for the top thermocouple. Both the deviations 0.81% and 1.2% lie within the engineering accuracy of 2%.

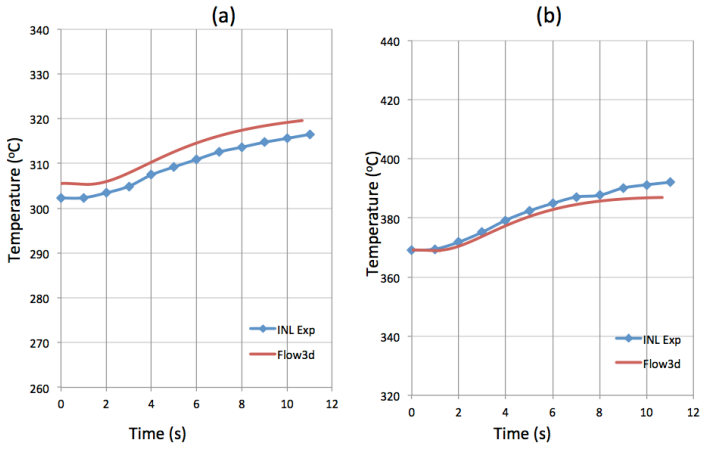

Figure 62. Predicted temperature profile vs. simulation for 200 gm charge, a-bottom of mold b- top thermocouple location

3.2 Fuels Development

3.2.1 Neptunium Reduction Experiments and Feedstock Purification

L. Squires, Idaho National Laboratory

Neptunium metal is an important constituent of transmutation fuel. Current supplies of pure neptunium metal for fuel fabrication needs are dwindling and it is therefore necessary to develop a technique to supply the metal. Large quantities of neptunium oxide exist across the DOE complex and much of this material is available at Idaho National Laboratory. A process is under development to directly reduce the oxide to metal using a chemical reduction technique. This process employees the Hot Uniaxial Press furnace with is in the Casting Laboratory glovebox, an argon atmosphere glovebox. It involves first heating the neptunium oxide starting material in a magnesium oxide crucible to drive off volatile impurities and then adding calcium metal as a reducing agent and calcium chloride salt. The mixture is then heated to 850^{o}C and the molten mixture is stirred using a stirrer specifically designed for the reduction process and the furnace. Once the reduction occurs the neptunium metal falls to the bottom of the crucible and upon cooling it can be removed as a metal button. There have been some doubts as to the purity of the resulting material but analysis has shown it to be 98-99% pure which is pure enough for fuel casting. Since different batches of starting material will be used in future runs it may become necessary to purify the final product. In which case a heat treatment under vacuum followed by a hydride/dehydride step have been proposed. Below are pictures (Figure 63) showing the furnace set up and the process products.

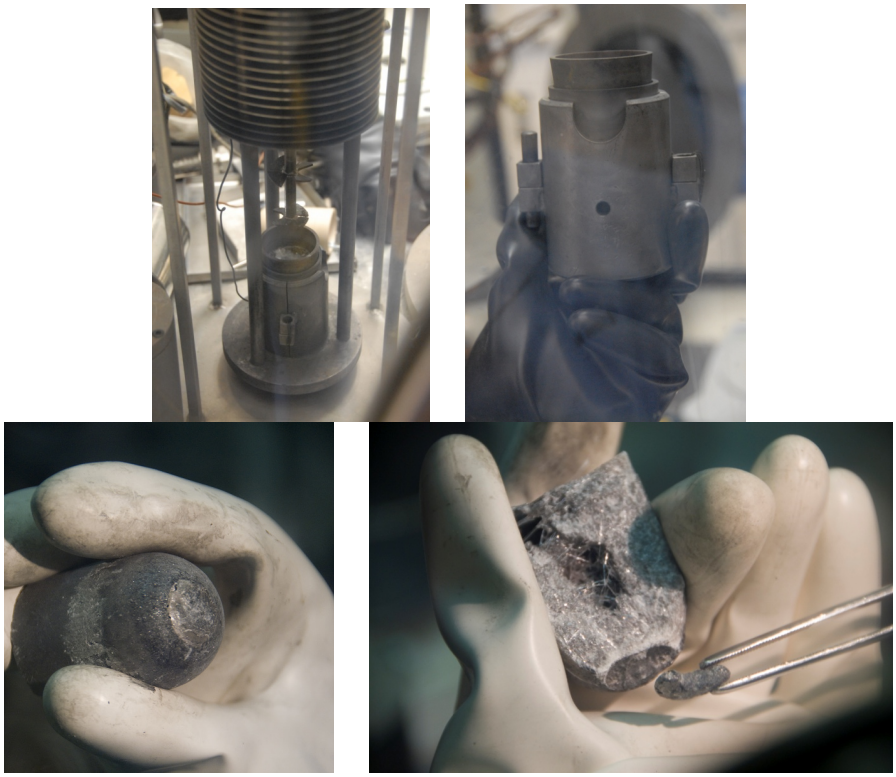

Figure 63. Top left: Hot Uniaxial Press insert loaded with reaction crucible and reagents. Top right: Close up of magnesium oxide crucible nested n a stainless steel crucible nested in the furnace insert. Bottom left: Solidified reagents post reduction with neptunium metal button clearly identifiable on the bottom. Bottom right: Removal of neptunium metal button

3.2.2 AmBB Accomplishments FY 2014

P. Lessing, Idaho National Laboratory

Experiments were conducted during FY 2014 to produce good purity Americium metal for use in tests within the ATR designed to trans-mutate Am (a minor actinide). Compositions will be developed and tested for ultimate use as an Americium Bearing Blanket (AmBB). The tests will be conducted in ATR on rodlets containing mixed-oxide pellets and metallic alloy slugs.

During FY 2014, americium was purified using impure metal obtained from LLNL. The LLNL material contains 5%Np, O, and 5% Pb as major impurities. During distillation in a tantalum tube, Am metal is deposited as shown in Figure 64. All the Np is left in bottom of tube; using short time/low temperature runs, the Pb was shown to segregate into outer regions of the solid distillate. The oxide is removed by the reaction $2La + 3/2\ O_2 \rightarrow La_2O_3$ (left in bottom). We have produced several grams of purified Am:

- g Am with no Np, but has high Pb
- g Am (approx.) removed by selective reaming of distilled Am; with no detectable Np, and containing very low Pb (< 0.0200 to 0.0803 % in 4 samples).

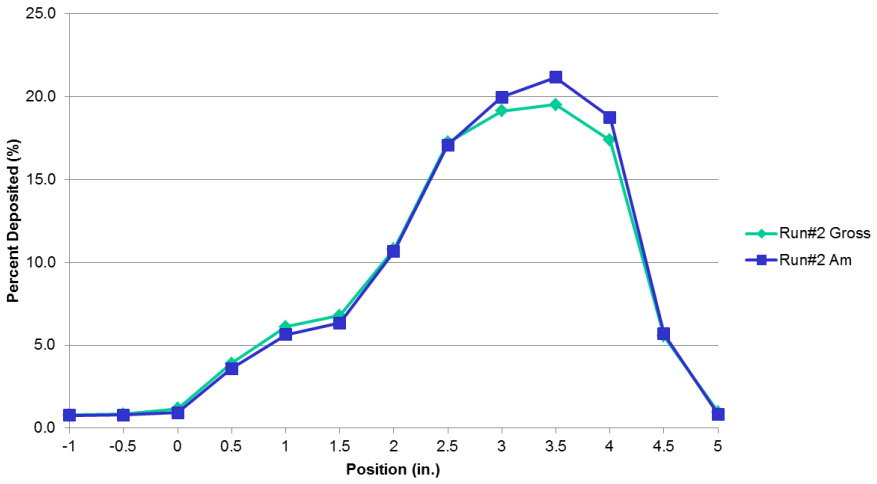

Figure 64. Percent Deposition plot indicates 75-80% of activity was deposited from 2-4 inches from the bottom of Ta crucible. Results are from a special, automated monitoring system featuring a Cadmium-Zinc-Telluride (CZT) detector. The system was developed at INL to monitor the progress and efficiency of the Am distillation process.

3.2.3 Minor Actinide Casting Experiments

R. Fielding, Idaho National Laboratory

Minor actinide casting in FY 2014 consisted of two main experiments; chemical analysis of previously cast rods to verify axial homogeneity and americium retention, and second a set of experiments to verify americium retention under casting conditions. In order to confirm axial chemical homogeneity samples were removed from the top and bottom of two cast pins and sent for chemical analysis. Following sampling the cast rods were broken up and remelted in an Y_2O_3 coated graphite crucible. The melting process was carried out under an approximate 600 torr pressure of flowing argon and heated to approximately 1450°C and held for 15 minutes. The resulting ingot of material was broken up, sampled, and remelted following the same heating procedure. Because the original cast pins were used as feedstock the material was melted 3 times totaling approximately 40 minutes at casting temperatures. When the

resulting ingots were broken up two random samples from each ingot were analyzed using ICP-MS to confirm americium retention.

Results from the chemical analysis of the rods showed the rods had good axial homogeneity. Figure 65 shows the results for the americium analysis. As shown the americium results were fairly consistent within the analysis level of error for each of the products, although for ingot #1 and ingot #2 one sample was low. This was caused due to the sampling method of the ingots. The ingots were sampled by breaking each one using a hammer and chisel and two conveniently sized pieces chosen and sent for analysis. Analysis of the original transuranic feedstock gave indication that the feedstock had a high level of secondary phase contamination such as oxides or nitrides. Because no casting took place during the americium retention test these second phase particles would have floated to the top of the melt adding to the dross which was observed. During sampling it was likely that some of the samples may have included more or less of this dross phase depending on where they were broken from. Based on these results it can be said that americium can be maintained during the casting process if casting is not done under a vacuum environment.

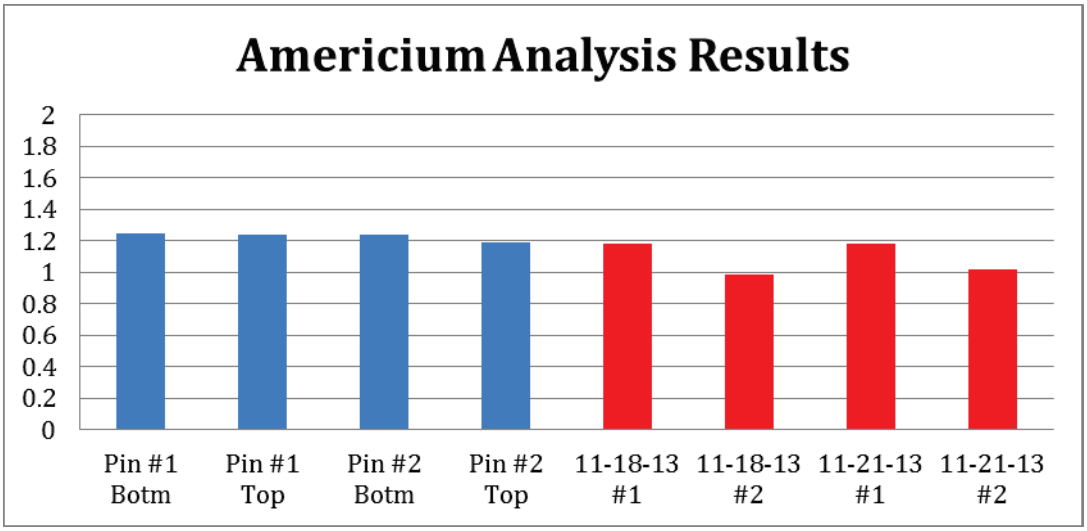

Figure 65. Americium levels of the cast-in pins and ingots. Note the red bars represent ingots and blue represent rod samples.

3.2.4 Fabrication of Metallic Fuel Samples

R. Fielding, Idaho National Laboratory

The metal fuel fabrication package is used to support fuel characterization and irradiation testing. Early in the fiscal additional fuel tests were made to supplement the AFC-4A irradiation test. The fuel slugs were cast, machined to final diameter and encapsulated in the standard AFC-OA irradiation hardware. To further support irradiation testing and sample fabrication the Bench-scale Casting II furnace was upgraded to provide better atmospheric contamination control. The original furnace designed called for the use of plastic tubing and compression fitting because a high vacuum level was not needed at the time. However, due to further testing and programmatic changes higher vacuum level was needed so the furnace was upgraded to utilize o-ring sealed vacuum fittings and stainless steel hoses.

The main thrust of the work this year was to determine which transmutation fuel samples were needed for characterization to fill in gaps in the fuel property database. An extensive inventory of the legacy fuel samples was undertaken to determine which samples were appropriately packaged to prevent excessive oxidation, the form of the samples, and which pieces could be used as feedstock to cast other samples needed for further characterization. Figure 66 shows an example of a fuel slug and feedstock samples. Following this inventory 12 alloys were identified that need to be cast for further characterization. The alloys are from the AFC-1 and AFC-2 series of irradiation tests as well as basic characterization samples that are needed for further phase diagram development. Currently three of the alloys have been cast; Pu-60Zr, Pu-40Zr, and Pu-30Zr. During casting it was observed that the casting hardware used was contaminating the melt, and possibly hindering the casting process. To avoid this contamination a new series of casting hardware was developed and used, which has proven to produce less contamination and improve overall castability.

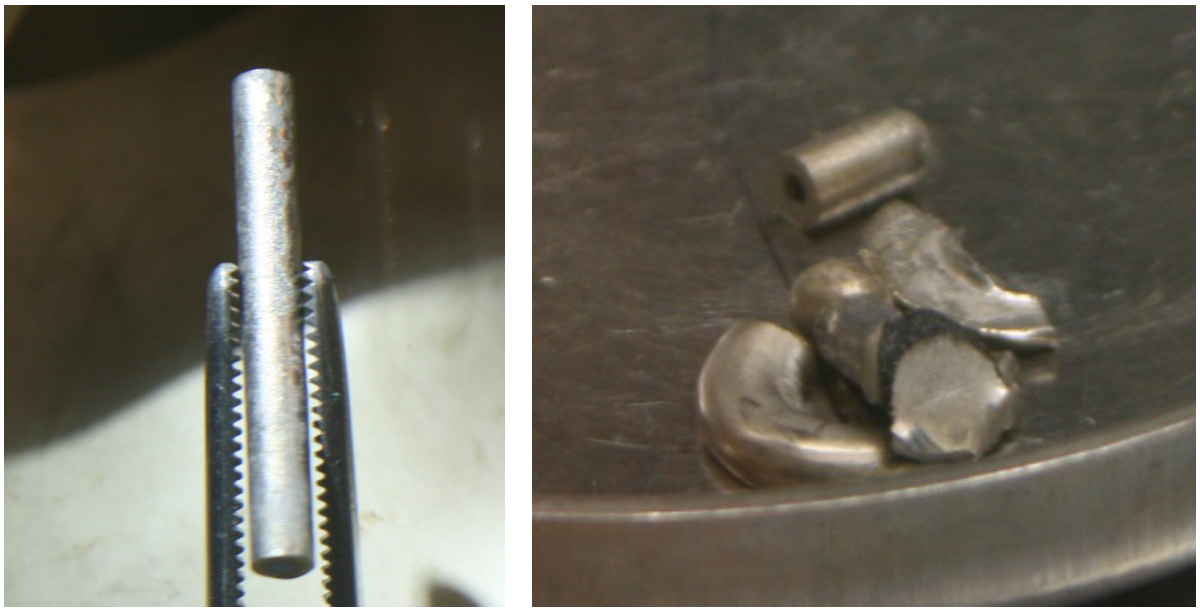

Figure 66. Legacy AFC-1 material: (Left) Archive slug which can be used as-is for further characterization and Right) remaining casting heel pieces which can be re-cast into a usable sample.

3.3 Cladding

3.3.1 Fast Reactor Cladding Development

S. Maloy, Los Alamos National Laboratory

Research performed on high dose irradiated HT-9 was summarized in a new revision of Ch. 18 of the Materials handbook (Rev. 6). Data included mechanical properties measured on the ACO3 duct after irradiation to 155 dpa which included tensile properties, fracture toughness and ductile to brittle transition temperature. In addition, revised sections were provided on irradiation creep and void swelling. An image of the cover page is shown in Figure 67. Authors include O. Anderoglu, M. Serrano de Caro, T. Saleh, LANL; M. Toloczko, PNNL; F. Garner, Radiation Effects Consulting; and T.S. Byun, PNNL (formerly at ORNL).

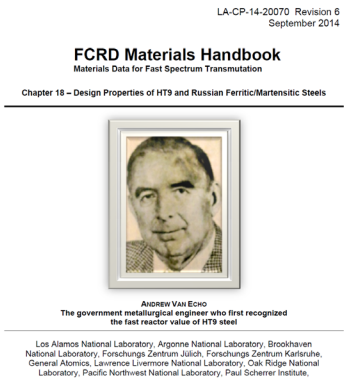
LA-CP-14-20070 Revision 6
September 2014

FCRD Materials Handbook
Materials Data for Fast Spectrum Transmutation

Chapter 18 – Design Properties of HT9 and Russian Ferritic/Martensitic Steels

ANDREW VAN ECHO
The government metallurgical engineer who first recognized the fast reactor value of HT9 steel

Los Alamos National Laboratory, Argonne National Laboratory, Brookhaven National Laboratory, Forschungs Zentrum Jülich, Forschungs Zentrum Karlsruhe, General Atomics, Lawrence Livermore National Laboratory, Oak Ridge National Laboratory, Pacific Northwest National Laboratory, Paul Scherrer Institute,

Figure 67. Cover page of Ch. 18 of Rev. 6 of the FCRD Materials Handbook.

3.3.2 Nanostructured Ferritic Alloy Development

D. Hoelzer, Oak Ridge National Laboratory

The project on development of "best practice" processing of the FCRD-NFA1 heat of 14YWT made excellent progress this fiscal year. Three 2.8 kg heats of FCRD-NFA1 were produced by hot extrusion at 850ºC, from which 9 plates were fabricated by cross rolling at 1000ºC. Three plates were supplied to the FCRD program for microstructural and mechanical properties studies and for fabrication of tubing for neutron irradiation studies. Six plates were supplied to the DOE-EPRI Program on Advanced Radiation Resistant Materials (ARRM) that is coordinating a global research effort to develop the next generation of materials for in-core components and fasteners of light water reactors. The advanced ODS 14YWT ferritic alloy was down selected as the candidate material for high-strength, radiation degradation resistance applications targeted for 2024. The microstructural studies conducted on FCRD-NFA1 revealed a high number density (~7 x 10^{23} m^{-3}) of Y-, Ti- and O-enriched nano-size (~2.0 +/- 0.8 nm diameter) particles dispersed within grains that have an average size of ~0.8 μm, small grain aspect ratio of ~1.02, and slight degree of bi-modal size distribution, plus a higher than normal concentration of ~20-150 nm size Ti(O,C,N) particles distributed in wavy patterns in the microstructure (see Figure 68). The mechanical property studies of: (1) tensile tests showed lower strengths, but higher ductilities from room temperature to 800ºC (see Figure 69), compared to previous 14YWT heats, and only a minor effect of anisotropy, (2) high-temperature creep strength that was comparable to the stronger MA957 alloy and (3) very low brittle-ductile fracture toughness transition temperature (-150ºC to -175ºC) with no anisotropic effects. These results show remarkable progress has been achieved on development of advanced ODS ferritic alloys.

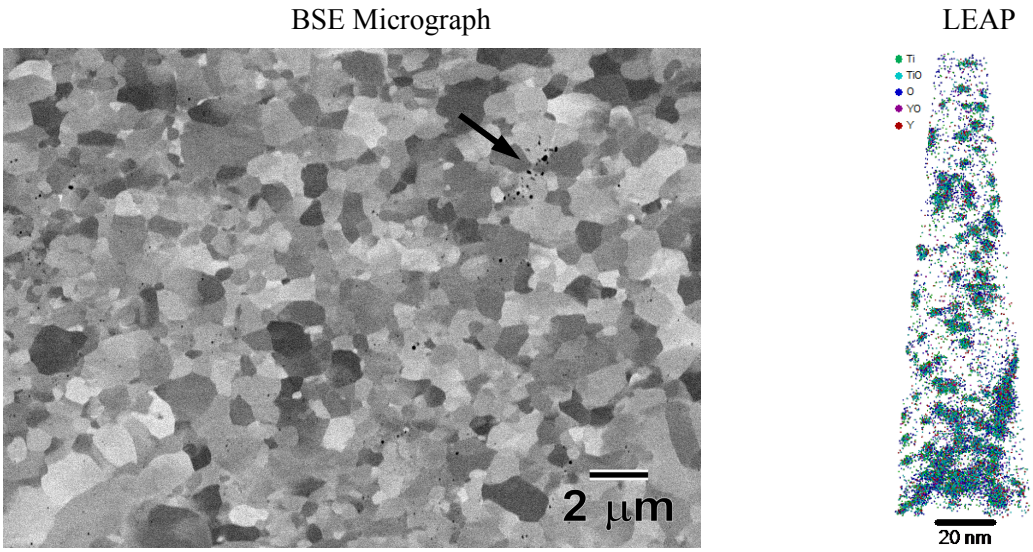

Figure 68. SEM backscattered electron micrograph (BSE) showing ultra-fine size, equiaxed grains and clusters of Ti(O,C, N) particles (arrow inset) and Local electrode atom probe (LEAP - UCSB) image showing the high number density of nano-size Y-, Ti- and O-enriched particles.

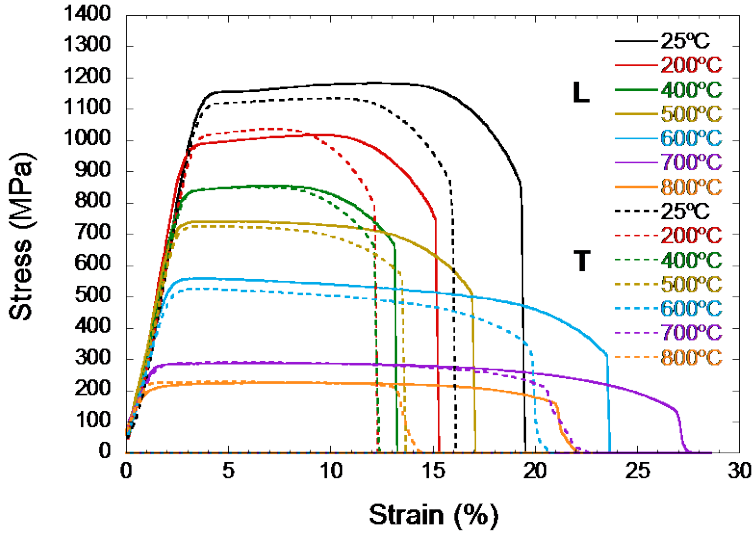

Figure 69. Tensile stress-strain curves of FCRD-NFA1 tested with 33-3 specimens fabricated with gage sections parallel to the extrusion (L - Longitudinal) and cross-rolled (T- Transverse) directions from room temperature to 800ºC.

Research was started this fiscal year on developing fabrication methods for ultimately producing thin wall clad tubing from the advanced ODS ferritic alloys. For the conventional fabrication method involving drawing, swaging and pilgering, three thick wall tubes were first produced by extruding ball milled powder of ODS 14YWT (14Cr) and ODS 9YWTV (9Cr) over a steel mandrel at 850ºC at ORNL (see Figure 70). After removing the mandrel and steel can from the enclosed ODS tubes, a tube section of 14YWT and 9YWTV were shipped to PNNL for developing the fabrication method using swaging and pilgering to reduce the wall thickness and diameter. In another method, the feasibility of solid-state cold spray deposition of ball milled and annealed 14YWT powder is being evaluated for producing thin wall tubes by the additive manufacturing approach.

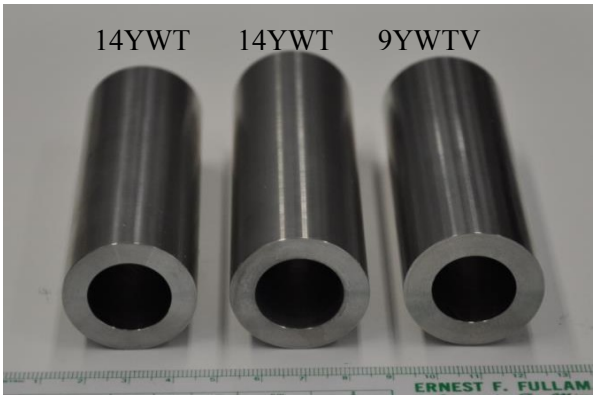

Figure 70. Extruded, thick wall tubes of 14YWT and 9YWTV.

3.4 Irradiation Testing

3.4.1 Megapie PIE Results

T. Saleh, Los Alamos National Laboratory

Irradiated, curved S1 style tensile samples from the T91 hemispherical beam window (calotte) were tested as part of the MEGAPIE international project. Figure 71 shows the results for room temperature tensile tests for control material vs material irradiated to 2.08 dpa/256°C and 4.5 dpa/312°C. The curved nature of the samples and the 1.5x1.7mm cross section leads to slightly unusual elastic and elongation behavior. The second figure shows the T91 MEGAPIE tests compared to the control and irradiated tests for the T91 samples in the ATR irradiation. These samples had a more traditional 1.5x.75mm cross section and higher dose (6.49dpa/296.5°C). Differences in elastic behavior and elongation are apparent, but the data scales well based on dose and temperature. Tabulated data follows with some additional data taken from Paul Scherrer Institute (PSI) tests on the samples from MEGAPIE at slightly different doses.

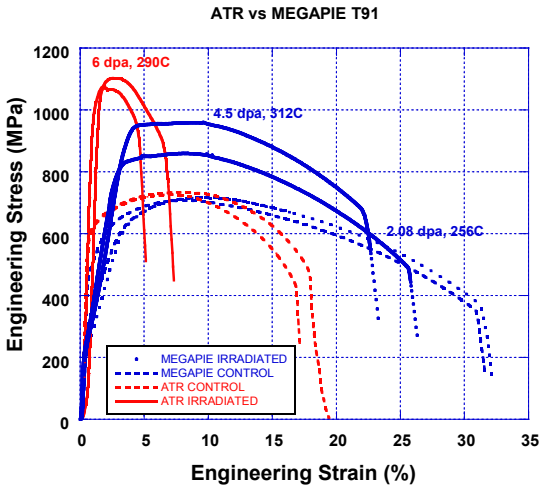

Figure 71. Results for room temperature tensile tests for control material vs material irradiated to 2.08 dpa/256°C and 4.5 dpa/312°C.

3.4.2 High Dose Irradiation Results

M. Toloczko and A. Certain, Pacific Northwest National Laboratory

Qualification of Ion Irradiations for High Dose Screening of Clad and Duct Materials

High burnup fuel for transmutation fast reactors continues to be a key focus, but the ability to qualify clad and duct to anticipated dose levels of 300+ dpa is well beyond what can be achieved with available fast neutron reactors. Ion irradiations are currently the only means to assess high dose effects, and in fact, ion irradiations have been used for this purpose over the last 30 years. Early applications of ion irradiations to study radiation effects often produced microstructures that were much different from neutron irradiations. With the resurgence in the desire to use ion irradiations, new experiments and historical assessments are being performed to learn how to produce microstructures more prototypic of fast reactor neutron irradiations. Using the latest information on conducting ion irradiations, MA957 ODS ferritic alloy microstructures were compared between 100 dpa ion and neutron irradiations. Void and precipitate microstructures compared between ion and neutron irradiations using a combination of transmission electron microscopy (TEM) and atom probe tomography (APT) were found to be very similar. For example at 400°C, little or no void swelling was found for either irradiation condition, the effect of irradiation on oxide particle size distribution was found to be similar, and as shown in Figure 72, alpha-prime was found for both irradiations conditions. Trends were similar for higher irradiation temperatures as well. This is one early example showing that ion irradiations have strong promise to at a minimum, act as an effective screening tool for high dose irradiation resistance down-select.

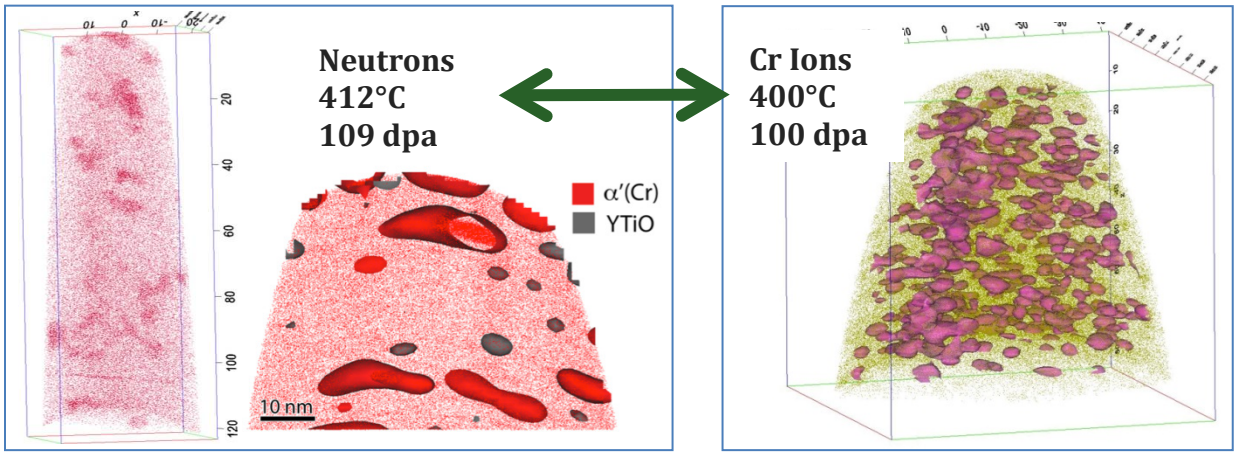

Figure 72. Comparison of alpha prime microstructures between ~100 dpa neutron and 100 dpa ion irradiations at ~400°C. Alpha prime of similar size was found for both irradiations.

14YWT Advanced ODS Ferritic Alloy High Dose Ion Irradiations

A series of high dose ion irradiations are being conducted to perform comparative studies between several candidate materials for transmutation fast reactor clad and duct. To provide a basis for a factor of improvement, not only are newer potentially more advanced alloys being irradiated, but historically relevant alloys with significant neutron irradiation experience are also being ion irradiated. For cladding where ODS ferritic alloys are considered the most likely candidate, the historic ODS alloy MA957 and the modern alloy 14YWT have been chosen while for duct applications where an ODS ferritic is impractical, the historic alloy is HT-9, and the more modern alloy is F82H. 500 dpa ion irradiations at temperatures from 400-500°C have now been completed on MA957 and 14YWT, and irradiations on HT-

9 are underway at this moment. Swelling, which is one of the key metrics in high dose irradiation resistance, was measured through post-irradiation microstructural observations. Figure 73 compares the response of MA957 and 14YWT to each other and to two other alloys, one of which is a non-optimized HT-9 (from an earlier study). As can be seen, both the MA957 and 14YWT perform much better than the other two alloys out in the 500 dpa range. When compared against each other, the more modern 14YWT does appear to be performing better, most likely due to a higher oxide particle and grain boundary surface area than for MA957. Information learned from these irradiations will be used to either select an existing alloy or be used to design an even better alloy.

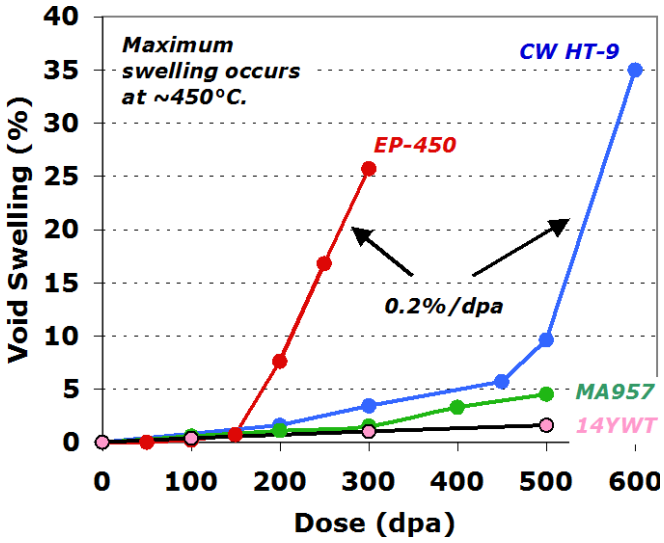

Figure 73. Void swelling of MA957, 14YWT, and two tempered ferritic-martensitic steels as a function of dose for ion irradiations.

Publications

1. M.B. Toloczko, F.A. Garner, V.N. Voyevodin, V.V. Bryk, O.V. Borodin, V.V. Mel'nychenko, and A.S. Kalchenko, "Ion-Induced Swelling of ODS Ferritic Alloy MA957 Tubing to 500 dpa," *Journal of Nuclear Materials*, 453 (1–3), October 2014, 323–333.
2. Byun, T.S., J.-H. Baek, O. Anderoglu, S.A. Maloy, and M.B. Toloczko, Thermal annealing recovery of fracture toughness in HT9 steel after irradiation to high doses, *Journal of Nuclear Materials*, 449(1-3), 2014, 263-272.
3. Byun, T.S., J.H. Yoon, D.T. Hoelzer, Y.B. Lee, S.H. Kang, and S.A. Maloy, "Process development for 9Cr nanostructured ferritic alloy (NFA) with high fracture toughness," *Journal of NuclearMaterials*, 449(1-3), 2014, 290-299.
4. Byun, T.S., J.H. Yoon, S.H. Wee, D.T. Hoelzer, and S.A. Maloy, "Fracture behavior of 9Cr nanostructured ferritic alloy with improved fracture toughness," *Journal of NuclearMaterials*, 449(1-3), 2014, 39-48.
5. Huang, Z., A. Harris, S.A. Maloy, and P. Hosemann, "Nanoindentation creep study on an ion beam irradiated oxide dispersion strengthened alloy," *Journal of NuclearMaterials*, 451(1-3), 2014, 162-167.

6. Was, G.S., Z. Jiao, E. Getto, K. Sun, A.M. Monterrosa, S.A. Maloy, O. Anderoglu, B.H. Sencer, and M. Hackett, "Emulation of reactor irradiation damage using ion beams," *Scripta Materialia*, 88, 2014, 33-36.
7. Baek, J.-H., T.S. Byun, S.A. Maloy, and M.B. Toloczko, "Investigation of temperature dependence of fracture toughness in high-dose HT9 steel using small-specimen reuse technique," *Journal of Nuclear Materials*, 444(1-3), 2014, 206-213.
8. Cunningham, N.J., Y. Wu, A. Etienne, E.M. Haney, G.R. Odette, E. Stergar, D.T. Hoelzer, Y.D. Kim, B.D. Wirth, and S.A. Maloy, "Effect of bulk oxygen on 14YWT nanostructured ferritic alloys," *Journal of Nuclear Materials*, 444(1-3), 2014, 35-38.
9. Mosbrucker, P.L., D.W. Brown, O. Anderoglu, L. Balogh, S.A. Maloy, T.A. Sisneros, J. Almer, E.F. Tulk, W. Morgenroth, and A.C. Dippel, "Neutron and X-ray diffraction analysis of the effect of irradiation dose and temperature on microstructure of irradiated HT-9 steel," *Journal of Nuclear Materials*, 443(1-3), 2013, 522-530.

3.4.3 Irradiation Testing in HFIR

J. McDuffee, R. Howard, R. Ellis, S. Voit, Oak Ridge National Laboratory

The objective of this work is to perform irradiation testing of fuel materials in the High Flux Isotope Reactor (HFIR) to obtain a fundamental understanding of the evolution of the microstructure of metal fuel materials as a function of elemental composition, temperature, and neutron fluence so as to better understand the in-service behavior and performance of the fuel. The use of rabbit capsules inserted into and ejected from the HFIR core during full power operation provides for control of the neutron fluence, an important parameter in the evolution of the microstructure. In FY 2014, five TEM-style rabbit capsules containing DU (depleted uranium) and DU-8.3%Zr samples were irradiated in HFIR to damage levels ranging from 0.003 to 1.1 dpa (displacements per atom). Irradiated samples are presently cooling prior to shipment to the Idaho National Laboratory. Also in the fiscal year, the HFIR rabbit capsule was redesigned to hold a new specimen geometry. The capsule redesign effort had four objectives; (1) utilize lesson learned from the TEM capsule design and reduce the radiation activity of capsule components to facilitate shipping, (2) redesign the inner sample holder to accommodate specimens of parallelepiped geometry, (3) design capsule to customer specified irradiation temperature requirements, and (4) minimize the axial temperature gradient in the parallelepiped specimens. All four design objectives were accomplished (see Figure 74). The Gd thermal neutron shield has been relocated outside the sample container and will be removed prior to shipping the sample capsule. The sample holder can now accommodate multiple samples of parallelepiped geometry. The target sample temperature of 700°C was achieved by controlling the radial gap between the Gd shield and the Ti sample capsule and a high thermal conductivity Mo sample holder was used to improve radial heat flow thereby reducing the axial temperature gradient to ~20°C.

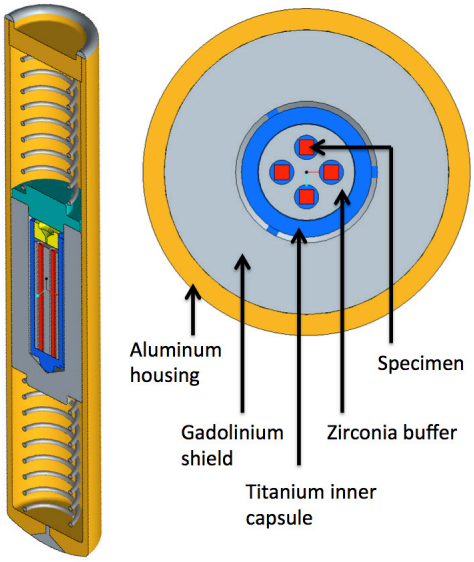

Figure 74. Parallelepiped rabbit design utilizing an outer gadolinium thermal neutron shield and a removable inner titanium specimen capsule.

3.4.4 FCRD Transmutation Fuels Irradiation Testing

K. Barrett, Idaho National Laboratory

Irradiation testing of AFC transmutation fuels is being performed in INL's ATR. The AFC-3 and AFC-4 series irradiation experiments are a continuation of the AFC-1 and AFC-2 scoping level experiments previously irradiated in ATR [1]. Upon reaching the programmatically desired burnup (defined as percent depletion of initial fissile material), or as directed by the AFC program, AFC-3 and AFC-4 experiments are discharged from ATR and shipped to the INL Materials and Fuels Complex (MFC) for postirradiation examination (PIE)

In addition to the AFC series fuel experiments, performance assessment of AmBB experiments in the ATR is being planned as part of a collaborative analysis program between CEA and DOE fuel development programs; however final design of the AmBB experiments was postponed until FY 2015 and therefore is not included in this report.

Accomplishments

In FY 2014, the AFC-3C capsules continued irradiation and the AFC-4A and AFC-4B capsules were initially inserted into ATR for irradiation cycle 155A. The AFC-3D capsules were not irradiated during cycle 155A due to higher than designed lobe power in position A-11. Due to the PIE results from AFC-2 rodlets identifying rodlet breach, it was decided that all AFC-3 and AFC-4A capsules would remain out of the ATR until the cause of breach was further examined and evaluated. Therefore, only the AFC-4B capsules were inserted into the A-12 position which had a lower lobe power cycle 155B than the other three ATR outboard A positions.

The AFC-4D test rodlet design and preparation began in FY 2014. An AFC-OA analysis plan [2] was issued to update the bounding safety analyses and the ATR experiment safety analysis. Enrichment calculations are being performed to meet AFC-4D test objectives and support fuel fabrication for the AFC-4D fuel.

Preliminary AFC-Re-Design

At the request of the AFC program, an independent review committee was convened to review the post-test analyses performed by the fuels development team, to assess the conclusions of the team for the cause of three experiment test failures (AFC-2A, AFC-2B, AFC-2E), to assess the adequacy and completeness of the analyses, to identify issues that were missed, and to make recommendations for improvements in the design and operation of future AFC transmutation fuels tests. The committee concluded that the most likely cause of failure in all three tests was a higher than anticipated heat generation rate in the fuel coupled with inadequate heat transfer thru the gas gap that exists between a test rod and the safety capsule. Several recommendations were made for improvements to the design and operation of future tests. A high priority was given to reducing the sensitivity of the gap thickness to the cladding temperature [3]. Some ideas for design changes were presented for the fuels development team to consider that will reduce this risk, and obtain additional data that would be useful in postirradiation examination. Other recommendations were made for out-of-pile testing, fabrication, sensitivity studies, and design analysis strategy. These recommendations were further examined and incorporated into an AFC preliminary re-design effort in FY 2014.

In FY2014, the AFC project team identified experiment objectives and requirements for the new design. Viable concepts were developed through brainstorming with the design and technical lead team. A sketch of a preliminary design has been drawn [Figure 75] consisting of a fueled rodlet

surrounded by an insulating sleeve and liquid metal, all contained inside of a capsule. Use of the insulating sleeve and liquid metal minimizes rodlet temperature sensitivity to manufacturing tolerances and provides larger clearances between components to aid disassembly during post-irradiation examination. This concept is slightly larger in diameter than the current AFC Outboard A design, and will likely need to be irradiated in the slightly larger diameter Small B positions in ATR.

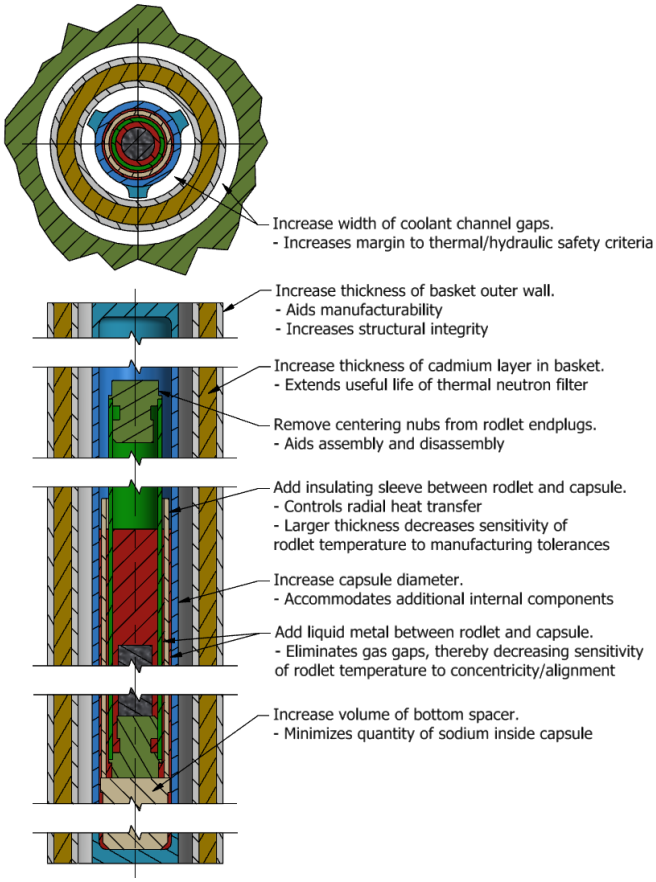

Figure 75. Preliminary AFC re-design sketch with overview of design improvements.

The design team is also identifying out-of-pile tests necessary to determine compatibility of sodium (liquid metal) with zirconium oxide (insulating sleeve) as well as to determine jump gap effects on heat transfer through small rodlet-to-capsule gas gaps used in the current and past AFC designs.

Future Work

The AFC-3C, AFC-3D, and AFC-4B capsules will continue irradiation in the ATR outboard "A" positions in FY 2015. The AFC-4A capsules will be evaluated to determine if they can be re-inserted in FY 2015. They were designed at 19 MW lobe power, however the inclusion of jump distance corrections to the cladding temperature calculations indicate AFC-4A capsules cannot be inserted in the ATR at more than 18 MW lobe power. In FY 2014, there was not an available outboard "A" position operating at this lobe power.

The AFC-4D experiments are currently being designed and analyzed for fabrication and insertion FY 2015. The AFC-OA ESAP will be revised in early FY 2015 to simplify the document, remove the center lobe power restriction, and include the AFC-4D and AFC-4E experiments.

Two AFC-4B capsules will be removed from the ATR after end of cycle 157B and will be stored in the ATR canal in preparation for shipment in the GE-100 from ATR to MFC for PIE in FY 2015.

A preliminary experiment plan will be prepared and issued in early FY 2015. Design and analysis for AFC-4C (new Outboard A capsules) will be completed by mid FY 2015. Final design and analysis for the AFC re-design and the AmBB experiments will be performed in FY 2015.

References

1. PLN-3608, "Project Execution Plan for the Fuel Cycle Research and Development AFC-OA Irradiation Experiments in the ATR," January 2013.
2. PLN-4778, "Analysis Plan for the AFC Outboard A Design Experiments," August 2014.
3. *Independent Review of AFC-2A, 2B and 2E Irradiation Tests*, FCRD-FUEL-2014-000578, January 2014.

3.4.5 FUTURIX-FTA Return

H. MacLean Chichester, Idaho National Laboratory

Ten years after signing the Implementing Arrangement between DOE and France's CEA to jointly conduct the FUTURIX irradiation experiments in the PHENIX reactor in France, the four pins in the FUTURIX-FTA fuel experiment returned to the U.S. The shipment arrived in South Carolina on July 22 and was received at INL on July 24 (See Figure 77 and Figure 76). Postirradiation examination of this experiment will begin in FY 2015. Identical fuels were irradiated in ATR in the AFC-1 test series. Results of the AFC-1 and FUTURIX-FTA experiments will be used to evaluate and identify any differences caused by the difference in neutron spectra between PHENIX (a typical fast reactor) and ATR (using a cadmium-lined basket to simulate fast reactor neutron spectrum in a thermal reactor).

Figure 77. Shipping vessel arriving in Charleston, South Carolina.

Figure 76. TN-106 cask containing the FUTURIX-FTA experiment in the HFEF Truck Lock

This page intentionally left blank.

Capability Development

SECTION 4

4. CAPABILITY DEVELOPMENT

A basic philosophy of AFC is the development and utilization of advanced scientific methods for the research and development of advanced, novel, high performance nuclear fuel systems. The Crosscutting Technologies area is focused on this guiding principal. Performing research on irradiated and highly radioactive fuel materials is difficult, time intensive, and technically challenging. Couple this with the desire to study the microstructural evolution of fuels and materials under irradiation provides the opportunity for the development of advances in nuclear fuels and materials R&D science. The activities in this technical area are examples of the innovative and creative science and engineering accomplished by the technical scientific and engineering staff.

4.1 Development of the Thermal Conductivity Microscope

D. Hurley, Idaho National Laboratory

The Thermal Conductivity Microscope (TCM) is designed to operate in a radiation hot cell environment via remote control manipulation. The TCM provides micron-level thermal property information that is commensurate with microstructure heterogeneity. The development of the TCM connects closely with INL's larger PIE effort to provide new validation metrics for fundamental computational material science models. Currently TCM is being used to provide important data on uranium bearing surrogate fuel samples.

One example of this work on surrogate fuel, shown on the upper right side of Figure 78, investigates the reduction in thermal conductivity of polycrystalline UO_2 irradiated with 4 MeV He^{++}. The conductivity of the thin surface layer corresponding to the plateau region of the damage profile was isolated by tuning the penetration depth of the thermal waves. Another example, shown in the lower right side of Figure 78, involves using the TCM to measure thermal anisotropy. Currently the TCM is being used to confirm the existence of thermal anisotropy in UO_2 caused by phonon-spin coupling.

The plans for FY15 include benchmarking the accuracy and reproducibility of the TCM using known thermal conductivity standards. Preliminary test conducted in FY 2014 indicate that conductivity results are accurate within ±5% and the reproducibility is less than 2%.

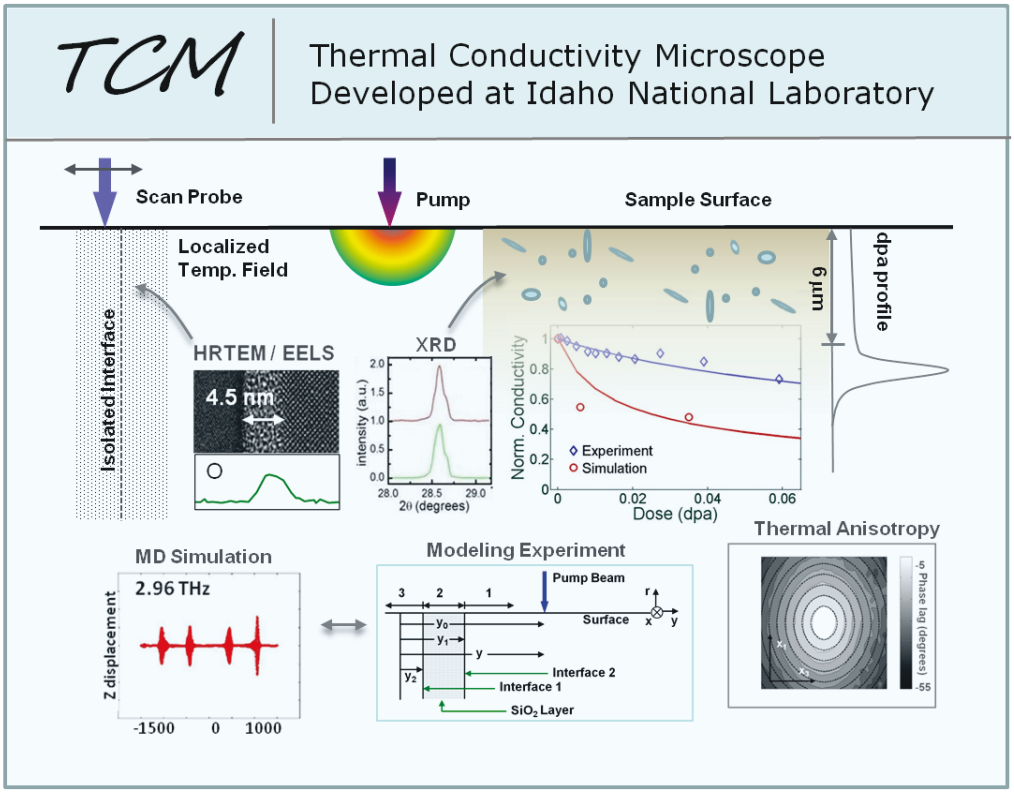

Figure 78. TCM measures local changes in thermal conductivity. The left side illustrates measurement of the Kapitza resistance of an individual, highly characterized interface. The right side demonstrates the use of the TCM to measure the conductivity of a thin surface layer damaged by energetic ions.

4.2 Thermophysical Properties Testing in the Fresh Fuels Glovebox

C. Papesch, Idaho National Laboratory

The fresh fuels glovebox located at MFC in the Analytical Laboratory was installed this year (Figure 79). This glovebox is an inert atmosphere box containing a variety of characterization instruments that will be used to support transuranic fuel and materials characterization for AFC irradiation testing and ATF fabrication and testing. The list of instruments that were installed and tested inside the glovebox in FY 2014 is as follows:

- Pulse Laser Flash analyzer (20°C to 2000°C between two furnaces)
- Differential Scanning Calorimeter (20°C to 1650°C)
- Pushrod Dilatometer (20°C to 1650°C)
- Differential Thermal Analyzer / Thermogravimetric Analyzer (20°C to 1600°C)
- Annealing furnace (20°C to 1200°C)
- Optical Metallograph
- Analytical Balance

While all of the thermophysical properties instruments and furnaces have been initially supplied with ultra-high purity argon and helium for use as testing atmospheres, there are connections available to

introduce specialty gases and gas mixes into the sample chambers. One potential use for a certified gas mixture is measuring the O/M ratio of mixed oxide fuels to determine stoichiometry. The instruments in this box will also be used to develop viable post irradiation testing methods for measuring thermal conductivity on metallic and ceramic fuels. The fresh fuels glovebox is scheduled to begin radiological operations in December 2014.

Contributors to the installation and readiness assessments of the fresh fuels glovebox include Brian Gray, Mark Anderson (Analytical Lab facility operations), Sadie Butler (Facility Manager, AL), Max Howell (Engineering), Cynthia Papesch, Craig Marshall (NS&T) MFC instrument and calibration and mechanical crafts.

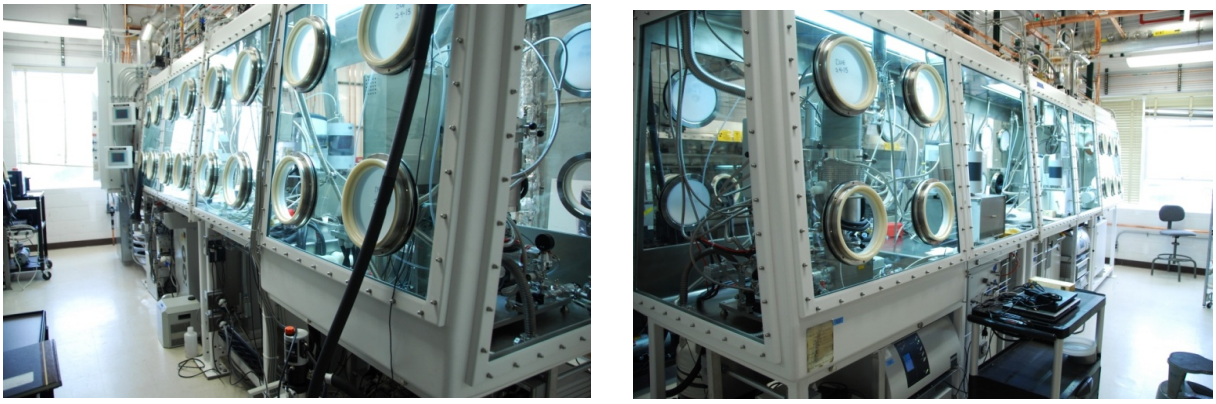

(a) (b)

Figure 79. Fresh Fuels Glovebox in MFC's Analytical Lab: (a) West side view; (b) East side view.

4.3 Advanced NDE Techniques Development and Path to Advanced PIE of ATR Irradiated Fuels

D. Byler, S. Vogel and K.J. McClellan, Los Alamos National Laboratory

The current "science based" approach to developing and testing new fuel forms requires that innovative and new techniques be developed and refined to extensively characterize nuclear fuel materials before, during and after irradiation to record and understand the microstructural and chemical evolution that occurs in the fuels during irradiation. The results from this characterization can produce data that is targeted to bridge the gaps in the current data sets to be used for improved predictive models and simulation and further aide in fuel development efforts. These efforts can effectively be used to streamline and advance the fuel licensing process to meet the needs of the nuclear fuels community and the path set forth by DOE to meet future nuclear power needs.

The emphasis of the current work is to develop, assess and demonstrate advanced non-destructive evaluation (NDE) techniques in support of advanced PIE efforts on fresh and irradiated nuclear fuels. As part of this effort, work was conducted in FY13 to determine a set of relevant techniques that could be used to improve the overall fuel characterization capabilities, given the constraints associated with highly radioactive materials. An assessment of relevant techniques and facilities available to DOE to perform the characterization was performed. It was determined that a set of x-ray, neutron and proton measurement techniques be further evaluated based on their ability to work with the highly radioactive

samples. There were a number of facilities with the techniques mentioned above, that could handle small quantities of high radioactivity samples, but only a few that could handle rodlets or entire fuel rods. Two of those were INL and LANL. As such, an assessment of the capabilities of each institution was performed, noting the strengths and weaknesses of each. Based on this assessment, a plan was developed in collaboration with INL to establish the process for evaluating both fresh and irradiated fuels, covering shipping, handling, testing and storage of fuel rodlets and materials.

During the early part of FY 2014, a set of clad depleted uranium dioxide (dUO_2) rodlets with engineered defects and chemistries were measured using neutron radiography (n-RAD), neutron resonance tomogrpahy and neutron scattering at LANL to assess the current set of capabilities with respect to spatial resolution and detection limits. A similar evaluation funded by LANL was previously performed in FY10 using proton and neutron radiography on clad dUO_2 pellets providing initial spatial resolutions and detection limits for the two techniques. Results from the current set of FY 2014 measurements are summarized below noting several technique improvements and refinements.

Two sets of clad dUO_2 rodlets sized to mimic LWR and fast reactor rodlets were evaluated using the neutron techniques. The rodlets contained pellets with various defects such as cracks and voids, variations in chemistry, different densities, tungsten wire inclusions for spatial resolution calibration, missing surfaces and additional rodlets containing compressed xenon gas at different pressures. The rodlets were measured with neutron resonance imaging, neutron scattering, and neutron tomography. The spatial resolutions and lower detection limits were established during this process. Refinements and interpretation of the extremely large datasets generated by the measurements were conducted to reconstruct the 3-dimensional (3-D) locations of chemistry, microstructure and phase content. Utilizing the SAMMY code developed at ORNL, a detailed analysis of the transmission spectra was also performed. Since the nuclear cross-sections are known, the code allows the refinement of the area density of the isotope present in the beam path, which in turn allows the derivation of the concentration of the isotopes present in a given sample. The initial results with known sample thicknesses yielded values within 20% of the expected density values. Also note that the analysis depends on parameters such as background and detector efficiency. Characterization and optimization of these values is currently ongoing.

In terms of advanced PIE capability refinement, is was demonstrated that by combining the results from neutron imaging, which uniquely allows the measurement of the concentration of isotopes, with neutron diffraction, crystallography (phases present, strains, crystal structure) and microstructure (defect concentrations, preferred orientation or texture of crystals) can also be obtained. This is shown in Figure 80, where a rodlet was fully tomographed and reconstructed to show the distribution of tungsten (artifact due to pellet processing) within the rodlet. By combining these techniques, a determination of the variation in densities and locations of impurities (such as the tungsten) within the rodlet can be attained. The technique can also be used to help to determine the crystallographic form of the tungsten, i.e. metallic tungsten, or a compound with tungsten in it. Additionally, by examining the resonances, gases such as xenon can be detected.

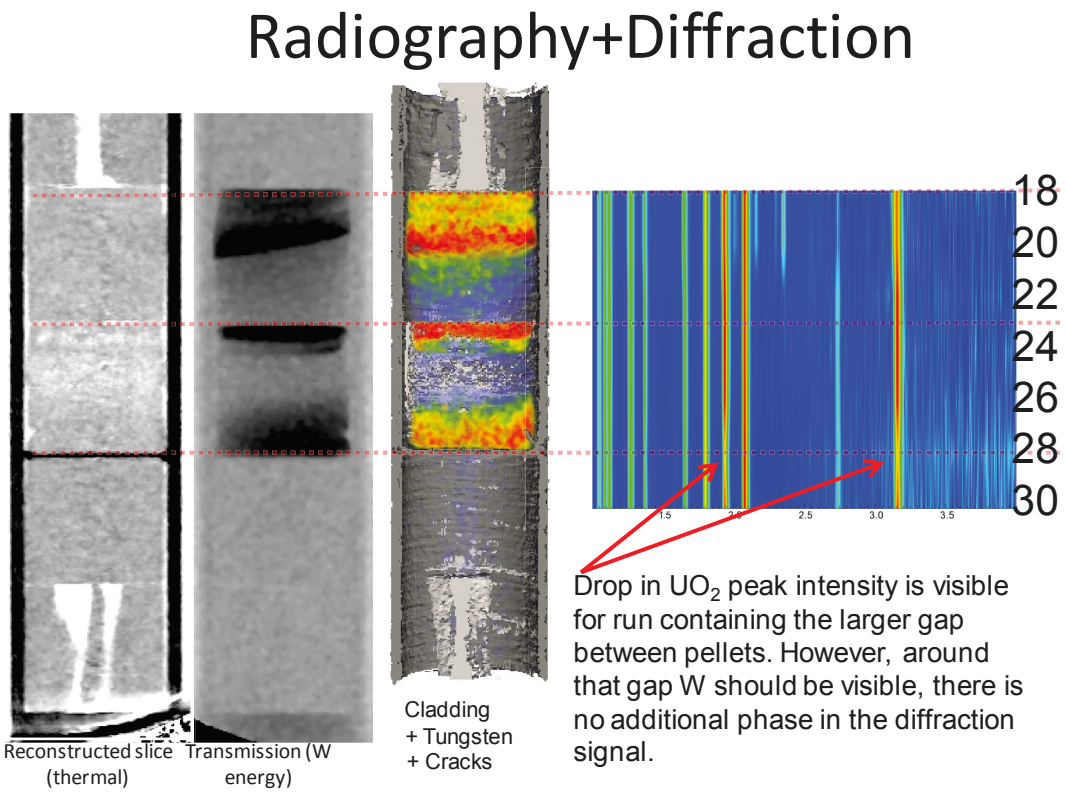

Figure 80. Neutron imaging and diffraction on dUO2 rodlet containing microstructure and void pellets.

In summary, these techniques set the foundation for a strong set of capabilities that have the ability to non-destructively examine fresh and irradiated fuel rodlets for 3-D chemistry, microstructure and phase content with spatial resolutions of 50 μm or less with interpolation and improved analytical routines. These techniques can be tailored to meet fuel development and modeling and simulation needs. Going forward, several additional improvements and refinements will be performed to prepare for evaluation of fresh and irradiated fuel rodlets; including further optimization of the experimental setup, data analysis and a reduction of background noise. Additionally, a new time-of-flight x-y neutron detector will be put into service to limit possible downtime.

Based on this assessment and the one done for INL, the path forward to testing fresh and irradiated fuel was developed. An idealized depiction of the process is shown in Figure 81.

This will rely heavily on coordination of shipping, irradiations and testing to provide data for modeling and simulation and to guide further PIE on fuel rodlets. The key concerns with this plan are the need for a certified shipping cask for irradiated fuels that meet the “Type B” criteria under the US Department of Transportation rules and regulations and the coordination of beamtime with shipping schedule.

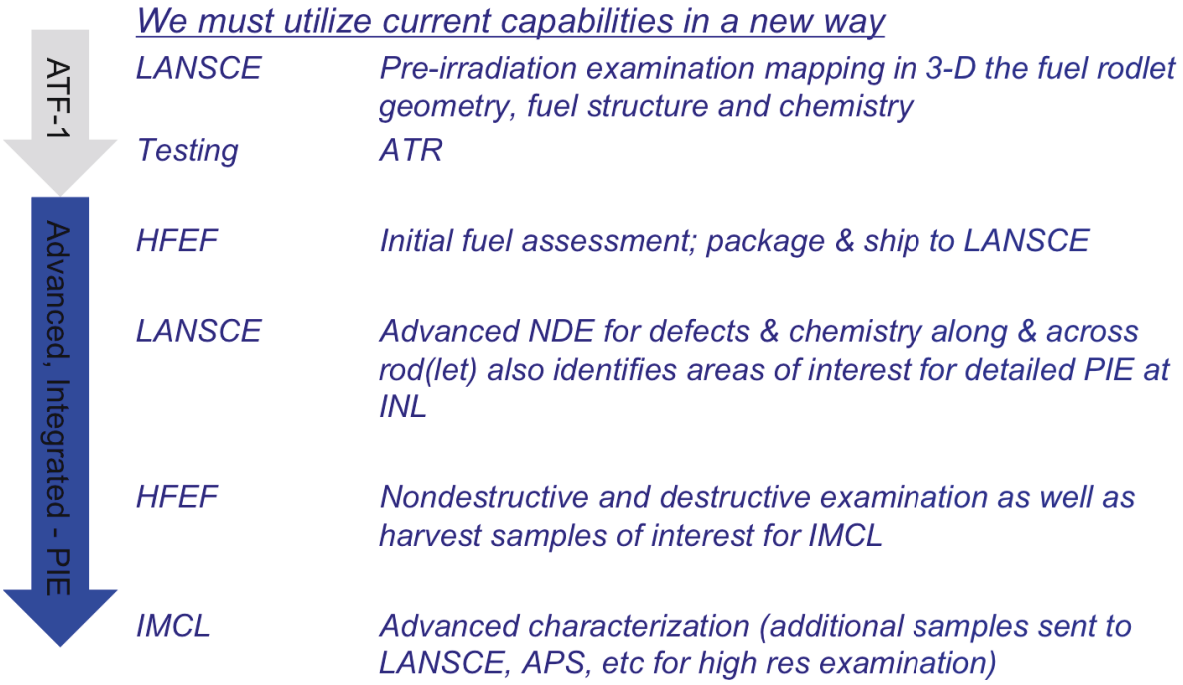

Figure 81. Depiction of A-PIE process applied to irradiated fuel rodlets that are shipped to LANL for NDE and back to INL for NDE and destructive examination

4.4 TREAT Experiment Planning

D. Wachs, Idaho National Laboratory

A transient testing research program is being developed to support assessment of ATF designs being proposed for LWR applications. Accident tolerant fuels are defined as fuel systems that, when compared to existing Zircaloy clad UO_2 designs, can tolerate loss of active cooling while maintaining or improving the fuel performance during normal operations, operational transients, design-basis events, and beyond design-basis events. ATF concept evaluation must be completed in time to support insertion of an ATF lead rod assembly into a commercial power reactor by 2022. To enable this goal, transient testing of ATF fuels under both overpower (e.g. Reactivity Initiated Accident (RIA) simulation) and undercooling (e.g. LOCA simulation) conditions must begin shortly. This series of ATF transient tests have been termed ATF-3.

The Transient Reactor Test (TREAT) facility is a versatile test facility able to subject experimental specimens to various transient nuclear conditions of interest (see the reactor core in Figure 82). TREAT resides at the Materials and Fuels Complex at INL. The reactor first achieved criticality in 1959 and was operated successfully until 1994, when its operations were suspended. During that time, the facility underwent various modifications and upgrades that maintained it in a "state-of-the-art" condition. DOE recently identified a broad need to reestablish transient testing capability in the United States. Resumption

of operations at the TREAT facility was identified as the preferred option for meeting these needs. As a result, an active project is underway to facilitate reactivation of the TREAT facility by 2018.

In parallel to the effort to resume operations at TREAT, the transient testing strategy to support ATF concept screening, development, and qualification is being developed. A proposal for the first set of transient experiments has been prepared for discussion with the ATF concept design leads. These tests emphasize assessment of the relative performance of the fuel designs under various enthalpy additions anticipated under pulse and ramp conditions. The TREAT test loop concept is provided in Figure 83.

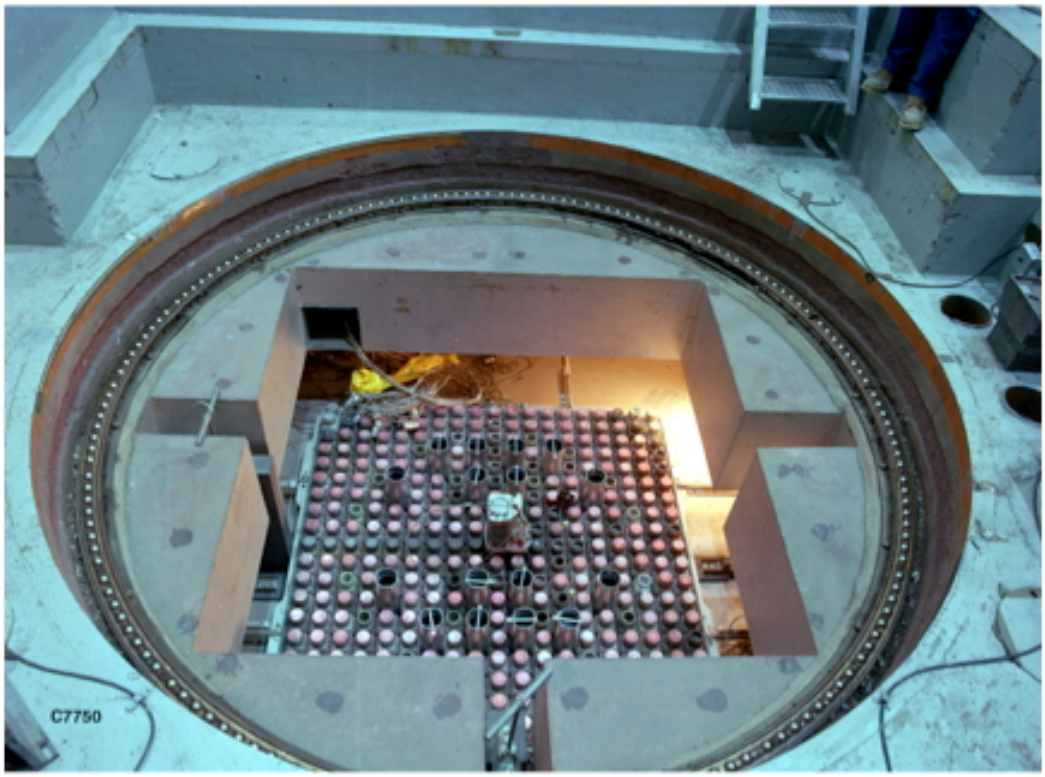

Figure 82. Overhead view of the Core of TREAT

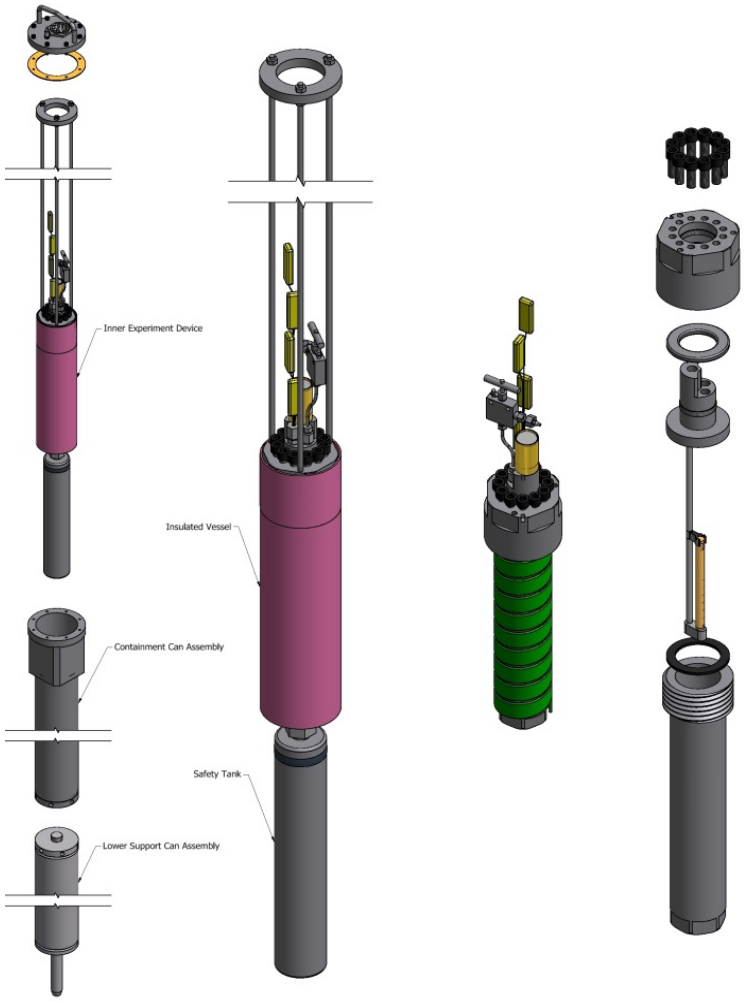

Figure 83. TREAT test loop for ATF fuel testing.

4.5 Minor Actinide Casting Experiments in the GACS

R. Fielding, Idaho National Laboratory

The glovebox advanced casting system (GACS) was installed and operated in a minor actinide qualified glovebox. This furnace was designed to provide a flexible casting development platform where both gravity casting into a permanent mold and counter gravity casting into a glass mold could be developed and studied. In addition to casting development the GACS will also be used to study melt properties, americium volatility studies, and general sample fabrication. The furnace was designed to be a flexible platform in which a number of experiments, alloys, and configurations can be run. The modular design of the furnace makes it possible to change out components, such as coils, crucibles, and molds to accommodate a variety of sizes or techniques as required.

The solid model of the GACS as it is currently configured for gravity casting and the installed furnace is shown in Figure 84. As can be seen in this figure the GACS is contained in a stainless steel shell which used standard ISO style vacuum flanges for all sealing surfaces. The mold and crucible are independently inductively heated allowing the ability to rapidly heat the crucible and mold which may be necessary to decrease the total amount of time the fuel alloy is heated thereby reducing volatility losses. A number of

thermocouples can be monitored throughout the heating cycles, a standard gravity casting utilizes four K-type thermocouples along the length of the mold with an option of monitoring up to six additional K-type thermocouples and a total of four B-type thermocouples can be used as well; two thermocouples are used on the crucible, one is used to monitor the crucible induction coil temperature and one thermocouple is a spare which can be used where needed. A total of five pressure transducers can be used to monitor the furnace system although currently only two are being utilized in the gravity pour configuration. The current design calls for a graphite crucible and a two-piece graphite mold with the pins being casting on the parting line of the mold.

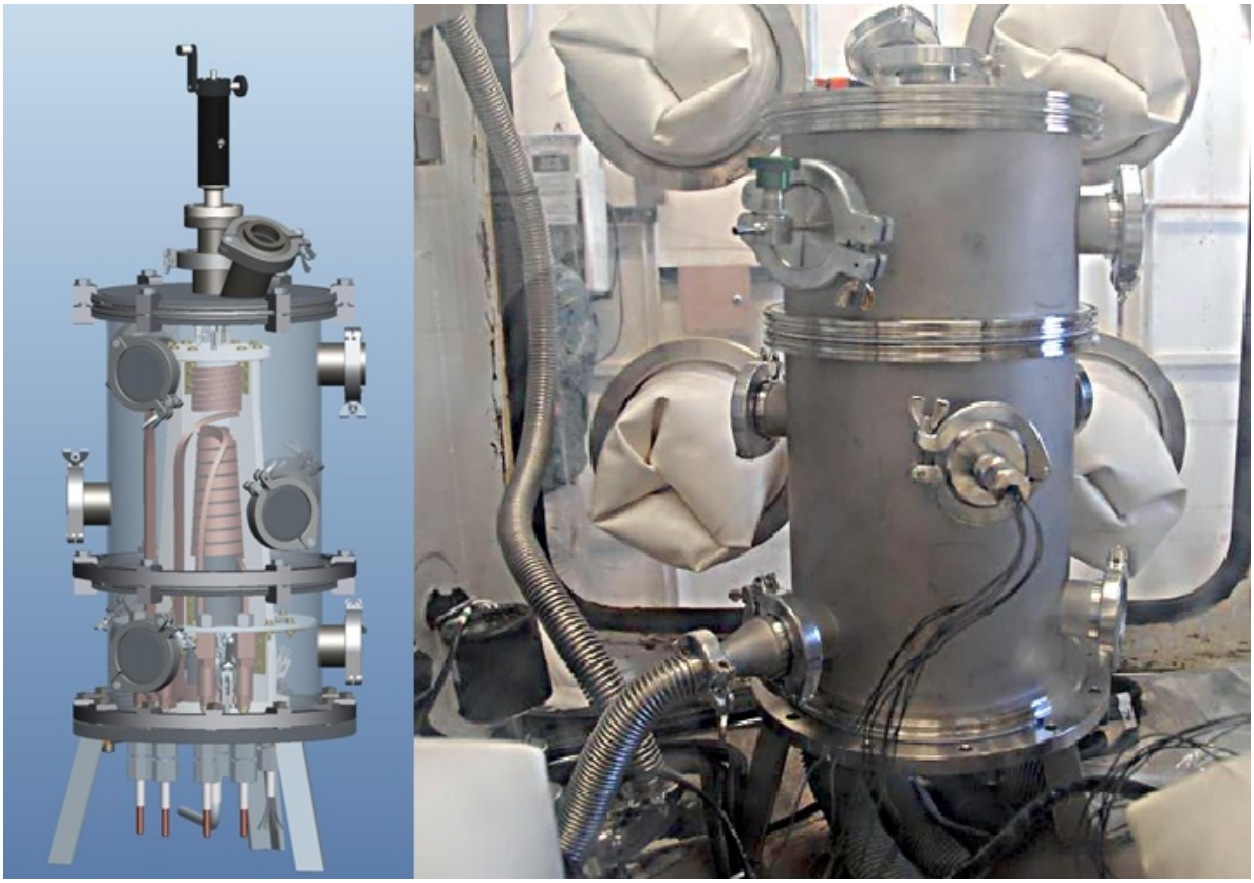

Figure 84. Schematic and photo of the GACS configured for gravity casting. Note- the linear actuator has been removed for the photo.

4.6 Advanced Instrumentation Development: Thermoacoustic Sensors

Over the last three years, AFC's advanced instrumentation work package has been developing and testing a self-powered and acoustically telemetered thermoacoustic (TAC) sensor. Currently the TAC sensor is being designed to operate in the Breazeale Nuclear Reactor to simultaneously measure neutron or gamma flux, gas temperature, and axial extension inside a fuel rod. Thus, a single sensor will be able to monitor at least three process measurements in real time.

This year the advanced instrumentation work package spearheaded collaboration between the INL, Penn State and Westinghouse to demonstrate TAC sensing technology in the Breazeale Nuclear Reactor. Westinghouse will be paying for deployment of the TAC sensor in the reactor (≈$500,000). The

demonstration of the TAC technology is scheduled for the summer of 2015. http://www.world-nuclear-news.org/ENF-Westinghouse-to-market-fuel-rod-sensors-by-2019-20061401.html

The TAC Breazeale reactor demonstration will validate a successful joint collaboration among a national laboratory, university, and industrial partner that is science-based and engineering driven. The TAC sensor is one of the few technologies in history of the INL in which industry has supported a development effort to leverage INL technology for a proof of concept demonstration while having a plan to in place to take the concept to market.

To prepare for a demonstration of the TAC technology in INL's ATR, the necessary acoustic/vibrational measurement infrastructure needs to be in-place on the reactor vessel. The advanced instrumentation team was able to deliver and successfully install the Acoustic/vibrational measurement infrastructure to monitor acoustic emissions within the ATR. The measurement infrastructure will allow acoustic/vibrational baselines to be developed for various operating conditions of ATR and will be useful to design acoustic based sensors such as TAC and vibro-acoustic transducers as well as develop online health diagnostics, prognostics, and predictive maintenance capabilities.

A significant component of the acoustic measurement infrastructure is a custom designed and architected Data Acquisition System (DAS) to demodulate TAC and vibro-acoustic signals from multiple receivers. The real-time conversion from acoustic signal into effective process and microstructure characterization data from multiple locations in the reactor will enable innovative control and diagnostic capabilities. The INL DAS system will automatically convert TAC sensor signals into dynamic amplitude, frequency and phase data. TAC Amplitude data is proportional to neutron or gamma flux. TAC frequency information will be proportional to temperature and the phase information will track axial elongation of the TAC sensor. Thus a single TAC sensor will be able to monitor at least three process measurements due to the INL DAS system. The INL DAS system was successfully tested in the Applied Research Laboratory Anechoic pool at Penn State.

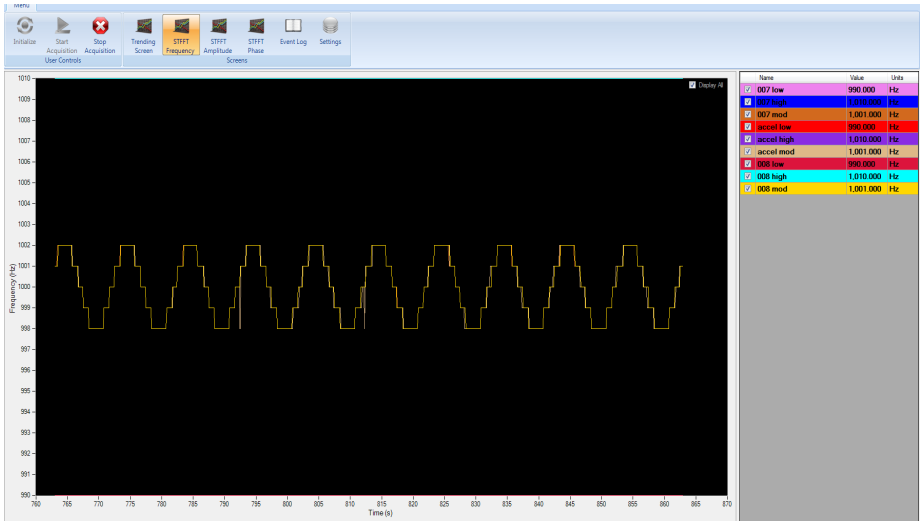

Figure 85. A screen shot of the frequency tracking display demonstrating the dynamic measurement from three simulated TAC sensors and three acoustic receivers.

Figure 85 shows a screen shot of the frequency tracking display demonstrating the dynamic measurement from three simulated TAC sensors and three acoustic receivers.

- Three simulated TAC signals: two static at 990 and 1010 Hz; one dynamic 998 to 1002 Hz

- Overlapping static signals are at the top and bottom of the screen (Hydrophone 7, Hydrophone 8, Accelerometer)
- Dynamic signals are shown center of the screen (three overlapping; Hydrophone 7, Hydrophone 8, Accelerometer). Steps in the dynamic signal are artifacts from the choice of DAS acquisition parameters

References

1. J. A. Smith, J. K. Jewell, *Promising Wireless In-Pile Sensing Methods*, INL/LTD-14-33110, FCRD, DOE Level 3 Milestone, September 29. 2014.
2. J. A. Smith, D. K. Kotter, R. A. Ali, S. L. Garrett, "Designing A TAC thermometer from A VHTR graphite structure," to be published in *Review Of Progress In Quantitative Nondestructive Evaluation,* 152, Boise ID, July 20-25, 2014, D. E. Chimenti, Editors, American Institute of Physics, Melville, NY, 2015. INL/CON-13-29454.
3. V. Agarwal, M. S. Tawfik, J. A. Smith, "Acoustic emission signal processing technique to characterize reactor in-pile phenomena," to be published in *Review of Progress in Quantitative Nondestructive Evaluation,* 152, Boise ID, July 20-25, 2014, D. E. Chimenti, Editors, American Institute of Physics, Melville, NY, 2015. INL/CON-13- 28878.
4. J. A. Smith, K. Jewell, B. Heidrich, S. Despain, "Advanced instrumentation for experiments," *DOE-NE AFC Integration Meeting*, August 28, 2014. INL/MIS-14-32916.

Documentation

SECTION 5

5. DOCUMENTATION

5.1 Additional Publications

Author(s)	Title	Publication	Date
Carmack, Jon	Accident Tolerant Fuel Development Program	Nuclear Plant Journal, vol 46	Jan-Feb, 2014
Bragg-Sitton, S.	Development of Advanced Accident-Tolerant Fuels for Commercial LWRs	Nuclear News	Mar 2014
Bragg-Sitton, S.	Development of Enhanced Accident-Tolerant Fuels for Light Water Reactors	2015 McGraw-Hill Yearbook of Science & Technology	Dec 2014
Collin, B.P.	Modeling and Analysis of UN TRISO Fuel for LWR Application Using the PARFUME code	Journal of Nuclear Materials vol 451	2014
Besmann, T.M., Ferber, M.K., Lin, H-T.L, Collin, B.P.,	Fission Product Release and Survivability of UN-Kernel LWR TRISO Fuel	Journal of Nuclear Materials vol 448	2014
Teague, M., Gorman, B., King, J., Porter, D., Hayes, S.	Microstructural Characterization of High Burn-up Mixed Oxide Fast Reactor Fuel	Journal of Nuclear Materials, 441, 267-273	2013
Teague, M., Gorman, B., Miller, B., King, J.	EBSD and TEM characterization of high burn-up mixed oxide fuel	Journal of Nuclear Materials, 444, 475-480	2014
Teague, M., Tonks, M., Novascone, S., Hayes, S.	Microstructural modeling of thermal conductivity of high burn-up mixed oxide fuel	Journal of Nuclear Materials, 444, 161-169	2014
Teague, M., Gorman, B.	Utilization of dual-column focused ion beam and scanning electron microscope for three dimensional characterization of high burn-up mixed oxide fuel	Progress in Nuclear Energy, 72, 67-71	2014
He, L.F, Gupta, M., Yablinsky, C.A., Gan, J., Kirk, M.A., Bai, X.M., Pakarinen, J., Allen, T.R.	In-situ TEM observation of dislocation evolution in Kr-irradiated UO2 single crystal	Journal of Nuclear Materials,443, 71-77	Nov-13
He, L.F., Pakarinen, J., Kirk, M.A., Gan, J., Nelson, A.T., Bai, X., El-Azab, A., Allen, T.R.	Microstructure evolution in Xe-irradiated UO2 at room temperature	Nuclear Instruments and Methods in Physics Research Section B: Beam Interactions with Materials and Atoms, 330, 55-60	Jul-14
Brown, N. R. Brown A. Aronson, M. Todosow, R. Brito, K. McClellan	"Neutronic performance of uranium nitride composite fuels in a PWR,"	Nuclear Engineering and Design, 275, 393-407 (2014)	2014
Brown, N. R. M. Todosow, K. J. McClellan.	"Uranium nitride composite fuels in a pressurized water reactor: exploration of multi-batch cycle length and UB4 admixture for reactivity control,"	Proceedings of PHYSOR 2014 – The Role of Reactor Physics Toward a Sustain Future; The Westin Miyako, Kyoto, Japan,	2014

5.2 AFC Level 2 Milestones

Work Package Title	Site	Work Package Manager	Milestone
AFC Campaign Management	INL	Beverly, Ed	Issue Quality Implementation Plan for ATF development – (implements quality processes in accordance with the FCRD QAPP.)
AFC Campaign Management	INL	Beverly, Ed	Issue Draft Advanced Fuels 2014 Accomplishments Report
AFC Campaign Management	INL	Beverly, Ed	Issue AFC 2013 Accomplishments Report (FY13)
LWR Fuels Irradiation Testing in ATR	INL	Barrett, Kristine	Acquire GE-100 Cask
LWR Fuels Irradiation Testing in ATR	INL	Barrett, Kristine	Initial ATF-1 test capsules ready for insertion into ATR cycle 157B
LWR Fuels Irradiation Testing in ATR	INL	Barrett, Kristine	Issue FY14 ATR Irradiation Report for AFC Metallic and LWR Fuels
Advanced Technique and Fuel Material Development	LANL	Byler, Darrin	Complete dry run using clad dUO2 rodlets with structures/defects tailored to define current advanced NDE capabilities
Advanced Technique and Fuel Material Development	LANL	Byler, Darrin	Report on assessment of Advanced PIE capabilities and path to first A-PIE of irradiated rodlets
Advanced Technique and Fuel Material Development	LANL	Byler, Darrin	Complete and issue summary report on Assessment of advanced sintering techniques for ATF fabrication
Severe Accident Test Station Installation and Testing	ORNL	Snead, Mary	Complete report on Mechanistic assessment and model input for SiC steam-oxidation at conditions consistent with beyond design basis accident conditions.
Severe Accident Test Station Installation and Testing	ORNL	Snead, Mary	Issue report documenting joint LANL and ORNL Advanced LWR cladding materials LOCA testing
Severe Accident Test Station Installation and Testing	ORNL	Snead, Mary	Complete in-cell installation of High-Temperature capability for Severe Accident Test Station.

Work Package Title	Site	Work Package Manager	Milestone
Innovative LWR Metallic Fuel	PNNL	Love, Diana	Complete corrosion testing of advanced metalic LWR fuel concept and issue status report documenting measurements
Advanced Accident Tolerant Ceramic Fuel Development	LANL	Nelson, Andy	Complete evaluation of reaction energetics and temperature thresholds for selected fuel systems of relevance to accident tolerant fuels
Advanced Accident Tolerant Ceramic Fuel Development	LANL	Nelson, Andy	Complete Structure-Property relation summary report for advanced composite accident tolerant fuel
Development of improved ATF engineering alloy - Mechanical testing of initial alloy	LANL	Maloy, Stuart	Complete summary report on ion irradiation testing and characterization of FeCrAl candidate alloys
ATF Cladding Production	ORNL	Yamamoto, Yuki	Report on the development of 2nd generation ATF FeCrAl alloys
ATF SiC Cladding Development	ORNL	Katoh, Yutai	Summary and near term technical gaps to address for applications of SiC to LWRs
Development of improved ATF engineering alloy	ORNL	Pint, Bruce	Complete report on production and properties of ORNL ATF FeCrAl candidate alloys
ATR ATF Loop Design	INL	Chichester, Heather	Issue ATR ATF Loop Conceptual Design Report
Halden ATF Test Planning and Fabrication	ORNL	Terrani, Kurt	Issue report summarizing Planning and Fabrication of ATF cladding in support of Halden Irradiation
Halden ATF Test Planning and Fabrication	ORNL	Terrani, Kurt	Issue report summarizing Design and Initial Results from Halden Irradiation on US-Contributed ATF Candidate Materials
Fabrication of Enriched Ceramic Fuel	LANL	McClellan, Ken	Fabricate composite ceramic fuel pellets and shipment to INL for ATF-1 test insertion in ATR cycle 158B
FUTURIX-FTA Return	INL	Chichester, Heather	FUTURIX-FTA received at HFEF
FUTURIX-FTA Return	INL	Chichester, Heather	Complete dry run with TN-106 complete, HFEF ready to receive FUTURIX-FTA shipment

Work Package Title	Site	Work Package Manager	Milestone
Advanced Fabrication Technique Development	INL	Fielding, Randy	Demonstrate advanced casting into integral FCCI barrier mold
Characterization of Metal Fuel Samples	INL	Papesch, Cynthia	Issue status report on AFC1 and AFC2 fuels characterization
Metallic Fuels Irradiation Testing in ATR	INL	Barrett, Kristine	Finalize test matrix for AFC-4C,4D advanced metallic fuels tests
Metallic Fuels Irradiation Testing in ATR	INL	Barrett, Kristine	Issue Preliminary Experiment Plan for New AFC Irradiation
PIE and reports (EBR-II, FFTF, AFC series, HFIR)	INL	Harp, Jason	Complete nondestructive PIE for AFC-2D,2E,3A,3B
Rev 6. of FCRD (AFCI) Materials Handbook	LANL	Maloy, Stuart	Complete Rev. 6 of AFCI Materials Handbook
Fuel Performance Modeling Applications	INL	Medvedev, Pavel	Summary report on Accident Tolerant Fuel Modeling and International Fuel Performance Collaboration
Technique Application to Highly Radioactive Samples	INL	Papesch, Cynthia	Initiate Hot Operations in Fresh Fuels Glove Box
Advanced Instrumentation for Experiments	INL	Smith, James	Complete report on in-pile measurement techniques

5.3 AFC Nuclear Energy University Project (NEUP) Grants

Active Projects Funded in 2011 – 2012

Lead University	Title	Principle Investigator
Case Western Reserve University	Improved Accident Tolerance of Austenitic Stainless Steel Cladding through Colossal Supersaturation with Interstitial Solutes	Frank Ernst
Ohio State University	Testing of Sapphire Optical Fiber and Sensors in Intense Radiation Fields, when subjected to very high temperatures,	Thomas E. Blue
University of Tennessee	Better Radiation Response and Accident Tolerance of Nanostructured Ceramic Fuel Materials	Yanwen Zhang
University of Florida	Development of Innovative Accident Tolerant High Thermal Conductivity UO_2 –Diamond Composite Fuel Pellets	James Tulenko
University of Wisconsin-Madison	Development of Advanced High Uranium Density Fuels for Light Water Reactors	James Blanchard
University of Kentucky	Elastic/Inelastic Measurement Project	Steven W. Yates
Idaho State University	Nanovision	Eric A. Burgett
Univ of Notre Dame	Microscopic Fuel Particles produced by Self-Assembly of Actinide Nanoclusters on Carbon Nanomaterials	Chongzheng Na

Active Projects Awarded in 2013

Lead University	Title	Principle Investigator
University of California, Berkeley	Developing Ultra-Small Scale Mechanical Testing Methods and Microstructural Investigation Procedures for Irradiated Materials	Peter Hosemann
University of California, Irvine	Multiphase Nanocrystalline Ceramic Concept for Nuclear Fuel	Martha Mecartney
University of Florida	Innovative Coating of Nanostructured Vanadium Carbide on the F/M Cladding Tube Inner Surface for Mitigating the Fuel Cladding Chemical Interactions	Yong Yang

University of South Carolina	U_3Si_2 Fabrication and Testing for Implementation into the BISON Fuel Performance Code	Travis Knight
Utah State University	Optical Fiber Based System for Multiple Thermophysical Properties for Glove Box, Hot Cell and In-Pile Applications,	Heng Ban
Purdue University	Correlating Thermal, Mechanical, and Electrical Coupling Based Multiphysics Behavior of Nuclear Materials Through In-Situ Measurements	ikas Tomar

Recently Awarded Grants in 2014

Lead University	Title	Principle Investigator
Ohio State University	Studies of Lanthanide Transport in Metallic Nuclear Fuels	Jinsuo Zhang
Texas A&M University	Development of high performance ODS alloys	Lin Shao
University of Arkansas	Computational and Experimental Studies of Microstructure-Scale Porosity in Metallic Fuels for Improved Gas Swelling Behavior	Paul Millett
University of Notre Dame	Assessment of Corrosion Resistance of Promising Accident Tolerant Fuel Cladding under Reactor Conditions	David Bartels
University of Tennessee	Enhanced Accident-Tolerant Fuel Performance and Reliability for Aggressive iPWR/SMR Operation	Ivan Maldonado
University of Wisconsin, Madison	Development of Self-Healing Zirconium-Silicide Coatings for Improved Performance of Zirconium-Alloy Fuel Cladding	Kumar Sridharan
Virginia Polytechnic Institute and State University	Thermal Conductivity in Metallic Fuels	Celine Hin
Virginia Polytechnic Institute and State University	SiC-ODS Alloy Gradient Nanocomposites as Novel Cladding Materials	Kathy Lu

This page intentionally left blank.

Appendix: Acronyms

6. APPENDIX: ACRONYMS

AFC	Advanced Fuels Campaign
AmBB	Americium Bearing Blankets
ANL	Argonne National Laboratory
AOO	Anticipated Operational Occurrence
APT	Atom Probe Tomography
ASU	Arizona State University
ATF	Accident Tolerant Fuel
ATR	Advanced Test Reactor
BDBA	Beyond Design Basis Accident
BNL	Brookhaven National Laboratory
CAD	Computer Aided Design
CAES	Center for Advanced Energy Studies
CEA	Atomic Energy Commission (France)
CNC	Computer Numerical Control
CNWG	Civil Nuclear Energy Research and Development Working Group
CRADA	Cooperative Research and Development Agreement
CRIEPI	Central Research Institute of Electric Power Industry (Japan)
CTR-N	carbothermic reduction/nitridization
CVD	Chemical Vapor Deposition
DBA	Design Basis Accident
DFEM	Densification-Based Finite-Element Model
DOE	Department of Energy
dpa	Displacements Per Atom
EBR	Experimental Breeder Reactor
ECCS	Emergency Core Cooling System
EFPD	Effective Full-Power Day
EOC	End of equilibrium Cycle
EPRI	Electric Power Research Institute
EURATOM	European Atomic Energy Community
FAS	Field Assisted Sintering
FBCVD	Fluidized Bed Chemical Vapor Deposition
FCF	Fuel Conditioning Facility

FCM	Fully Ceramic Microencapsulated
FCRD	Fuel Cycle Research and Development
FCT	Fuel Cycle Technologies
FFTF	Fast Flux Test Facility
FIB	Focused Ion Beam
FOA	Funding Opportunity Announcement
FS	Flash Sintering
FY	Fiscal Year
GACID	Global Actinide Cycle International Demonstration
GACS	Glovebox Advanced Casting System
GE	General Electric
HFEF	Hot Fuel Examination Facility
HFIR	High-Flux Isotope Reactor
IAC	Industry Advisory Committee
IAEA	International Atomic Energy Agency
IFBA	Integral Fuel Burnable Absorber
INERI	International Nuclear Energy Research Initiative
INL	Idaho National Laboratory
IRP	Integrated Research Project
ITU	Institute for Transuranium Elements
JAEA	Japan Atomic Energy Agency
JFCS	Joint Fuel Cycle Studies
KAERI	Korean Atomic Energy Research Institute
LANL	Los Alamos National Laboratory
LANSCE	Los Alamos Neutron Science Center
LEAP	Local Electrode Atom Probe
LLNL	Lawrence Livermore National Laboratory
LOCA	Loss of Coolant Accident
LTA	Lead Test Assembly
LTR	Lead Test Rod
LWR	Light Water Reactor
LWRS	Light Water Reactor Sustainability Program
MA	Minor Actinide
MBM	MOOSE-BISON-MARMOT

MFC	Materials and Fuels Complex
Mo	Molybdenum
MOTA	Materials Open Test Assembly
MOX	Mixed Oxide
MPM	Mechanical Properties Microscope
MSC	Master Sintering Curve
NDE	Non-Destructive Examination
NE	Office of Nuclear Energy
NEAMS	Nuclear Energy Advanced Modeling and Simulation
NEUP	Nuclear Energy University Program
NFA	Nano-Strengthened Ferritic Alloy
NRAD	Neutron Radiography Reactor
NRC	Nuclear Regulatory Commission
NTD	National Technical Director
ODS	Oxide Dispersion Strengthened
OECD-NEA	Org for Economic Cooperation and Development-Nuclear Energy Agency
OMB	Office of Management and Budget
ORNL	Oak Ridge National Laboratory
PCT	peak clad temperature
PIE	Post-irradiation Examination
PNNL	Pacific Northwest National Laboratory
PWR	Pressurized Water Reactor
R&D	Research and Development
RD&D	Research, Development, and Demonstration
RIAR	Research Institute of Atomic Reactors (Russia)
SATS	Severe Accident Test Station
SEM	Scanning Electron Microscope
SET	Separate Effects Test
SiC	Silicon Carbide
SFR	Sodium Fast Reactor
SPS	Spark Plasma Sintering
SRNL	Savannah River National Laboratory
TAF-ID	Thermodynamics of Advanced Fuels-International Database
TCM	Thermal Conductivity Microscope

TD	Theoretical Density
TEM	Transmission Electron Microscope
TGA	thermogravimetric analysis
TMI	Three Mile Island
TREAT	Transient Reactor Test Facility
TRISO	Tristructural Isotropic
TRL	Technology Readiness Level
TRU	Transuranic
UNF	Used Nuclear Fuel
USC	University of South Carolina
WEC	Westinghouse Electric Company
XRD	X-Ray Diffraction